




EX LIBRIS
UNIVERSITATIS
ALBERTENSIS

The Bruce Peel
Special Collections
Library



Digitized by the Internet Archive
in 2025 with funding from
University of Alberta Library

<https://archive.org/details/0162014937831>

University of Alberta

Library Release Form

Name of Author: Hanna Christin Krüger

Title of Thesis: Modelling H₂S biofiltration to predict solid sulphur formation

Degree: Master of Science

Year this Degree granted: 2001

Permission is hereby granted to the University of Alberta Library to reproduce single copies of this thesis and to lend or sell such copies for private, scholarly or scientific research purposes only.

The author reserves all other publication and other rights in association with the copyright in the thesis, and except as herein before provided, neither the thesis nor any substantial portion thereof may be printed or otherwise reproduced in any material form whatever without the author's prior written permission.

University of Alberta

Modelling H₂S biofiltration to predict solid sulphur formation

by

Hanna Christin Krüger



A thesis submitted to the Faculty of Graduate Studies and Research in partial fulfillment
of the requirements for the degree of Master of Science

in

Chemical Engineering and Microbiology and Biotechnology

Department of Chemical and Materials Engineering

Department of Biological Sciences

Edmonton, Alberta

Fall 2001

University of Alberta

Faculty of Graduate Studies and Research

The undersigned certify that they have read, and recommend to the Faculty of Graduate Studies and Research for acceptance, a thesis entitled Modelling H₂S biofiltration to predict solid sulphur formation, submitted by Hanna Christin Krüger in partial fulfillment of the requirements for the degree of Master of Science in Chemical Engineering and Microbiology and Biotechnology.

Dedication

The beginning of wisdom is this: Get wisdom, and whatever else you get, get insight.

Proverbs 4:7

Abstract

In this study, the treatment of H_2S -contaminated air streams in a biofilter under pseudo-steady state conditions was described with a general mathematical model. The model accounts for chemical oxidation, biological oxidation, and dispersion, to successfully model solid sulphur formation. The biological oxidation of H_2S is a two-step process involving a solid sulphur intermediate, which is further oxidised to sulphate under appropriate conditions. The biological oxidation of sulphur is the rate-limiting step in H_2S biofilters. H_2S can also be oxidised chemically to sulphur, in the presence of air and water. Experiments were performed to measure chemical oxidation and dispersion in a column packed with peat. The experimental data indicate that up to 70 percent of H_2S removal in biofilters results from chemical oxidation. Chemical H_2S oxidation was linear at concentrations of up to 3000 ppm. The model predicts sulphur plugging and porosity decrease within the biofilter bed over time.

Acknowledgements

I would like to express my most sincere thanks and appreciation to all of those who have guided and supported me along the way, who have enriched my personal as well as academic life by their interest in my work. Especially, I would like to thank:

- Drs. William McCaffrey and Phil Fedorak for their supervision, guidance and encouragement, and for their support of the interdisciplinary degree program;
- Drs. Fraser Forbes and Karen Budwill for being a part of my committee, and for being there to answer my numerous questions about modelling and biofiltration;
- The support staff of the Department of Chemical and Materials Engineering, especially Andrée Koenig for her help with everything lab-related, Tuyet Le for showing me where things are and how they work, Tina Barker for the SEM work, Richard Cooper and Walter Boddez for keeping my equipment in working order, and AnnMarie Brereton and Marilee Barry for all things administrative;
- Dr. Richard Coleman and Irene Gaudet at the Alberta Research Council, for lending me equipment and answering numerous questions about biofiltration;
- My colleagues in both Biological Sciences and Chemical Engineering, for their friendship and advice over the course of my program;
- My family and friends for their love, support and encouragement over the past two years. Special thanks goes to my fiancé, Richard Janzen, without whom this would not have been possible;
- The University of Alberta and The Natural Sciences and Engineering Research Council of Canada (NSERC) for their financial support.

Table of Contents

1.0 Introduction	1
1.1 The biofiltration process	1
1.2 Statement of research	1
1.2.1 Problem and hypothesis	1
1.2.2 Objectives	2
1.2.3 Significance	2
1.3 Thesis outline	3
2.0 Theory and background	4
2.1 Hydrogen sulphide	4
2.2 H₂S in the oilfield	5
2.2.1 Sour gas	5
2.2.2 Flaring	7
2.2.3 Flaring issues	8
2.2.4 Alternatives to flaring	10
2.3 Biofiltration	11
2.3.1 Biofilter basics	11
2.3.2 H ₂ S biofilters	13
2.4 Chemistry of H₂S biofilters	17
2.4.1 Biological oxidation	19
2.4.2 Chemical oxidation	22
2.4.3 Solid sulphur formation	26
2.4.5 Biological sulphur	27
2.4.6 Hydrogen polysulphides	29
2.5 H₂S degradation kinetics	31
2.5.1 Biological H ₂ S degradation	31

2.5.2 Chemical H ₂ S oxidation	35
2.6 ARC work	36
2.6.1 Analysis of steady state	37
2.6.2 Sulphur balance	38
2.7 Modelling of biofilters	41
2.7.1 Historical background	41
2.7.2 Issues to consider in modelling	46
3.0 Biofilter model	47
3.1 Model development	47
3.2 Assumptions	50
3.3 Parameters	53
3.4 Modelling details	55
3.4.1 Overall H ₂ S removal	55
3.4.1.1 Mass balance over the gas phase	55
3.4.1.2 Mass balances over the biofilm	57
3.4.1.3 System solution	59
3.4.2 Formation of a solid phase	59
4.0 Experimental	63
4.1 Overview of approach	63
4.2 Column design and construction	64
4.2.1 Materials	64
4.2.2 Column construction	65
4.2.3 Substance delivery	67
4.3 Experimental procedure	67
4.3.1 Chemical oxidation studies	67
4.3.2 Tracer studies	69

4.4 Experimental methods	70
4.4.1 Scanning electron microscopy	70
4.4.2 Energy dispersive x-ray spectroscopy	70
4.4.3 Moisture content	71
4.4.4 Wet chemical methods	71
4.4.5 Combustion analysis	71
4.4.6 Interparticle porosity	72
5.0 Results and discussion	73
5.1 Tracer studies	73
5.1.1 Background	73
5.1.1.1 Tanks-in-series model	74
5.1.1.2 Dispersion model	75
5.1.2 Tracer study results	76
5.1.3 Flow pattern calculations and discussion	81
5.1.3.1 TIS model	81
5.1.3.2 Dispersion model	82
5.1.4 Conclusions from the tracer studies	84
5.2 Chemical oxidation studies	85
5.2.1 SEM and EDX analyses	85
5.2.2 Quantitative sulphur recovery	94
5.2.3 Kinetics of H ₂ S removal	101
5.2.4 Conclusions from the chemical oxidation studies	108
5.3 Model predictions	109
5.3.1 Modelling H ₂ S removal	109
5.3.1.1 Concentration profiles	109
5.3.1.2 Sensitivity to Pe	112
5.3.1.3 Sensitivity to A and δ	113

5.3.1.4 Overall parametric sensitivity studies	116
5.3.2 Modelling sulphur formation	119
5.4 Biofilter applications	123
5.4.1 Replacement for flaring	123
5.4.2 Pre-treatment alternative to flaring	125
5.4.3 Microbially soured wells	127
5.4.4 Microbial column regeneration	129
6.0 Conclusions and recommendations	131
7.0 References	133
<i>Appendix A – ARC raw data</i>	<i>144</i>
<i>Appendix B – Model code</i>	<i>152</i>
<i>Appendix C – Chemical oxidation experiments data</i>	<i>162</i>
<i>Appendix D – Determining rate laws</i>	<i>164</i>
<i>Appendix E – Edmonton water quality parameters</i>	<i>169</i>
<i>Appendix F – RTD analysis</i>	<i>170</i>
<i>Appendix G – Biofilter calculations</i>	<i>172</i>

Index of Tables

Table 1:	H ₂ S toxicity levels (after PCF 2000a; PITS 1997)	5
Table 2:	Details and parameters of selected H ₂ S biofilters discussed in the literature (after Smet et al. 1998)	14
Table 3:	Oxidation states of inorganic sulphur compounds (after Suzuki 1999)	18
Table 4:	Michaelis-Menten parameters found in selected biofilter studies	34
Table 5:	Summary of chemical oxidation kinetics observed in aqueous solutions	36
Table 6:	Sulphur balances for various time periods during laboratory-scale Biofilter 1 operation, from Dec. 9, 1992 to Mar. 12, 1993 (Data from Coleman and Dombroski 1995)	40
Table 7:	Summary of key features of selected biofilter models (after Devinny et al. 1999)	42
Table 8:	Parameters used in the biofilter model	54
Table 9:	Residence time distributions for tracer studies performed on two sizes of biofilter columns, using triplicate pulse injections of methane	77
Table 10:	Bed porosity for the two columns, as calculated assuming an ideal, perfectly mixed reactor	81
Table 11:	Average number of tanks-in-series needed to approximate ideal reactor RTD, for the two columns with various packing materials	82
Table 12:	Reactor Peclet numbers calculated using different boundary conditions, in response to a pulse tracer input of methane	83
Table 13:	Composition analysis (normalised weight percent) determined by EDX scans of three isolated particles on a webbed sub-section of the foam control	91
Table 14:	Composition analysis (normalised weight percent) determined by EDX scans for sulphur-coated foam from the top of the H ₂ S biofilter. The three particles were all found on webbed sub-sections of the foam.	92

Table 15:	Composition analysis (normalised weight percent) based on EDX scans for control and sulphur-coated peat from the top of the biofilter. The two particles on the sulphur-coated peat were chosen at random, and appear to be composed largely of sulphur.	92
Table 16:	Sulphur in the effluent of an H ₂ S biofilter. The sulphate in the effluent was measured and converted to the corresponding amount of sulphur.	98
Table 17:	Chemical oxidation in the H ₂ S biofilter	100
Table 18:	Effect of inhibition on the apparent kinetic parameters in H ₂ S biofiltration	108

Index of Figures

Figure 1: Estimated flaring from upstream oil and gas sources in Alberta (after PCF 2000b)	7
Figure 2: Enzymatic oxidation pathway of inorganic sulphur compounds (after Suzuki 1999)	19
Figure 3: Performance of a 1 m laboratory-scale H ₂ S biofilter inoculated with <i>T. thiooxidans</i> (Experiment 3, Biofilter 2, Budwill and Coleman 1999). The curves shown are H ₂ S inlet (●) and outlet concentrations (■), and percent removal (▲).	38
Figure 4: Pre-inoculation sulphur balance for laboratory-scale Biofilter 1, during the time period of Dec. 9, 1992 – Feb. 5, 1993 (after Coleman and Dombroski 1995). The curves shown represent the percentage of inlet H ₂ S out as H ₂ S (◆) and SO ₄ ²⁻ (●), and the percentage unaccounted for (▲) over time.	39
Figure 5: Transport processes occurring in a biofilter (after Hodge and Devinny 1995)	47
Figure 6: Schematic of biofilter subdivisions. Each subdivision is assumed to be ideally mixed (after Deshusses et al. 1995a).	48
Figure 7: Schematic of the biofilter model for one layer (after Deshusses et al. 1995a).	49
Figure 8: Schematic diagram of the H ₂ S biofilter used in the chemical oxidation experiments	66
Figure 9: Normalised concentration profiles obtained for the 1 m tracer study column, using various different packings.	78
Figure 10: Normalised concentration profiles for tracer studies obtained for the 42 cm H ₂ S biofilter, before and after sulphur deposition (1000 ppm H ₂ S for 1 week).	78
Figure 11: Concentration curves in closed vessels for various extents of backmixing, as predicted by the dispersion model (after Levenspiel 1972)	84
Figure 12: SEM micrograph of sulphur-coated peat	86
Figure 13: SEM micrograph of selected particles, believed to be mainly sulphur, on sulphur-coated peat	87

Figure 14: SEM micrograph of selected particles found on a webbed section of sulphur-coated foam _____	88
Figure 15: SEM micrograph, at higher magnification, of selected particles found on a webbed section of sulphur-coated foam _____	89
Figure 16: Chemical sulphur deposition over time in the H ₂ S biofilter, at 3000 (♦) and 1000 (■) ppm inlet H ₂ S concentration. _____	95
Figure 17: Sulphur recovery from the H ₂ S biofilter matrix after the completion of the chemical oxidation experiments. From inlet to outlet, the columns represent sections BF-1 (::), BF-2 (■■), BF-3(≡), and BF-4(♦♦). _____	96
Figure 18: Observed removal rate in a 1 m laboratory-scale H ₂ S biofilter, inoculated with <i>T. thiooxidans</i> . Data are shown are from experiments conducted at the ARC in 1995 and 1999 (Budwill and Coleman 1999; Coleman and Dombroski 1995). _____	102
Figure 19: Total biological activity versus inlet concentration in an H ₂ S biofilter. Values of <i>r</i> were calculated from ARC data (Budwill and Coleman 1999; Coleman and Dombroski 1995), and <i>r</i> _{chem} was calculated with kinetic constants derived from experimental data. _____	104
Figure 20: Modelling inhibition kinetics for H ₂ S self-inhibition in an H ₂ S biofilter. The curve shown is the model prediction obtained using a product inhibition model. Values of <i>r</i> and <i>r</i> _{chem} were calculated from ARC data (Budwill and Coleman 1999; Coleman and Dombroski 1995). _____	107
Figure 21: H ₂ S removal profiles in the gas phase, along the length of the biofilter, as predicted by the model. The curves are for inlet concentrations of 3000 (●), 2000 (■), 1000 (♦), and 500 (▲) ppm. All model parameters are as reported in Table 8. _____	110
Figure 22: H ₂ S removal profiles in the biofilm, as predicted by the biofilter model. The inlet H ₂ S concentration is 2000 ppm, and all other parameters are those found in Table 8. _____	111
Figure 23: Effect of Peclet number on gas phase H ₂ S concentration profiles along the length of the biofilter. Peclet numbers of 1000 (■), 100 (▲), 17 (♦), 5 (●), 2 (◇) and 1 (★) are shown. The inlet concentration is 2000 ppm, and the remaining parameters are those reported in Table 8. _____	113
Figure 24: Effect of the specific surface area (<i>A</i>) on the H ₂ S gas phase concentration profile along the biofilter. The curves are for surface areas of 1100 (♦), 950 (■), 800 (▲), 400 (●) and 100 (★) m ² /m ³ . The inlet concentration is 2000 ppm; all other parameters are those reported in Table 8. _____	114

- Figure 25: Effect of the biofilm thickness on the gas phase H_2S removal profiles in the biofilter. Biofilm thicknesses of 200 (◆), 175 (■), 100 (▲), 50 (●) and 30 (★) μm are shown. The inlet concentration is 2000 ppm, and the remaining parameters are those reported in Table 8. _____ 115
- Figure 26: Sensitivity of the model to the values of parameters A (◆), Pe (■), and δ (×). The reference value for the midpoint concentration is the H_2S concentration predicted at the midpoint of the biofilter ($z=0.5$), when the inlet concentration is 2000 ppm. The reference values for the parameters are those reported in Table 8. _____ 118
- Figure 27: Sulphur deposition over time at 1000 (■) and 3000 (◆) ppm inlet H_2S concentrations. The lines represent model predictions at 1000 (---) and 3000 (—) ppm. The points represent the data from the chemical oxidation experiments. The error bars are ± 20 percent, as in Figure 16. _____ 120
- Figure 28: Model predictions of the changes in the volume of sulphur formed (V_S) and porosity (E) over time, due to chemical oxidation at influent H_2S concentrations of 1000 (---) and 3000 (—) ppm. _____ 121
- Figure 29: Model predictions of the changes in the volume of sulphur formed (V_S) and porosity (E) over time, due to chemical and biological oxidation at influent H_2S concentrations of 1000 (---) and 3000 (—) ppm. _____ 122

Nomenclature

A	support material interfacial area per unit volume, m^2/m^3
ARC	Alberta Research Council
atm	atmosphere
C	concentration, kg/m^3
C^*	dimensionless concentration
C_h	gas phase H_2S concentration, kg/m^3
C_{in}	inlet H_2S concentration, kg/m^3
CSTR	continuously stirred tank reactor
d	days
D	dispersion coefficient, m^2/s
D_a	dispersion coefficient of H_2S in air, m^2/s
D_h	diffusion coefficient of H_2S in water, m^2/s
D_i	dispersion coefficient, m^2/s
E	porosity
EC	elimination capacity, $\text{kg}/\text{m}^3\text{s}$
EDX	energy dispersive x-ray analysis
E_{new}	new value of porosity, calculated at each time step
$E(t)$, E_i	exit age distribution of the tracer leaving the vessel
$E(\Theta)$	residence time distribution (RTD)
Expt.	experiment
ΔG^0	Gibbs free energy change of a reaction, kJ/mol
h	hours
H	characteristic length of a reactor, m
HAP	hazardous air pollutant
H_h	Henry's law coefficient for H_2S , $(\text{kg}/\text{m}^3)/(\text{kg}/\text{m}^3)$
H_o	Henry's law coefficient for O_2 , $(\text{kg}/\text{m}^3)/(\text{kg}/\text{m}^3)$
ID	inner diameter
k	reaction rate constant

K_i	inhibition constant, kg/m^3
k_s	chemical reaction rate constant, $(\text{kg/m}^3)^{0.38} \text{s}^{-1}$
K_s	biological half saturation constant, kg/m^3
min	minutes
n	number of tanks in series
N	number of biofilm subdivisions, x-direction
NMR	nuclear magnetic resonance
n_s	chemical reaction order
OD	outer diameter
ODE	ordinary differential equation
Pe	Peclet number
Pe_r	reactor Peclet number
P	product concentration, kg/m^3
PFR	plug flow reactor
P_x	partial pressure
Q	volumetric flow rate, m^3/s
r	H_2S removal rate in the gas phase, $\text{kg/m}^3\text{s}$
R	H_2S removal rate in the biofilm, $\text{kg/m}^3\text{s}$
r_{biol}	biological H_2S oxidation rate, $\text{kg/m}^3\text{s}$
$r_{\text{biol},\text{SO}_4}$	biological sulphur oxidation rate (to sulphate), $\text{kg/m}^3\text{s}$
r_{chem}	gas phase H_2S removal rate during chemical oxidation, $\text{kg/m}^3\text{s}$
r_{inhib}	biological activity rate under inhibition kinetics, $\text{kg/m}^3\text{s}$
r_k	rate constant for chemical sulphur formation
$r_{s,\text{chem}}$	chemical sulphur formation rate, $\text{kg/m}^3\text{s}$
RTD	residence time distribution
s	seconds
SEM	scanning electron microscopy
S_h	liquid phase H_2S concentration, kg/m^3
SRB	sulphate-reducing bacteria
t, t_i	time at which tracer measurements were taken at exit, min
Δt_i	time interval between tracer measurements, min

TIS	tanks-in-series
t_m	mean residence time, min
U	superficial gas velocity, m/s
UV	ultraviolet
V	biofilter volume, m ³
V_m	maximum H ₂ S biological uptake rate, kg/m ³ s
VOC	volatile organic compound
w	counter for axial sub-divisions in biofilter
W	number of z-direction divisions in biofilter
x	radial distance in biofilter, m
z	axial distance in biofilter, m
Z	height of biofilter, m
Δz	height of one layer in the biofilter (Z/W), m
[]	concentration
δ	biofilm thickness, m
Θ	dimensionless time, defined as t_i/t_m
ρ	density, kg/m ³
σ^2	variance

1.0 Introduction

1.1 The biofiltration process

Biological waste treatment is becoming increasingly popular for use as an air pollution control technology. Biofilters are multiphase biological reactors that are based on the aerobic treatment of biodegradable contaminants. Their operation involves forcing a polluted air stream to flow through a bed packed with an organic or inorganic support material, to which pollutant-degrading microorganisms are attached in a biofilm. Biofiltration is technically feasible and efficient for the treatment of hydrogen sulphide (H_2S) gas. Therefore, it has potential application to the oil and gas industry, where waste streams of H_2S -containing gases are routinely flared or vented to the atmosphere.

Extensive research has been conducted on many topics related to biofiltration, but biofiltration systems have only been subject to a minimum amount of modelling. The scale-up of laboratory-scale biofilters for application in industry is usually dictated by empirical knowledge. Mathematical models are useful in visualising pollutant removal in a biofilter, and can be used for design, scale-up, and optimisation of the biofiltration process.

1.2 Statement of research

1.2.1 Problem and hypothesis

The biofiltration of H_2S results in the formation of a solid product, sulphur, in the biofilter bed. This product is formed both by chemical and biological means. Over time, the build-up of sulphur leads to a decrease in the porosity of a biofilter, which leads to decreased biofilter performance. Eventually, process shutdowns are required for replacement of the packing material. This constitutes a significant obstacle to the use of

biofilters in the oilfield, where flare locations are often remote and not routinely serviced by operators. It is generally assumed in H₂S biofiltration that the appearance of a solid product is due to sub-optimal conditions of moisture and nutrients for the microbial culture in the biofilter bed. However, data from research conducted in non-inoculated biofilters suggests that solid sulphur is formed in H₂S biofilters even in the absence of a microbial presence. Evidence for abiotic H₂S oxidation also exists in the literature. The hypothesis proposed for this project is that a significant amount of the sulphur formed in an H₂S biofilter is actually formed abiotically. A model incorporating both chemical and biological oxidation terms to describe the formation of solid sulphur in an H₂S biofilter bed would be useful in better understanding the fundamental processes that lead to biofilter bed plugging.

1.2.2 Objectives

The objectives of this research were to study and quantify the rate of chemical H₂S oxidation in a biofilter, and to model the decrease in porosity and accumulation of solid sulphur caused by the combination of chemical and biological sulphur deposition processes in a biofilter.

These objectives were achieved in two stages. First, several key model parameters were determined through experimentation. A series of chemical oxidation experiments at high H₂S loading rates were performed in a laboratory-scale biofilter packed with coarse sphagnum peat. These experiments were complemented with tracer tests as a means of assessing channelling and dispersion in the filter bed. Second, a mathematical model was proposed for predicting H₂S removal and sulphur plugging in a biofilter.

1.2.3 Significance

Recent trends in biofilter application are shifting towards the treatment of increasingly higher concentrations of pollutants. This model provides a more comprehensive

understanding of the consequences of treating higher concentrations of H_2S in biofilters. No specific studies have addressed the problem of solid product formation in biofilters, or modelled the fundamental processes that lead to sulphur accumulation in H_2S biofilters. The knowledge gained from such a model is useful in understanding the relative importance of chemical and biological sulphur deposition processes in H_2S biofilters. This information is valuable in identifying measures for improving the H_2S biofiltration process.

1.3 Thesis outline

This thesis is divided into five sections. Immediately proceeding this brief introduction (Section 1), a literature review is presented in the following section (Section 2). The background information covers a review of flaring and biofiltration. There is considerable detail outlining H_2S biofilters and the chemical and biological reactions occurring in them. After a brief discussion of the kinetics of H_2S degradation, a historical background of biofilter modelling is presented.

Section 3 presents the details of the model development. This followed by a description, in Section 4, of the column set up, experimental procedures and analytical techniques used in this study. The results of the experiments are presented in Section 5, which also includes a discussion of how the experimental results contributed to the model. Final conclusions and recommendations are presented in Section 6. Several appendices contain details such as raw data and specific calculations performed during data analysis.

All symbols and abbreviations used in this thesis are presented in the nomenclature pages immediately preceding this section.

2.0 Theory and background

2.1 Hydrogen sulphide

Hydrogen sulphide (H_2S) is a naturally occurring gas found in a variety of geological formations. It is formed biogenically by the natural anaerobic decomposition of organic material. It can also be formed chemically. H_2S is encountered in a variety of industrial processes, including sewage and wastewater treatment, pulp and paper processing, the production and refining of petroleum, and the production and mining of metals and sulphur. Other names for H_2S include sour gas, acid gas, stink damp, and sulphuretted hydrogen. H_2S is the most reduced of the inorganic sulphur compounds.

H_2S gas is colourless, denser than air, and extremely toxic. It is extremely soluble in water ($\sim 0.1 \text{ M}$ at 25°C , P_x of 1 atm), with pK_1 around 7 and pK_2 around 13 (Suzuki 1999). At low concentrations, H_2S gas has a rotten egg smell, and will cause throat and eye irritations. It quickly deadens the sense of smell, and is lethal at high concentrations. H_2S toxicity levels are shown in Table 1. H_2S enters the body through the lungs, and causes the respiratory system of the body to shut down, which eventually causes the heart to stop (Beauchamp et al. 1984). The occupational exposure limit (for an 8-hour workday) for H_2S in the province of Alberta is 10 ppm (PITS 1997). The Alberta Ambient Air Quality Guidelines designate 10 ppb as the maximum allowable amount of H_2S in the air (PCF 2000a). This is generally the level at which individuals can detect the rotten egg smell of H_2S .

From 1976 to 1996, there were 31 occupational fatalities due to hydrogen sulphide exposure in Alberta (PITS 1997). Because it is denser than air, H_2S does not disperse rapidly in enclosed spaces. In the open, H_2S is generally diluted rapidly by ambient air, or lifted into the atmosphere by methane (CH_4), which is less dense than air. H_2S gas is also corrosive and has embrittling effects on pipelines as well as being harmful to crops and

vegetation. From 1980 to 1997, corrosion accounted for more than 73 percent of sour gas pipeline failures in Alberta (PCF 2000a).

Table 1: H₂S toxicity levels (after PCF 2000a; PITS 1997)

H ₂ S exposure (ppm)	Possible health effects
<1	Smell is detectable.
10	No known adverse health effects, though some people may experience tearing of the eyes, headaches, or loss of sleep after prolonged exposure. The effects are reversible, and are not considered serious for the general population.
20 – 200	Eye and respiratory tract irritation, loss of smell, headaches, nausea. Mandatory workplace evacuation levels vary by province.
100	Immediately dangerous to life and health (persons without adequate respiratory protection may be fatally injured or suffer immediate, irreversible or incapacitating health effects).
200	Continued exposure may cause lung tissue to swell and fill with fluid (pulmonary edema) as well as inflammation of the eye and eyelids (keratoconjunctivitis).
500 – 700	Affects the central nervous system, exposure for a few minutes results in loss of reasoning, loss of balance, unconsciousness and cessation of breathing.
700 – 1000	Immediate loss of consciousness, permanent brain damage and death occur if rescue is not immediate.

2.2 H₂S in the oilfield

2.2.1 Sour gas

Oil and gas reservoirs around the world contain small amounts of H₂S and other sulphur compounds, typically at concentrations of about 1 – 2 percent (PCF 2000a). This H₂S is formed anoxically by chemical reactions within sedimentary rocks. At temperatures above 140°C, the calcium sulphate (CaSO₄) in gypsum can react with organic materials to

produce H_2S and compounds such as calcium carbonate (CaCO_3) (PCF 2000a). This process results in large volumes of H_2S in deeply buried sedimentary rocks, such as those found in the foothills of the Canadian Rockies. Many petroleum-bearing rock formations contain iron, which bonds with the sulphur to neutralise the H_2S , thereby forming sweet gas reservoirs. Sweet gas consists mostly of CH_4 , with a low concentration of other short-chain hydrocarbons, such as ethane (C_2H_6), propane (C_3H_8), butane (C_4H_{10}), and pentane (C_5H_{12}). Sour gas contains H_2S in addition to the short chain hydrocarbons, and requires sweetening before it can be marketed.

There are various ways to define sour gas. A *pipeline* is considered sour if it carries gas containing more than 1 percent H_2S (PCF 2000a). Many people in the oil and gas industry adopt this definition to distinguish between sweet and sour gas. According to Alberta worker safety regulations, any *well or processing facility* handling gas with more than 10 ppm H_2S (0.001 percent) is defined as a sour gas worksite, and appropriate warning signs must be posted (PCF 2000a).

Approximately one third of the total natural gas production in Canada is sour, and of this, about 85 percent is produced in Alberta (PCF 2000a). The average H_2S content of Alberta sour gas is 5 – 10 percent, though the concentration can range from trace amounts to more than 90 percent (PCF 2000a). The sales of sour gas and byproducts represent a significant portion of the total upstream industry revenues from oil and gas production in Canada. In 1998, approximately \$3.2 billion worth of sour gas and \$40 million worth of elemental sulphur were produced and sold (PCF 2000a).

There are few conclusive studies on the effects of sour gas production on animal and human health, and further research is still required. A medical diagnostic review commissioned by the government-industry Acid Deposition Research Program (ADRP), conducted between 1983 and 1989 found no differences in most health outcomes between a community near extensive sour gas operations and one without (PCF 2000a). However, this same study also found that there were more respiratory symptoms reported in children aged 5 to 15 who lived downwind from gas processing plants. Studies

performed on beef and dairy herds near sour gas operations have produced mixed results. Some results actually showed improvement of herd health, while other indicators were negative (Scott 1998; Waldner et al. 1998).

2.2.2 Flaring

The production of crude oil results in the release of dissolved solution gases, which typically contain hydrocarbons, carbon dioxide (CO₂), and possibly H₂S. Depending on the circumstances, this solution gas can be either an asset or a liability. Factors that determine whether the gas is marketable include gas composition, volumes produced, access to pipelines and processing facilities, and the stage of oilfield development. Together, these factors determine the potential revenues versus production costs of solution gas. When it is not economic to conserve and market the solution gas, it is captured and directed to a flare system for combustion. Depending on the situation, flaring may involve burning all of the combustible gases associated with oil production, or combustion of only the hydrogen sulphide fraction, once the marketable hydrocarbons have been separated and collected. The majority of solution gas flaring in Canada occurs at oilfield battery sites in Alberta (Stroscher et al. 1998). Flaring is also used for emergency use in the case of operational upsets. There are five types of flaring that occur in the petroleum industry. The breakdown is shown in Figure 1.

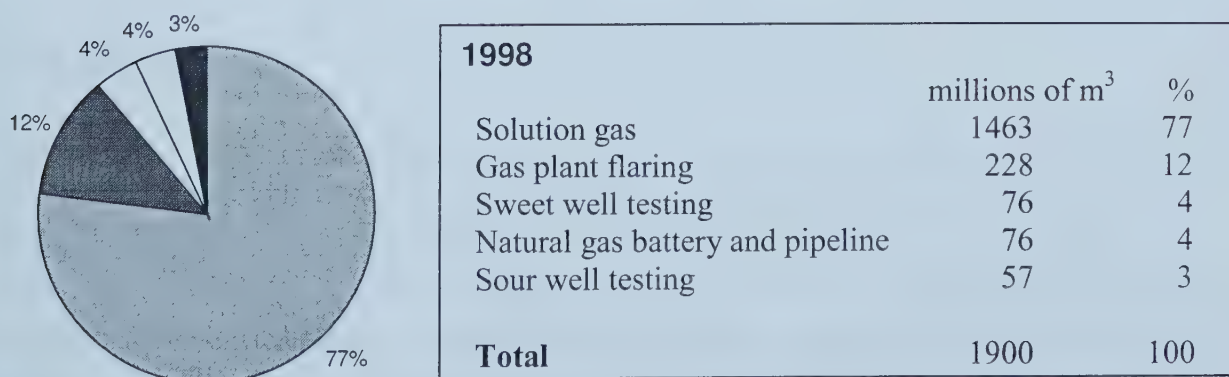


Figure 1: Estimated flaring from upstream oil and gas sources in Alberta (after PCF 2000b)

The products of the combustion in the flare stacks are emitted directly to the atmosphere. Flares are often visible from major highways, and cause a great deal of public concern. Some flares have been identified as sources of odours, bright lights, noise and smoke, and have been the cause of air quality related health concerns by members of the public. The Alberta Energy and Utilities Board (EUB), is the regulating agency for waste solution gas flaring in Alberta. A recent policy review identified three distinct groups of concerns with respect to solution gas flaring: local health and environmental impacts, waste of non-renewable resources (resource conservation), and potential global environmental impacts (EUB 1997). Specific concerns include climate change due to the release of greenhouse gases, including carbon dioxide and methane, the possibility of acid rain and the impact of flaring on human and animal health.

Approximately 94 percent of the total solution gas production in Alberta is captured and marketed, while the remainder is treated as a waste product and disposed of by flaring or venting (Johnson et al. 2001). In 1999, a total of 4499 oil and bitumen batteries reported (solution gas) flaring and/or venting with a combined gas volume totalling 1.42 billion m³ (Johnson et al. 2001). Approximately 0.938 billion m³ of this gas were flared, at 3715 different battery sites (Johnson et al. 2001). The measurement of both the flow and volume of waste gases is quite infrequent; it is difficult to obtain accurate estimates of the total volume of flaring in Alberta. EUB data from 1998 indicate that approximately 1000 solution gas flares in Alberta are burning gas containing H₂S (PCF 2000b).

2.2.3 Flaring issues

The majority of the flares in Alberta operate as diffusion flames, which is a combustion process in which there is no premixing of the fuel and the air. Diffusion flames are difficult to operate with exactly the right proportions of oxygen and fuel, even under ideal conditions. This often leads to some level of incomplete combustion, as evidenced by black smoke coming off of the flare stacks (PCF 2000b). Currently, the efficiencies of flares are unknown. Estimates range from 20 to 99 percent, leading to large uncertainties in the effects of flares on the environment (Flakstad 2000; Johnson 1999).

It is estimated that 75 – 80 tonnes of sulphur are released daily from solution gas flaring in Alberta (Stroscher 1996). At 100 percent combustion efficiency, this would be released into the environment as sulphur dioxide (SO_2). However, as the efficiency of combustion decreases, other sulphur compounds are emitted, including H_2S , carbonyl sulphide, carbon disulphide and mercaptans (Stroscher 1996). Other compounds that have been identified in inefficient flare gas emissions include carbon monoxide (CO), polycyclic aromatic hydrocarbons, volatile organic compounds (VOCs), oxides, unburned hydrocarbons and particulate matter (Johnson 1999; PCF 2000b; Stroscher 1996). Many of these incomplete combustion products pose significant health threats to living organisms in their vicinity. The 1995 national emissions inventory found that 19.3 percent of VOC emissions and 14.6 percent of sulphur dioxide emissions in Canada came from the upstream oil and gas industry (PCF 2000b).

The characterisation of emissions from flaring in Alberta is a topic that is currently under extensive research, as very little research has been conducted in this area in the past (Flakstad 2000). The composition of flaring emissions is influenced by such factors as flare design, operating conditions, and composition of the waste gases. Gas flow rates to wells may fluctuate widely, depending on the operation of the wells feeding them as well as the downstream operation of facilities such as gas plants that may necessitate shutdown (Johnson et al. 2001). Thus, it is difficult to identify both the nature and volume of the emissions from solution gas flares. This is further complicated by the fact that most flares draw from more than one well. The ability of a flare to efficiently burn hydrocarbon products is a complex issue, and methods for the detailed examinations of flares are rather limited.

Historically, the decision to flare waste gases has been a purely economic one. However, this is changing as regulations for air emissions become stricter. In the United States, SO_2 is a regulated pollutant, and as such the flaring of H_2S may no longer be simply an economic decision: a sulphur recovery plant may be necessary to meet air quality standards (Sublette and Sylvester 1987a). Increasing environmental awareness is leading to interest in ways to reduce the volume of gases flared in the oilfield each year.

2.2.4 Alternatives to flaring

Since research on flaring efficiency was released in 1996, an impetus to reduce flaring has resulted in the creation of voluntary initiatives, new research, regulatory guidelines, and technological developments (PCF 2000b). The Clean Air Strategic Alliance (CASA) brings together government, industry, environmental and health organisations to collaborate on air quality issues in Alberta. As a result of the CASA recommendations made to the EUB in 1998, new flaring guidelines were introduced in 1999. The initial goal of these guidelines is a 25 percent reduction in solution gas flare volumes by the end of 2001, compared with 1996 volumes (PCF 2000b). The guidelines also require that companies work to improve the efficiency of all flaring, and consult with area residents, especially those living within 500 metres of solution gas flare installations (PCF 2000b).

Conventional processes for the removal of contaminants from air streams include physicochemical methods such as alkaline, oxidative and catalytic scrubbing, as well as adsorption onto activated carbon, thermal incineration, and biotechnological methods including biofiltration, bioscrubbing, and biotrickling filters. Chemical methods such as incineration are expensive, and require significant amounts of fuel and water as well as extensive equipment. Adsorption onto activated carbon is also costly, and the spent carbon is a hazardous waste that requires appropriate disposal. Although the term “filtration” is actually appropriate for physical separation, the term “biofiltration” implies the biochemical destruction of pollutants through the activities of microorganisms immobilised on solids (Baltzis et al. 1997). Since toxicants are metabolised, rather than being retained in the biofilter matrix, biofiltration is a destructive treatment technology that does not involve cross-media transfer of contaminants (Kennes and Thalasso 1998). The spent matrix material is generally quite innocuous, and can be disposed of by landfilling or landfarming. As regulations to restrict air emissions become increasingly stringent, biological air pollution control technologies are becoming more cost effective (Devinny et al. 1999). A comprehensive review article comparing different treatment methods for waste gases that are contaminated with odorous sulphur compounds was published by Smet et al. (1998).

Studies done at the Alberta Research Council (ARC) in Vegreville have proposed biofiltration as a safe, low-cost alternative to solution gas flaring (Budwill and Coleman 1999). In their studies, influent H₂S concentrations of up to 2500 ppm were removed completely using a peat biofilter inoculated with *Thiobacillus thiooxidans*. Based on these results, the suggestion was made that biofilters could be used to effectively remove the H₂S from waste gas streams, instead of sending them to the flare stack. Extrapolation of the results from laboratory-scale biofilter experiments showed that this technology has the potential to be used at small sour gas batteries, producing less than 1 tonne of H₂S per day (Budwill and Coleman 1999).

The application of sulphur oxidising bacteria to remediate products from the oilfield is not new. A research group at the University of Tulsa, Oklahoma, has proposed an anaerobic microbial desulphurisation process, using *Thiobacillus denitrificans* to remove H₂S from natural gas (Sublette and Sylvester 1987a, b). This process has also been suggested to treat sour water (Jenneman et al. 1999; Sublette 1989). There is also an aerobic bacterial gas desulphurisation process, the Shell-Paques process, which has been in use commercially since 1993 (New Paradigm 2001). This process uses thiobacilli to oxidise H₂S to elemental sulphur.

2.3 Biofiltration

2.3.1 Biofilter basics

Biofiltration is a technology based upon the aerobic metabolism of contaminants by microorganisms immobilised on a stationary support material. The basic premise behind the operation of a biofilter is that the waste gas stream is first humidified and then forced to flow through a bed packed with an organic carrier material such as peat moss, or compost. Inorganic support materials, such as synthetic beads can also be used. Microorganisms are attached to the surface of this support material, in a conglomeration known as a biofilm. The contaminant partitions into the liquid film and is biodegraded by

the microorganisms residing in the biofilm. The degradation is an enzyme-catalysed process. Biofilters require minimal inputs of energy and raw materials, have low capital and operating costs, and produce few or no waste products. More importantly, biofiltration is widely accepted by the public because it is viewed as a “natural process.” The biofiltration of volatile organic compounds produces mostly innocuous end products such as CO₂, H₂O and biomass (Devinny et al. 1999; van Groenestijn and Hesselink 1993). Several excellent review articles on biofiltration exist in the literature (Kennes and Thalasso 1998; McNevin and Barford 2000; van Groenestijn and Hesselink 1993; Wani et al. 1997).

To be successfully treated in a biofilter, contaminants must be biodegradable as well as non-toxic to the microorganisms effecting the removal. Compounds that are most susceptible to removal by biofiltration include low molecular weight and highly soluble organic compounds with simple bond structures (Devinny et al. 1999). Organic compounds such as alcohols, aldehydes, ketones, and simple aromatics demonstrate excellent biodegradability. Phenols, chlorinated hydrocarbons, polyaromatic hydrocarbons, and highly halogenated hydrocarbons show moderate to slow degradation. Inorganic compounds such as ammonia and hydrogen sulphide are also degraded well in biofilters. In addition to the contaminant, which generally serves as an energy and/or carbon source for the microorganisms in the biofilter, moisture, air (oxygen), and nutrients must also be present in sufficient amounts for degradation to occur.

There are two basic types of biofilters: classical (gas phase) biofilters, and biotrickling filters (trickling biofilters). Gas phase biofilters use a porous medium, usually of an organic material, such as peat moss, bark, or compost. They do not involve a liquid stream circulating through the bed of solids. Rather, moisture is supplied via humidification of the inlet air stream. Biotrickling filters are usually packed with ceramic or plastic media, and involve the recirculation of a nutrient-rich liquid stream within the reactor. Biotrickling filters are common in wastewater treatment, and have hydraulic loading rates starting at approximately 1.2 m³/m²d (Metcalf & Eddy 1991). The biofilters used in these experiments and at the ARC are intermediates between gas phase and

trickling biofilters. There is a small liquid stream (approximately $0.05 \text{ m}^3/\text{m}^2\text{d}$) trickling through the biofilter bed, but this stream is not recirculated.

Microbial reactions have been used to treat waste gases since the 1920s (Devinny et al. 1999). Since then, the use of biological processes to treat gas phase contaminants has become increasingly widespread, especially in Europe and Japan (Kennes and Thalasso 1998; Ottengraf 1986). Some commercial biofilters are now being operated in the United States as well, with the estimated biofiltration market for 2000 reaching over \$100 million US (Devinny et al. 1999). Two major market applications are odour control and the biofiltration of VOCs and hazardous air pollutants (HAPs) in the wood products and pulp and paper industries. Traditionally, biofilters have been used in applications with moderate to high flow waste streams with low levels of contaminants (Devinny et al. 1999; Kennes and Thalasso 1998; Wani et al. 1997), but this is continuing to change as biofiltration research develops.

2.3.2 H₂S biofilters

Hydrogen sulphide has been treated in biofilters, biotrickling filters, and bioreactors. Originally, biofilters were used to treat only low levels of H₂S, as odour abatement strategies (McNevin and Barford 2000). Increasingly, new research has shown that H₂S can be successfully removed at relatively high concentrations (>2000 ppm) (Allen and Yang 1991; Coleman and Budwill 1999).

Microorganisms capable of H₂S oxidation, as listed by Cho et al. (1991b), include *Beggiatoa*, *Xanthomonas*, *Thiobacillus*, *Hyphomicrobium*, *Rhodobacter*, *Chromatium*, *Ectothirhodospira*, *Thiothrix*, and cyanobacteria. Most authors use the indigenous microorganisms within the matrix material to effect the desired degradation (Allen and Yang 1991; LeBeau and Milligan 1994). Studies done at the ARC (Coleman and Dombroski 1995) were among the first to investigate the concept of deliberately inoculating biofilters with bacteria selected to oxidise specific contaminants. Many of the

H₂S biofilters currently under investigation have been deliberately inoculated with *Thiobacillus* strains (Arvin et al. 1993; Budwill and Coleman 1999).

A summary of key H₂S biofilter papers published in the literature is presented in Table 2.

Table 2: Details and parameters of selected H₂S biofilters discussed in the literature (after Smet et al. 1998)

Authors	Matrix material	Inoculation	Max. removal capacity (g H ₂ S/ m ³ h)
Budwill and Coleman 1999	Peat	<i>T. thiooxidans</i>	826
Kowal et al., cited in Smet et al. 1998	Dry, activated sludge	No	500
Yang and Allen 1994a	Compost	No	130
Degorce-Dumas et al. 1997	Dry wastewater sludge (BSE); peat	No	129
Wani et al. 1998a, b, c, d; 1999	Compost, hog fuel, perlite	No	81
Bonnin et al., cited in Smet et al. 1998	Mearl ^a	<i>Thiobacillus</i> sp.	70
Cho et al. 1991a	Fibrous peat	<i>Thiobacillus</i> HA43	50
Zhang et al., cited in Smet et al. 1998	Peat	Domestic sewage sludge	30.4
Hirai et al. 1990	Fibrous peat	Domestic sewage sludge	25.4
Cho et al., cited in Smet et al. 1998	Peat	<i>T. thioparus</i> DW44	24.5
Zhang et al., cited in Smet et al. 1998	Peat	<i>Hyphomicrobium</i> I55	15
LeBeau and Milligan 1994	Topsoil, peat, and cypress or wood mulch	No	0.00282 g/kg h (no density data given)

^a Pure carbonate material, such as oyster shells and coral

T. thiooxidans is classified as part of the group generally known as “colourless sulphur bacteria,” a term originally used by Winogradsky, which includes prokaryotes that can grow under aerobic conditions in the dark (Kuenen 1989). *Thiobacillus* cells are small, gram-negative, and rod-shaped, with no known resting stages (Kuenen 1989). They obtain energy for growth from the oxidation of inorganic reduced sulphur compounds, such as H₂S. The full name for this physiological type of bacterium is “obligate chemolithoautotroph.” These organisms are obligate autotrophs, meaning that they have a strict requirement to fix CO₂ as a carbon source. This is beneficial when designing an H₂S biofilter, as it eliminates the need to supply an external carbon or energy source (Coleman and Dombroski 1995). While *T. thiooxidans* can oxidise sulphur compounds over a wide range of pH (1 – 9), an acidic pH is required for growth (Suzuki 1965). The internal pH of a microbial cell is usually around 7 (Prescott et al. 1993), but the bulk phase pH in an H₂S biofilter is generally around 2 – 3, because *T. thiooxidans* are acidophilic. *T. thiooxidans* are not inhibited until the pH falls below 1 (Devinny et al. 1999).

Studies done at the ARC have shown that biofiltration of H₂S using *T. thiooxidans* as an inoculum is highly effective (Budwill and Coleman 1999; Coleman 1993, 1994; Coleman and Dombroski 1995; Dombroski et al. 1995). Up to 2500 ppm influent H₂S were successfully removed (>99.9 percent) in this work, using coarse sphagnum peat as a solid support (Budwill and Coleman 1999). The studies began in 1992, and have included laboratory-scale, pilot-scale and full-scale demonstration biofilters. The high sulphur loading rates used at the ARC were unprecedented in the literature when they were first published. The maximum removal efficiency is still much higher than what has been reported in the literature. High loading rates resulted in sulphur accumulation on the peat; ongoing washing with water was found to prolong the life of the biofilter matrix (Budwill and Coleman 1999; Dombroski et al. 1995). Because *T. thiooxidans* is autotrophic, studies were done to examine whether H₂S oxidation could be enhanced by increased concentrations of CO₂. The data from these experiments proved inconclusive, due to the already high efficiency of the biofilters at atmospheric CO₂ contents (Budwill and

Coleman 1999). Further information about the ARC biofilter experiments, including the data that led to the creation of this thesis project, can be found in Section 2.6.

Allen and Yang (1991; 1992) operated laboratory-scale biofilters packed with compost to remove H_2S concentrations of up to 2660 ppm, with removal rates of 99 – 100 percent. The indigenous microbial population within the compost was used to obtain removal, and the results showed a 2-week acclimation period during which sulphur-oxidising organisms were presumably enriched in the biofilter. This acclimation period could be eliminated by pre-exposure of the compost to H_2S , or by the addition of a small amount of sewage sludge to increase the initial resident microbial population (Allen and Yang 1992). The authors found a significant relationship between H_2S oxidation and the gas loading rate. High gas flow rates result in uneven gas distributions and high pressure drops, which reduce the efficiency of the system. They introduced the concept of the maximum H_2S loading capacity, which differs for every matrix material, and is defined as the maximum amount of H_2S that can be introduced to a system without inhibiting its microbial activity. This capacity depends on the microbial community and sulphur oxidising capacity of the bacteria in the matrix. Overloading was indicated by the appearance of “a white coloured substance on the compost,” a sudden decrease in removal efficiency, and higher concentrations of elemental sulphur within the compost (Allen and Yang 1991). The whitish deposit was identified as being either elemental sulphur or sulphate salts (Allen and Yang 1992). Another problem encountered in this work was the acidification of the biofilter system, which led to corrosion, reduced efficiency, and system upset.

A number of studies by Wani et al. (1998a, b, c, d) describe the transient and steady state behaviour of biofilters treating reduced sulphur pulping odours (including H_2S) and VOCs. The different media used include mixtures of compost and perlite (4:1), hog fuel and perlite (4:1) and compost, hog fuel and perlite (2:2:1). Hog fuel is a mixture of raw bark, wood waste, and other extraneous materials that are pulverised and used as a fuel for power boilers in a pulp mill. The authors investigated the effects of biofilter starvation, caused by either no-contaminant-loading phases, where only humidified air

was passing through the biofilters, or idle phases, where no air was passing through the biofilter. Extended periods of starvation (up to 3 months) resulted in longer re-acclimation phases, as did the idle phase as compared with the no-contaminant-loading phase. This last effect was due to the drying out of the matrix when no air was passing through the filter. Studies of the transient behaviour of biofilters are important due to the fluctuating nature of industrial biofilter loading (Wani et al. 1998a). In field operation, a biofilter would need to respond effectively to sudden changes in operating conditions, shutdowns, and contaminant shock loading. The biofilters in the Wani et al. (1998a) study responded to H_2S concentration spikes by recovering their initial rates within 2 – 8 h. After a starvation time of 3 months, full capacity was reached within 120 – 140 h (Wani et al. 1998a). The sorption capacity of the medium was found to play an important role in contaminant removal during transient operation. This is a similar finding to that of Deshusses et al. (1995a). At high concentrations, H_2S is thought to self-inhibit its biodegradation (Wani et al. 1998a), but the limit for microbial growth is not clear. Wani et al. (1998d) observed first and fractional order removal kinetics, at concentrations below 450 ppm H_2S .

2.4 Chemistry of H_2S biofilters

H_2S undergoes both chemical and biological oxidation in a biofilter. The main discrepancy in the literature about H_2S oxidation, both chemical and biological, is in the labelling of the chemical species ‘sulphide,’ which has an oxidation state of -2. Hydrogen sulphide is an acid, and is present in various dissociated forms depending on the pH of its environment. ‘Sulphide’ is interchangeably designated in the literature as HS^- , S^{2-} and H_2S . Wherever possible, in this thesis, the true chemical species has been shown, but some authors designate reduced sulphur species only as ‘sulphide.’

In the metabolism of inorganic sulphur compounds, the extreme chemical reactivity of these compounds as well as their metabolic intermediates and products make the elucidation of the metabolic pathways extremely difficult (Suzuki 1999). It is also

difficult to separate chemical and biological oxidation, particularly because the reactivity of inorganic reduced sulphur compounds results in spontaneous reactions with oxygen (Kuenen 1975). Both chemical and biological sulphide reactions compete for sulphur and reactive sulphur intermediates in biotic systems, making measurement of in situ rates difficult (McNevin et al. 1999).

In order to understand the reactions in the following sections, it is important to have a general understanding of the various forms of inorganic sulphur. The oxidation states of various sulphur compounds are shown in Table 3.

Table 3: Oxidation states of inorganic sulphur compounds (after Suzuki 1999)

-2	0	+2	+4	+6
H ₂ S	S	SO	SO ₂	SO ₃
HS ⁻	S ₈			
S ²⁻	S ⁰			
Hydrogen sulphide	Elemental sulphur	Sulphur monoxide	Sulphur dioxide	Sulphur trioxide
		H ₂ SO ₂	H ₂ SO ₃	H ₂ SO ₄
		Sulphoxylic acid	Sulphurous acid	Sulphuric acid
			SO ₃ ²⁻	SO ₄ ²⁻
			Sulphite	Sulphate
	S-----		-----SO ₃ ²⁻	
		Thiosulphate		
H ₂ S-----				-----SO ₃
		Thiosulphuric acid		
	S-----		-----SO ₃ ²⁻	
		Tetrathionate		
	S-----			-----SO ₃
H ₂ S-----S _n				
Polysulphane				
S ²⁻ -----S _n				
Polysulphide				

2.4.1 Biological oxidation

Reduced inorganic sulphur compounds can be oxidised by aerobic microorganisms to either sulphur or sulphate, depending on enzymatic conditions and oxygen content (Jensen and Webb 1995). Under oxygen-limited conditions, sulphur-oxidising bacteria oxidise H_2S to elemental sulphur (Kuenen 1975). If sufficient oxygen is present, sulphate is preferentially produced because then more energy is gained for bacterial growth than from the formation of sulphur (Janssen et al. 1995). The conversion of H_2S to sulphate in the presence of air and water is a two-step process, involving the formation of a solid sulphur intermediate before complete oxidation to sulphate. The rate-limiting step for biological H_2S degradation seems to be the biological utilisation of sulphur that results in the formation of sulphate. Favourable conditions for solid sulphur formation include either low $[\text{O}_2]$ and low $[\text{S}^{2-}]$, or high $[\text{O}_2]$ and high $[\text{S}^{2-}]$. At high concentrations of sulphide (designated interchangeably as H_2S , S^{2-} or HS^-), the biological oxidation of H_2S is thought to be zero-order (Yang and Allen 1994b).

In a recent review article, Suzuki (1999) showed that the microbial oxidation of inorganic sulphur compounds is governed by both chemical and enzymatic reactions. The enzymatic oxidation proceeds mainly via the reaction pathway shown in Figure 2.

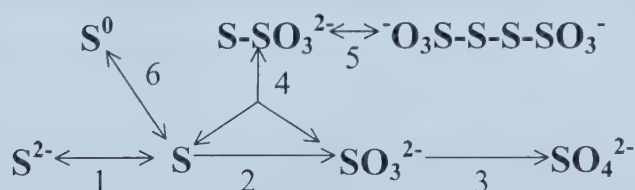


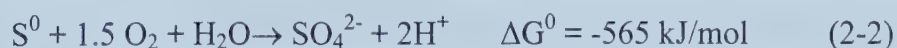
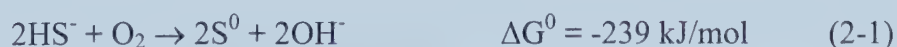
Figure 2: Enzymatic oxidation pathway of inorganic sulphur compounds (after Suzuki 1999)

Reaction 1 is the fastest of the reactions shown in Figure 2, and is shown as reversible because of some anaerobic reactions that can occur with *Thiobacillus ferrooxidans* cells (Suzuki et al. 1994). The “S” shown should be considered as “reactive sulphur” (Suzuki

et al. 1994), that is converted to elemental sulphur (S₈) when accumulated. The stoichiometric presence of a solid sulphur intermediate has been experimentally verified using oxidation studies in which further sulphur oxidation was inhibited by N-ethylmaleimide (Chan and Suzuki 1993). When reaction 2 is not fast enough, sulphur accumulates in the system (Suzuki et al. 1994). When reaction 3 is slower than reaction 2, sulphite accumulates and the reaction of sulphur with sulphite (reaction 4) yields thiosulphate as the oxidation product (Suzuki et al. 1994). Cheng et al. (1999) proposed that solid sulphur is simultaneously oxidised to thiosulphate and sulphite, by the action of *T. thiooxidans*.

T. thiooxidans can oxidise sulphur in various oxidation states, including elemental sulphur and sulphide (Suzuki et al. 1993). At an acidic pH, sulphur oxidation is inhibited by the accumulation of sulphite (Suzuki et al. 1994). This may explain the accumulation of solid sulphur in H₂S biofilters (which have an acidic pH) at high loading rates. Gadre (1989) suggests that elemental sulphur is deposited at extremely acidic conditions (below pH 2), due to the incomplete oxidation of sulphide. For experiments at pH 2.3, Suzuki et al. (1993) observed rapid microbial oxidation of H₂S with three distinct stages of oxygen consumption. The initial phase is the rapid oxidation: $\text{H}_2\text{S} + \frac{1}{2} \text{O}_2 \rightarrow \text{S} + \text{H}_2\text{O}$ (reaction 1). The second phase is the slightly slower oxidation stage: $\text{S} + \text{O}_2 + \text{H}_2\text{O} \rightarrow \text{H}_2\text{SO}_3$ (reaction 2), and the third phase is the slowest oxidation stage: $\text{H}_2\text{SO}_3 + \frac{1}{2} \text{O}_2 \rightarrow \text{H}_2\text{SO}_4$ (reaction 3). At high concentrations, sulphate also acts as an inhibitor to sulphur oxidation by microbial cultures (Yang and Allen 1994a).

Based on experiments in aerobic bioreactor systems, Buisman et al. (1990a) proposed the following two-stage biological sulphide oxidation reaction, at pH 8.0 and 25°C:



The sulphur intermediate (S⁰), is thought to be a membrane-bound polymeric sulphur compound (Buisman et al. 1990a). Reaction 2-1 occurs much faster than reaction 2-2

(Buisman et al. 1990a). At oxygen concentrations below 0.1 mg/L, that is, under oxygen-limiting conditions, sulphur is the major end product of sulphur oxidation, and reaction 2-2 does not occur (Janssen et al. 1995). Sulphate is the major end product formed under conditions of sulphide (HS^-) limitation, or when the system is underloaded (Janssen et al. 1995).

The biological sulphide oxidation rate, at pH 8.0 and 25°C, is 75 times faster than the chemical oxidation rate, for sulphide concentrations around 10 mg/L (Buisman et al. 1990b). At higher concentrations (i.e. 100 mg/L), the biological oxidation rate is only 7 times faster than the chemical one (Buisman et al. 1990b).

In another experiment, Buisman et al. (1990a) showed that practically no sulphate is formed in a cell suspension if the sulphide concentration exceeds 5 mg/L, and oxygen concentration is less than 9 mg/L. Under these conditions, with pH 8.0, the main reaction product observed was sulphur. Less than 10 percent sulphate production was observed at low oxygen concentrations, even when the sulphide concentration in the reactor exceeded 10 mg/L. For high sulphide concentrations (>20 mg/L), increasing the oxygen concentration did nothing to increase sulphate production, but it did increase the sulphide oxidation rate. However, for sulphide concentrations less than 20 mg/L, the sulphate production rate increased sharply with increasing oxygen concentration. The authors concluded that sulphate production can be suppressed by controlling the oxygen concentration in aqueous solutions. At high sulphide concentrations (>20 mg/L), the oxygen concentration should be increased in order to increase the sulphide oxidation rate. At low sulphide concentrations (<20 mg/L), the oxygen concentration should be kept low in order to suppress the oxidation of sulphur to sulphate (Buisman et al. 1990a; Nelson 1989).

McNevin et al. (1999) studied the adsorption and biological degradation of sulphide on peat. Based on their results, they concluded that aerobic biofilters remove sulphide by a two-stage process, involving an initial chemical oxidation to elemental sulphur followed by a slower biological oxidation to sulphate. The elemental sulphur formed by chemical

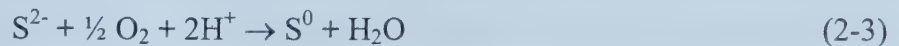
oxidation is incorporated into the membrane of sulphur-oxidising microorganisms to be further oxidised to sulphate. They suggest that the use of peat in their experiments provided a catalytic surface for chemical sulphide oxidation, and that the high surface area of peat provides excellent mass transfer qualities for oxygen dissolution. McNevin et al. (1999) found different results than Buisman et al. (1990a), who found that biological oxidation was faster than chemical oxidation. This is likely due to differing environmental conditions used in these studies. The Buisman et al. (1990a) study was performed in a stirred, liquid-phase reactor at pH 8.0 with oxygen limitation while the McNevin et al. (1999) study was performed in a biotrickling filter packed with peat, at pH 6.0 and excess oxygen.

To summarise, H_2S is biologically oxidised primarily to sulphur and sulphate, with the form of the final product depending on the concentrations of sulphide and oxygen in the system. Cheng et al. (1999) proposed that the different oxidation products are indicative of different oxidation mechanisms. They postulated that two pathways of sulphur compound oxidation exist: one that is related to bacterial growth, and one that is used to provide energy and results in sulphate production. The differences in free energy obtained from the two oxidation reactions can be seen in equations 2-1 and 2-2. At high concentrations of sulphur, bacterial growth (2-1) but not sulphate production (2-2) is inhibited (Cheng et al. 1999).

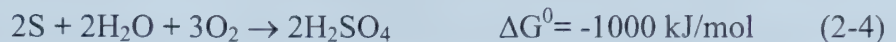
2.4.2 Chemical oxidation

In the presence of air and water, H_2S undergoes a spontaneous chemical oxidation reaction. The extent of the oxidation reaction depends on the ratio of molecular oxygen to sulphide concentrations (Kuhn et al. 1983). Many different reaction products have been reported in the literature. The major products of the chemical oxidation of H_2S appear to be solid sulphur (Chen and Morris 1972; McNevin et al. 1999), thiosulphate (Chen and Morris 1972; Degorce-Dumas et al. 1997; Janssen et al. 1995) or sulphate (Wainwright 1984). The form of the final product is dependent on such factors as pH, oxygen concentration, and H_2S loading rates.

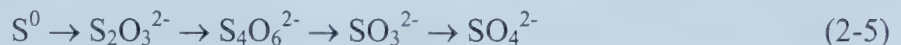
Under conditions of excess dissolved oxygen, chemical oxidation occurs according to the equation (McNevin et al. 1999; Wainwright 1984):



Solid sulphur can be chemically oxidised to sulphate according to the following equation (Wainwright 1984):



The pathway is thought to involve various intermediates (Wainwright 1984), with intermediates that resemble those of microbial oxidation:



While the oxidation shown in equation 2-5 is rapid in aerobic soils, microbial sulphur oxidation is thought to dominate under conditions where water and oxygen are in sufficient supply (Wainwright 1984). Thiobacilli are also capable of oxidising most of the intermediate compounds shown above, such as thiosulphate and tetrathionate (Kuenen 1975), so it is difficult to distinguish the source of sulphur oxidation in an inoculated biofilter.

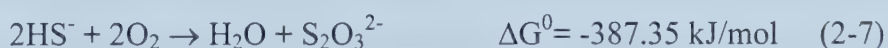
Using a biofilter packed with dry wastewater sludge, Degorce-Dumas et al. (1997) observed an initial efficiency of 65 percent in their sterilised biofilter. This was attributed to various physicochemical phenomena, including adsorption, absorption, and chemical oxidation of the influent H_2S . Chemical oxidation in the biofilter was found to produce mainly thiosulphate, plus some sulphate. In the biotic biofilter, the final sulphur balance under influent H_2S concentrations ranging from 2410 – 3260 mg/m^3 was (Degorce-Dumas et al. 1997):

$$100\% \text{ S-}\text{H}_2\text{S (removed)} = (60 \pm 10)\% \text{ S-S}^0 + (40 \pm 10)\% \text{ S-SO}_4^{2-} \quad (2-6)$$

This may correspond with the findings of Wainwright (1984) regarding the oxidation of sulphide in aerobic soils, discussed previously. In aerobic and abiotic conditions, the chemical oxidation of S^{2-} to S^0 was considered to be rapid, whereas the oxidation of S^0 to SO_4^{2-} was slow. Lindemann et al. (1991) found no $S^0 \rightarrow SO_4^{2-}$ oxidation, over the course of 40 d, in control experiments that were not inoculated with thiobacilli.

Janssen et al. (1995) investigated both biological and chemical sulphide oxidation in a fed batch reactor, using a mixed culture of thiobacilli. They observed a distinctly two-stage process, during which only sulphur and thiosulphate were formed initially, followed by sulphate formation accompanied by an increase in oxygen demand. The formation of sulphur and sulphate as end products from the oxidation could be controlled both instantaneously and reversibly by the amount of oxygen supplied. Under highly oxygen-limited conditions, with an oxygen/sulphide consumption ratio below $0.7 \text{ mol h}^{-1}/\text{mol h}^{-1}$, thiosulphate and sulphur were abundantly formed. Sulphate was the primary oxidation product when the oxygen/sulphide consumption ratio was greater than 1. The authors concluded that chemical oxidation is faster than biological oxidation under highly oxygen limited conditions. The chemical sulphide oxidation rate was found to be first order, with a reaction rate constant of 0.87 h^{-1} .

The reaction pathway for chemical sulphide oxidation is thought to proceed as follows (Degorce-Dumas et al. 1997; Janssen et al. 1995):



Both chemical and biological oxidation reactions were found to occur in the bioreactor. Approximately 60 percent of the added sulphur was oxidised to thiosulphate, and the remaining 40 percent to colloidal sulphur (Janssen et al. 1995). However, Suzuki et al. (1993) state that thiosulphate is a known by-product of biological sulphur oxidation, especially at neutral pH; it occurs both as an intermediate product in the $H_2S \rightarrow H_2SO_4$ reaction, as well as by a secondary reaction of $S + SO_3^{2-} \rightarrow S_2O_3^{2-}$.

Chen and Morris (1972) found that the aqueous oxidation of sulphide by O_2 happens very slowly in acid solutions, in which H_2S is the predominant sulphide species. A high sulphide-to-oxygen ratio results in the precipitation of sulphur whereas a low ratio results in direct oxidation to thiosulphate. This is in agreement with what other authors have suggested. The reaction products of sulphide oxidation are pH dependent (Chen and Morris 1972; Kuhn et al. 1983). For example, regardless of the sulphide-to-oxygen ratio, thiosulphate is the principal product observed in laboratory solutions at $pH > 8.5$ (Chen and Morris 1972). The other authors cited previously who also observed primarily thiosulphate production (Janssen et al. 1995) were generally working at $pH\ 8 - 8.5$, which may explain their results. Sulphide has a higher holding capacity for sulphur at a higher pH, and above $pH\ 7.5$ the precipitation of sulphur becomes more and more difficult (Chen and Morris 1972). This may explain the lack of sulphur precipitation observed in buffered H_2S biofilter experiments. The oxidation of SO_3^{2-} to SO_4^{2-} is thought to be inhibited by sulphide solution, and even after several weeks of experimentation, complete oxidation of sulphide to SO_4^{2-} (in abiotic systems) is not often achieved (Chen and Morris 1972; Lindemann et al. 1991).

O'Brien and Birkner (1977) did a study of the kinetics of oxygenation of reduced sulphur species in aqueous solution. They found that the chemical oxidation was first-order with respect to reduced sulphur at all pH values, and nearly first-order with respect to oxygen at $pH\ 7.55$. An overall kinetic model was developed, and suggests the presence of parallel reactions between reduced sulphur species and oxygen to form sulphite, thiosulphate, and sulphate. No sulphur was ever observed in their experiments. The authors postulated that the formation of solid sulphur is a function of the sulphide-to-oxygen ratio ($[S^{2-}]/[O_2]$). A high ratio, along with a total reduced sulphur concentration greater than $10^{-3}\ M$ favours the formation of sulphur, whereas sulphide, thiosulphate and sulphate are formed when $[S^{2-}]/[O_2]$ is small (O'Brien and Birkner 1977). They also concluded that sulphate is the favoured reaction product below $pH\ 6$.

The rate of abiotic sulphide oxidation is affected by various factors, including the length of the induction period, temperature, pH, sulphide ion concentration, oxygen

concentration, neutral salt content, and the presence or absence of bacteria and organic species (Kuhn et al. 1983). The reaction order for chemical sulphide oxidation, with respect to oxygen, depends on the total sulphide concentration, calculated as $S = [H_2S] + [HS^-] + [S^{2-}]$ (Buisman et al. 1990b). When reacting at low concentrations (0.05 – 1 mM), sulphide and oxygen form primarily thiosulphate (20 – 40 percent), sulphate (40 percent), and sulphite (10 percent), but hardly any sulphur (Kuenen 1975). At high concentrations (>1 mM), sulphur is one of the main oxidation products (Kuenen 1975).

2.4.3 Solid sulphur formation

A major operational difficulty in H_2S biofilters is sulphur plugging at high loading rates. Normally, biofilters can be run for periods of years without replacement of the biofilter matrix (Wani et al. 1999), but this is not the case for H_2S biofilters operating at high sulphur loading rates. Furusawa et al. (1984) observed the appearance of both CS_2 -extractable sulphur as well as ‘organic’ sulphur (associated with carbon compounds) at high H_2S loading rates. Allen and Yang (1992) observed whitish discoloration of the compost packing in their H_2S biofilter, that was accompanied by a rapid drop in pH and elevated temperatures, indicating enhanced biological activity. More than half of the sulphur that accumulated in their column was found to be water soluble (Allen and Yang 1992). With *T. ferrooxidans*, Hazeau et al. (1988) observed the appearance of an insoluble sulphur compound, whose oxidation rate was reduced in the absence of sulphate. Degorce-Dumas et al. (1997) found 60 percent sulphur and 40 percent sulphate in their biofilters after periods of high H_2S loading.

Low concentrations of influent H_2S do not result in sulphur accumulation in a biofilter, but above certain breakthrough point concentrations, the accumulation of solid sulphur as well as potentially inhibitory levels of sulphide can become a problem in H_2S biofilters (Allen and Yang 1991; Sublette et al. 1998). Degorce-Dumas et al. (1997) observed growth inhibition in their biofilter at H_2S loading rates of greater than 3000 mg/m³. Sulphate in high concentrations is also inhibitory to H_2S degradation; Yang and Allen (1994a) found that a sulphate level above 25 mg-S/g was inhibitory to sulphur-oxidising

microbes. The three most important factors that control the formation of sulphur in aerobic, biological systems are: the sulphide-to-oxygen ratio, the sulphide concentration, and the sulphide loading rate (Buisman et al. 1990a).

It is not possible to convert all influent H_2S to sulphur in an aqueous system (Janssen et al. 1995). In a series of bioreactor experiments at pH 8.0 and 25°C, some sulphate formation was always observed, either directly due to an oversupply of oxygen, or indirectly due to the formation of thiosulphate under oxygen-limiting conditions. The maximal sulphur formation was observed not at the stoichiometric value of $(\text{O}_2/\text{S}^{2-})_{\text{consumption}} = 0.5$, but at values between 0.6 and 1.0. The authors speculated that this was because of the chemical formation of thiosulphate. The maximum observed sulphur yield was 73 ± 10 percent (Janssen et al. 1995).

The formation of sulphate and sulphur as end products in a bioreactor system can be controlled by manipulating the amount of oxygen supplied. Solid sulphur is formed by *T. thiooxidans* under oxygen-limiting conditions (Janssen et al. 1995). High sulphide to oxygen loading ratios also result in solid sulphur deposition; less than 10 percent sulphate is produced at low oxygen concentrations (Buisman et al. 1990a). Gadre (1989) found 79 percent elemental sulphur and only 21 percent sulphate from H_2S oxidation in a fixed film bioreactor, also under oxygen-limiting conditions, and Tichý (1994) used neutrophilic thiobacilli to produce biological sulphur under oxygen limitation. Even at high oxygen concentrations, high sulphide loading results in less than 5 percent of the incoming sulphide being chemically converted to sulphate, with the rest precipitating as solid sulphur (Janssen et al. 1995).

2.4.5 Biological sulphur

Though there is the possibility of both extracellular deposition and intracellular accumulation, most species of *Thiobacillus* may precipitate elemental sulphur externally to their cells during growth on sulphide or thiosulphate (Kuenen 1989). This is possibly indicative of differing mechanisms of sulphur compound oxidation. Extracellular sulphur

precipitation is best explained as a consequence of sulphide conversion to sulphur at the surface of the cell, presumably in the periplasmic space, catalysed by enzyme systems located in or external to the bounding membrane of the cell (Kuenen 1989).

There has been some debate in the literature as to the nature of solid sulphur intermediate produced by biological systems. The notion of biological sulphur, or hydrophilic sulphur, was first introduced by Steudel (1989). Hydrophilic sulphur is considered to be a form of elemental sulphur produced by sulphide-oxidising bacteria under certain conditions, that consists of long-chain polythionates, possibly in association with elemental sulphur (Chan and Suzuki 1993; Hazeau et al. 1988; Pronk et al. 1990; Steudel 1989). It is soluble only in polar organic solvents (such as acetone) and in water, and has an oxidation state of zero. Commercially available chemical sulphur, also called sulphur flower, is soluble in CS₂. Tichý (1994) performed an analysis of biologically produced sulphur, and determined it to be composed of 91.3 percent elemental sulphur, with the balance being mineral salts and fractions of microbial biomass. The particles were between 1 and 6 µm in size (Tichý 1994). The hydrophilic nature of the sulphur is believed to be due to the adsorption of polythionates or microbial surfactants (Steudel 1989).

Long chain polythionates are formed according to the pathway depicted by reaction 5 in Figure 2. However, when the further oxidation of biologically formed sulphur (reaction 2 in Figure 2) is inhibited, the sulphur product that accumulates is elemental sulphur, and not hydrophilic sulphur (Chan and Suzuki 1993). The biologically produced sulphur intermediate is also sometimes called polysulphide, or colloidal sulphur.

When elemental sulphur forms in aqueous solution, it actually forms colloidal sulphur (Meyer 1977). Colloidal sulphur contains a mixture of different chemical species. Work done in the early 1900s indicates that colloidal sulphur can contain polythionates of the formula SO₃⁻-S_x-SO₃⁻, with an x value of 10 – 25 (Meyer 1977). Chen and Morris (1972) found that polysulphide ions, S_x²⁻, may be formed through the interaction of sulphur and an aqueous solution of sulphide. Neutral elemental sulphur and large polysulphide ions,

S_x^{2-} and HS_x^- , are not soluble in water, and eventually precipitate (Meyer 1977). This process is accelerated by light, which induces S-S scission. Hartler et al., quoted in Chen and Morris (1972), found that the rate of sulphur dissolution in aqueous sodium sulphide solutions is influenced by several factors, including the rate of mass transfer of reactants and products, the specific active surface of the sulphur, and the rate of chemical reaction. The formation of polysulphide ions from sulphur and sulphide has an autocatalytic effect on the rate of sulphur dissolution (Chen and Morris 1972; Kuenen 1975).

Microbes can grow on both chemically and biologically produced sulphur; this is sometimes aided by the production of surface-active agents (Bryant et al. 1983). Biologically produced sulphur oxidises significantly faster than chemically produced sulphur, and results in higher rates of sulphuric acid production (Tichý 1994). This is partly because its hydrophilicity allows better contact with water and bacteria, and also because biologically produced sulphur has a higher specific surface area than chemically produced sulphur (Tichý 1994).

2.4.6 Hydrogen polysulphides

Polysulphides are mixtures of molecules of the type $X-S_n-X$ in which n values range between 1 and 10 (Meyer 1977; Raymont 1975). They are formed when neutral sulphur atoms combine with monosulphide species (O'Brien and Birkner 1977), or when H_2S dissolves in and reacts with liquid sulphur (Hyne and Wassink 1991). Polysulphide molecules are not branched. The sulphur chains can be terminated by hydrogen, a halogen, or other inorganic or organic terminal groups. Tetra- and pentasulphide species are the predominant polysulphide species in neutral and slightly alkaline solutions (O'Brien and Birkner 1977). Polysulphide compounds are the sulphur analogues of alkanes, $H-(CH_2)_n-H$, therefore their official IUPAC name is sulphane (Meyer 1977). Most of the literature on polysulphides was published in the 1950s and 60s.

Polysulphides are highly unstable in air and spontaneously decompose to H_2O and S_8 (Clark et al. 1994). It is difficult to analyse for hydrogen polysulphides in air, except by

doing gas density analyses. However, the sulphanes are fairly stable in solution, especially in the presence of sulphur (Meyer 1977). They form an equilibrium mixture in which the elemental sulphur is saturated with sulphane with an average chain length between 4 and 7 (Meyer 1977). Apparently the dissolved sulphur has a stabilising effect, because the mixture decomposes quickly if elemental sulphur is extracted (Meyer 1977).

In solution, the proton exchange in sulphanes is slow enough to yield a characteristic NMR spectrum for each chain length value n (Schmidbaur et al. 1964). UV spectra can also be useful in analysing polysulphides (Fehér and Hitzemann 1958; Giggenbach 1971). However, these measurements can be difficult because at high pH the sulphides oxidise readily, even with only traces of dissolved O_2 (Meyer 1977). Organic polysulphides can be analysed using chromatography (Meyer 1977).

Because gaseous H_2S often contains small amounts of additional sulphur, it may be represented non-stoichiometrically by the formula H_2S_x , where x is slightly larger than one (Dalla Lana 2001). Condensation of sulphanes with chlorosulphanes, formed by the reactions of sulphur or hydrogen sulphide with chlorine, can form heavy oils with the composition $H-S_x-H$, where x can be as high as 354 (Fehér and Winkhaus 1956; Meyer 1977). If more than 12 percent H_2S is present in natural gas, elemental sulphur precipitates and tends to plug the tubing and the bottom of the well (Meyer 1977), likely due to the presence of polysulphides. The presence of H_2S_x has implications for the use of H_2S biofilters in the oilfield. Any polysulphides present in the flare gas stream would decompose to H_2O and elemental sulphur immediately upon entering the biofilter, thereby exacerbating the problem of sulphur plugging.

2.5 H₂S degradation kinetics

2.5.1 Biological H₂S degradation

Generally, the substrate utilisation rate of a pollutant by microbial flora can be expressed using the Michaelis-Menten relationship (Deshusses et al. 1995a; Yang and Allen 1994b; Wani et al. 1999):

$$-\frac{dC}{dt} = \frac{V_m C}{K_s + C} \quad (2-8)$$

where C is the substrate concentration, V_m is the maximum substrate utilisation rate, and K_s is the Michaelis constant, also called the half saturation constant. A smaller value of K_s indicates a higher affinity of the biomass for the substrate (Chung et al. 1998).

Yang and Allen (1994b) found that H₂S oxidation is first-order at low concentrations (<200 ppm), zero-order at high concentrations (>400 ppm), and fractional-order in the intermediate concentration range of H₂S in the inlet gas. Under steady state conditions, meaning that the microbial population is not changing with time, there are three situations that can be encountered in a biological system, and corresponding equations can be developed from the Michaelis-Menten expression.

The first of these occurs if the substrate concentration is very high (i.e. $C \gg K_s$). Here, the rate expression approaches zero order in the substrate concentration:

$$-\frac{dC}{dt} = V_m = k_0 \quad (2-9)$$

where k_0 is the zero-order rate coefficient. Under these conditions, the liquid film is saturated with dissolved pollutant, and the (empirical) rate of reaction depends solely on

the capacity of the microbial population present to degrade the pollutant (Ottengraf 1977). For inlet H_2S concentrations of greater than 400 ppm, k_0 was found to be 26.1 ppm/s (Yang and Allen 1994b). This represents the maximum elimination capacity of the microbes for H_2S , in a compost biofilter with a retention time of 16 s.

If the inlet substrate concentration is very low (i.e. $C \ll K_s$), a first-order kinetic dependence is obtained:

$$-\frac{dC}{dt} = k_1 C \quad (2-10)$$

where k_1 is the first-order rate coefficient. Under these conditions, the rate limiting step is the mass diffusion of pollutant to the surface of the biofilm, where it will be quickly degraded by the microorganisms present; the overall rate is dependant on the gas phase concentration of the pollutant (Ottengraf 1977). For inlet concentrations of H_2S less than 200 ppm, Yang and Allen (1994b) obtained a first-order rate coefficient of 0.54 s^{-1} .

Finally, in regions of intermediate inlet concentration (i.e. $K_s \approx C$), the biological reaction follows fractional-order kinetics, because no simplifying assumptions can be made with regards to the Michaelis-Menten kinetic expression. In this operating range, kinetics are usually expressed by empirical relationships, such as the diffusion limiting model described by Ottengraf (1977):

$$\frac{C}{C_0} = \left(1 - \frac{H}{U_g} \sqrt{\frac{k_0 D_e a}{2mC_0 \delta}} \right)^2 \quad (2-11)$$

where H is the height of the filter bed, U_g is the gas velocity, a is the interfacial area per unit volume, D_e is the effective diffusion coefficient, m is the gas/liquid distribution coefficient of the substrate, and δ is the biolayer thickness. To use this equation, a fractional-order reaction coefficient, k_f , can be defined as (Yang and Allen 1994b):

$$k_f = \sqrt{\frac{k_0 D_e a}{2mC_0 \delta}} \quad (2-12)$$

For inlet H₂S concentrations of between 200 and 400 ppm, k_f was found to be 0.064 s⁻¹ (Yang and Allen 1994b).

Hirai et al. (1990) did an experiment to measure the removal kinetics of H₂S on a peat biofilter. After an acclimation period of 19 d at inlet H₂S concentrations of 80 – 150 ppm, the maximum removal coefficient (V_m) and saturation constant (K_s) were found to be 5.0 g-S/d kg-dry peat and 55 ppm respectively. The Michaelis-Menten type of expression used in this study was:

$$-\frac{dC}{dt} = \frac{V_m C}{K_s + C} \cdot \frac{S_a}{F} \cdot \alpha \quad (2-13)$$

where S_a is the cross sectional area of the column, F is the gas flow rate, and α is a conversion coefficient to convert from ppm to kg-dry peat/g-S.

A similar experiment by Wani et al. (1998d), using compost and wood-based biofilters for the elimination of H₂S yielded V_m and K_s values of 142.6 g/m³h and 59.3 ppm respectively. The inlet concentration of H₂S varied between 10 and 500 ppm. Neither constant varied significantly in different biofilters. Mass transfer and microbial degradation in the biofilter were lumped into one kinetic model. The biofilters were modelled as plug flow reactors using the equation:

$$\frac{\left(\frac{V}{Q}\right)}{(C_0 - C_e)} = \frac{K_s}{V_m} \frac{1}{C_{in}} + \frac{1}{V_m} \quad (2-14)$$

In a biofilter, the ‘true’ rate of biological degradation is often masked by adsorption and chemical removal processes (McNevin and Barford 1998). Furusawa et al. (1984) found

that a γ -irradiated peat biofilter showed a constant removal of 12 percent of the inlet H_2S , when the inlet concentration was 125 ppm. This may have been due to either absorption or chemical oxidation. The rate constant for this intrinsic H_2S removal was 0.44 g H_2S /d kg-dry-peat. The overall H_2S removal kinetics were independent of H_2S concentration, but the rate constant varied with the inlet H_2S concentration.

A summary of the Michaelis-Menten constants for H_2S biofiltration found in the literature is shown in Table 4.

Table 4: Michaelis-Menten parameters found in selected biofilter studies

Authors	Matrix material	Microbial strain	V_m (g $\text{H}_2\text{S}/\text{m}^3 \text{ h}$)	K_s (ppm)
Cho et al. 1991a	Fibrous peat; inoculated with culture for all runs	<i>Thiobacillus</i> sp. HA43, isolated from domestic sewage sludge	108 (γ -ray sterilised peat)	39
			120 (non-sterilised peat)	93
			322 (peat & domestic sewage sludge)	78
Chung et al. 1998	Ca-alginate beads with immobilised cells	<i>Thiobacillus</i> <i>novellus</i> CH 3	263 – 642 (autotrophic)	84 – 186
			309 – 628 (mixotrophic)	74 – 152
Hirai et al. 1990	Peat	Aerobically digested domestic sewage sludge	25	55
Wani et al. 1998d, 1999	Compost, hog fuel and perlite	Indigenous	136 – 147	44 – 59

For the experiments done by Cho et al. (1991a), summarised above, it is worth noting the differences in biological removal rates under different conditions. Significant numbers of heterotrophic bacteria were isolated from the non-sterilised peat and peat & domestic sewage sludge-seeded peat, as compared with the γ -ray sterilised peat. However, the difference between the first two runs is still not overly significant over the course of 1

day, suggesting that most of the removal for runs one and two is autotrophic. The highest removal rates were obtained in the biofilters seeded with domestic sewage sludge in addition to the inoculum, suggesting either a significant population of other H₂S-degrading microorganisms, or enhanced activity of the inoculum due to the high concentration of organic compounds in the sludge (Cho et al. 1991a). Significant removal due to heterotrophic populations in an H₂S biofilter is unlikely; heterotrophs would fail to proliferate to any great extent in an autotrophic environment (Gadre 1989; Sublette and Sylvester 1987a).

2.5.2 Chemical H₂S oxidation

Many different rate expressions for chemical H₂S oxidation exist in the literature, under widely varying conditions of pH, oxygen, and sulphide concentrations. Some of the rates published are quite contradictory; this likely has to do with differing reaction mechanisms, both speculated and observed (Kuhn et al. 1983). All proposed chemical oxidation rate laws are of the form:

$$R = k[S]^m [O]^n \quad (2-15)$$

Values of m, n and k vary with ionic strength and pH (Buisman et al. 1990b). The only exception to this general form was proposed by Janssen et al. (1995), who found that the chemical oxidation of H₂S is first order, with $k = 0.87 \text{ h}^{-1}$.

A summary of chemical oxidation rate expressions found in the literature is shown in Table 5. The basic rate law is shown in equation 2-15. Values of k, m, and n reported vary widely. All of the published sulphide oxidation rates were obtained in aqueous solutions; the values would be expected to differ significantly in a biofilter.

Table 5: Summary of chemical oxidation kinetics observed in aqueous solutions

Authors	k (M/min)	m ^a	n ^b	Conditions
Buisman et al. 1990b	2.8E-07	0.41	0.39 log [S]	[S]: 0.15 – 28 mM [O]: 0.21 – 1.1 mM pH: 8.0 T: 25°C
Chen and Morris 1972	0.00017 – 0.37	1.34	0.56	[S]: 0.08 – 0.16 mM [O]: 0.02 – 0.05 mM pH: 6.0 – 12.5 T: 25°C
Jolley and Forster 1985	44.3 – 67.6	1.15	0.69	[S]: 0.05 – 0.2 mM [O]: 0.6 mM pH: 7.0 T: nr ^c
O'Brien and Birkner 1977	0.97-1.97	1.02	0.80	[S]: 0.022 – 1.21 mM [O]: 0.21 – 1.1 mM pH: 4, 7.55, 10 T: 25°C
Wilmot et al. 1988	1.6E-06	0.38	0.21	[S]: 0.09 – 0.3 mM [O]: 0.16 – 0.62 mM pH: 7.0 T: 20°C
Zhang and Millero 1994	log k = 12.25 – 3060/T+0.45*I ^d	1	1	[S]: 0.025 mM [O]: saturated pH: 8.0 T: 5 – 65°C

^a m: reaction order with respect to sulphide^b n: reaction order with respect to oxygen^c nr: not reported^d I: ionic strength

2.6 ARC work

The background work for this thesis project was done at the ARC in Vegreville, Alberta, under the direction of Drs. Karen Budwill and Richard Coleman (Budwill and Coleman 1999; Coleman and Dombroski 1995). The ARC raw data relevant to the current project are shown in Appendix A. The graphs and tables shown in this section were constructed from these data; cumulative data plots were not shown in the original ARC reports. This

thesis project is considered an extension of the ARC work in that the data obtained by the ARC were used in this project as being representative of overall H₂S removal rates, encompassing biological H₂S removal, chemical H₂S removal, and biological sulphur degradation. Together with the chemical removal data obtained in this project, these data form the basis of the kinetic expressions for the model described in Section 3.

2.6.1 Analysis of steady state

Steady state models are representative only for data that were collected at steady state, where (theoretically) the important parameters (i.e. concentrations, flow rates) are not changing with time. Various analyses were done of the ARC data, to determine periods of steady state operation. The three measurements relevant to steady state H₂S removal are inlet concentration, outlet concentration, and percent removal. Difficulties arose in establishing what constitutes steady state for biofilter operation. There are various places within the data where a constant removal efficiency and outlet concentration were obtained over a prolonged period of time, while the inlet concentration was still fluctuating widely. An example is shown in Figure 3.

In Figure 3, removal rates of 92 to 100 percent and outlet concentrations of close to zero were maintained while inlet concentrations fluctuated between 80 and 2500 ppm. This suggests that the biofilter used at ARC was over-designed for the inlet specifications; the entire length of the biofilter was not necessary to obtain complete conversion. It is also likely that there was significant channelling and/or short circuiting occurring within the biofilter matrix. This thesis project is aimed at understanding and modelling the processes occurring within the biofilter, in order to optimise the length of biofilter required to attain complete H₂S removal.

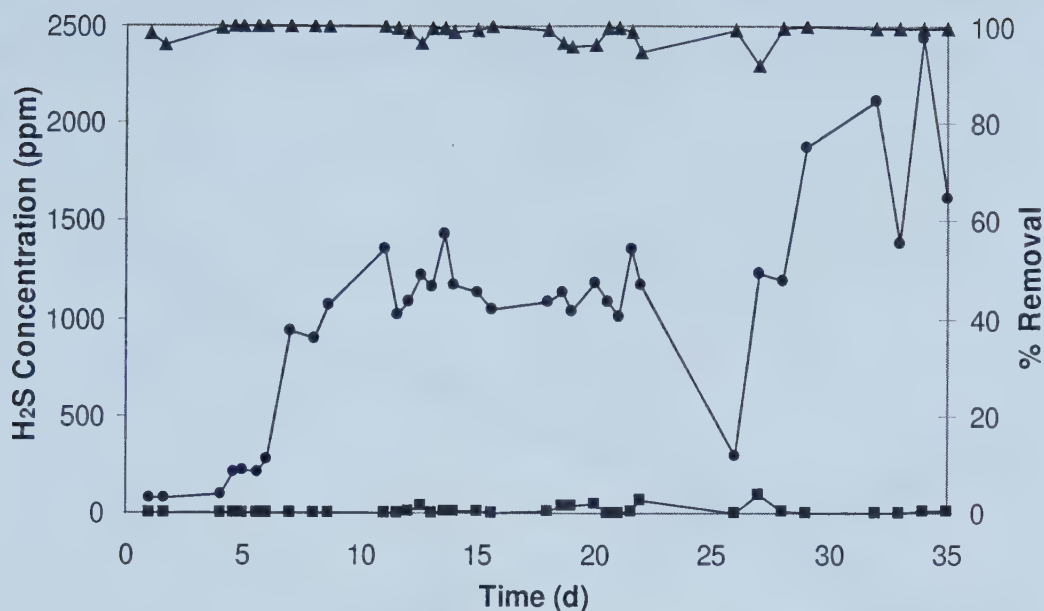


Figure 3: Performance of a 1 m laboratory-scale H₂S biofilter inoculated with *T. thiooxidans* (Experiment 3, Biofilter 2, Budwill and Coleman 1999). The curves shown are H₂S inlet (●) and outlet concentrations (■), and percent removal (▲).

2.6.2 Sulphur balance

Sulphur deposition was a serious problem in the ARC biofilters (Budwill and Coleman 1999). This leads to the question of the origin of the sulphur deposits in the biofilter. In previous work at the ARC (Coleman and Dombroski 1995), there was a period of almost 2 months where the biofilter was operating without an inoculum. Data collected during that time suggest that there was abiotic H₂S removal, as well as possibly some sulphur deposition occurring during this time. The pre-inoculation sulphur balance for this experiment is shown in Figure 4.

Even though the chemical oxidation of H₂S is well known (Kuhn et al. 1983), the biofilter experiments at the ARC did not include any control runs with uninoculated biofilters. One reason for this includes the fact that the water-based chemical conversion of H₂S depends on the relative humidity of the air entering the biofilter, as well as on the

moisture content in the biofilter (Budwill 2000a). This was deemed to be too difficult to control, and the ARC experiments were focussed on biological conversion (Budwill 2000a).

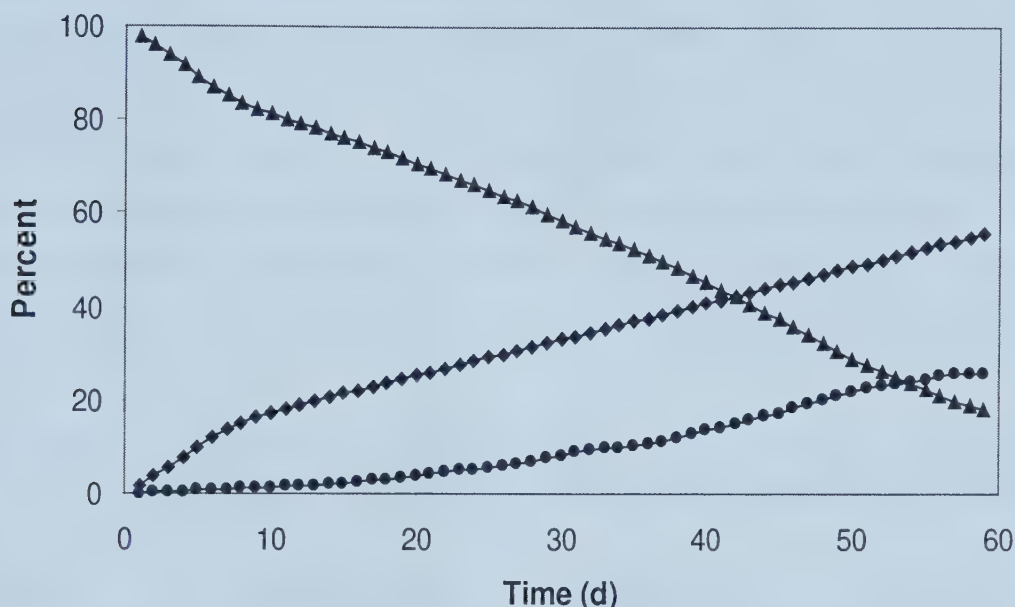


Figure 4: Pre-inoculation sulphur balance for laboratory-scale Biofilter 1, during the time period of Dec. 9, 1992 – Feb. 5, 1993 (after Coleman and Dombroski 1995). The curves shown represent the percentage of inlet H₂S out as H₂S (♦) and SO₄²⁻ (●), and the percentage unaccounted for (▲) over time.

The percentages plotted in Figure 4 are cumulative percentages of the total moles of H₂S flowing into the biofilter during the time period shown. After 2 months, 56 percent of the influent H₂S emerged from the biofilter unchanged, 26 percent was converted to sulphate, and the remaining 18 percent was unaccounted for. The experiment ran for 1 month after inoculation, and by the end, only 10 percent of the influent H₂S was unaccounted for. The overall sulphur balances for one particular biofilter experiment are shown in Table 6.

The last line in Table 6 shows the theoretical amount of sulphur that would have been formed in the biofilter, if all of the sulphur unaccounted for was deposited as solid sulphur. This number was calculated by assuming a one to one conversion (on a mole

basis) of H_2S unaccounted for (in moles) to solid sulphur. As seen in Table 6, nearly all of the sulphur potentially deposited was deposited during the pre-inoculation stage. This suggests that it is primarily chemical in origin. *T. thiooxidans* can grow on both chemically and biologically formed sulphur, though biological sulphur is preferred (Knickerbocker et al. 2000; Tichý 1994). The removal of H_2S is a two-step process involving a solid sulphur intermediate (McNevin et al. 1999) that is degraded to sulphate under optimal conditions (Wainwright 1984). The ARC biofilter was operating with inlet H_2S concentrations of between 10 and 40 ppm, which is well within the range (up to 2500 ppm) of what this size of biofilter can successfully remove (Budwill and Coleman 1999). At such low concentrations, significant sulphur deposition in the biofilter is unlikely, because sulphur intermediates are consumed as fast as they are being formed.

Table 6: Sulphur balances for various time periods during laboratory-scale Biofilter 1 operation, from Dec. 9, 1992 to Mar. 12, 1993 (Data from Coleman and Dombroski 1995)

Indicator	Pre-inoculation (Dec. 9 – Feb. 5)	Post-inoculation (Feb. 5 – Mar. 12)	Overall (Dec. 9 – Mar. 12)
% out as H_2S	56	16	37
% out as SO_4^{2-}	26	83	53
% unaccounted for	18	1	10
g S (hypothetical)	1.20	0.06	1.19

The data shown in Figure 4 and Table 6 led to the hypothesis that a significant portion of the H_2S removal in the ARC biofilter was abiotic. This is supported by numerous papers in the literature (Degorce-Dumas et al. 1997; Janssen et al. 1995; McNevin et al. 1999) and was discussed in Section 2.4.2. Since no formal abiotic control experiments were done at the ARC, a number of experiments, described in Section 4, were designed to investigate this chemical oxidation reaction.

While most of the influent H_2S in the ARC biofilter was converted to sulphate, sulphur plugging and drying out of the matrix bed was a serious problem at high loading rates;

the life span of the filter bed was only approximately 50 d (Budwill and Coleman 1999). This constitutes a significant operational difficulty, especially for future scale-up and field operations. To date, no biofilter models incorporating the formation of a solid product have been published. The goal of this thesis project was to use the chemical H_2S removal data, along with data collected previously by the ARC, in order to successfully model solid sulphur deposition in an H_2S biofilter.

2.7 Modelling of biofilters

2.7.1 Historical background

Many people have shown that biological waste treatment processes are cost-effective for the treatment of high volume gas streams containing low levels of pollutants (Kennes and Thalasso 1998; Wani et al. 1997). However, despite their use in many industries worldwide, biofilter treatment processes have only been subject to a minimum amount of modelling (Allen and Yang 1991; Baltzis et al. 1997; Deshusses et al. 1995a). Scale-up and design of industrial biofilters is usually dictated by empirical knowledge, since there is a lack of comprehensive knowledge of the individual processes involved in contaminant elimination. Biofilters are often considered as mysterious “black boxes” within which pollutants vanish as a result of the action of enigmatic microbes (Deshusses et al. 1995a).

Historically, there have been three main goals for modelling biofilters: understanding the relationships between column parameters and pollutant removal, design, and process optimisation (Devinny et al. 1999). The earliest model was proposed in the early 1980s, and was based on the existing models for submerged biofilm processes developed by Jennings et al. (1976) and Ottengraf (1977). These models assumed basic mass balances, plug flow in the air stream, and simple reaction kinetics. The basis of biofilm modelling came from an extension by Ottengraf and van Den Oever (1983) of the submerged

biofilm model. Ottengraf's model (1986) remains the most commonly referenced biofilter model, and most current models were developed from it. Recently, the nature of biofilter modelling has changed slightly, because of advances in computing power (Devinny et al. 1999). The trend is shifting from simplified models with many assumptions to complex models that use numerical approaches to solve large numbers of equations. Biofilter models differ mainly in the following four areas: 1) model for fluid flow; 2) model for biodegradation reaction in the biofilm; 3) details of interphase transport; and 4) role of the support medium (Amanullah et al. 1999). Table 7 presents a summary of selected key biofilter models and their principal features.

Table 7: Summary of key features of selected biofilter models (after Devinny et al. 1999)

Model	Characteristics	Solution	Validated using
Ottengraf 1986	Simple, steady-state model, assumes zero- or first-order kinetics	Analytical	Compost & peat biofilter
Shareefdeen et al. 1993	Steady state model with oxygen limitation and substrate inhibition	Numerical, trial and error to obtain the biofilm concentration profile	Peat moss and perlite biofilter
Shareefdeen and Baltzis 1994	Transient model with oxygen limitation; patchy biomass coverage	Quasi-steady state, numerical solution	Peat moss and perlite biofilter
Deshusses et al. 1995a,b	Dynamic model; includes sorption and cross-inhibition with two pollutants	Numerical, finite difference	Compost biofilter
Zarook et al. 1998	Steady state model; accounts for axial dispersion	Numerical, finite difference	Peat moss biofilter
Amanullah et al. 1999	Transient and steady state model; very comprehensive parameter coverage	Numerical, integration of ODEs	Computer simulation, replicated key published models

Ottengraf's model was first published in 1983 (Ottengraf and van Den Oever 1983), but is best described in Ottengraf (1986). The model is a modification of the submerged biofilm model by Jennings et al. (1976), to include gas-liquid biofilm interfaces. Three basic situations, believed to be common in waste air treatment are described: first-order kinetics, zero-order kinetics with reaction rate limitation, and zero-order kinetics with diffusion rate limitation, all with excess available oxygen. Ottengraf (1986) used Michaelis-Menten type rate expressions to describe substrate elimination in the biofilm. Analytical solutions describing each of the three kinetic scenarios give the biofilm concentration profile. This profile is exponential, linear or quadratic for first-order, zero-order with reaction limitation, and zero-order with diffusion limitation, respectively. The major shortfall of analytical solutions to biofilter models is that they cannot be used to describe interactions among multiple substrates, transient operation, or changes within the reaction order or reaction conditions within the biofilter (Deshusses et al. 1995a).

Shareefdeen et al. (1993) published a model that is quite similar to that of Ottengraf and van den Oever (1983), but with differences in the microkinetics. This model assumes a double limitation by both the carbon substrate (methanol) and oxygen; the resulting kinetics are described by a Haldane-type expression. A number of further studies by the same authors have shown that oxygen is particularly important (in terms of rate limitation) whenever polar compounds are removed via biofiltration (Baltzis et al. 1997). Shareefdeen et al. (1993) assumed that one of the rate-limiting substrates is depleted before it reaches the biofilm-solid interface. Self-inhibition by substrates at high concentrations is also accounted for. The model assumes that the biofilter is at steady state. Additionally, this model allows for the calculation of active biofilm thickness at every location in the biofilter bed, rather than assuming one thickness throughout. Experiments were carried out in order to optimise the packing in the column (Shareefdeen et al. 1993). Peat alone was found to lead to channelling and poor gas contact; performance was significantly improved by the addition of perlite particles. This model could not accurately describe short-term transient behaviour. Most model parameters were determined in non-biofilter systems, and it was assumed that they would apply equally well to biofilter systems.

The difference between steady state and unsteady state biofiltration is that transient operation involves an extra physical process, namely, adsorption onto the packing medium (Baltzis et al. 1997). In an extension of their 1993 model, Shareefdeen and Baltzis (1994) introduced sorption of the pollutant onto the packing material and partial coverage of the support medium by a biofilm, in order to model transient changes occurring in biofilters. Under steady state conditions, the model reduces to that of Shareefdeen et al. (1993). The assumption of partial coverage allows for direct adsorption of the pollutant onto solid particles, as described by a Freundlich isotherm. This problem was very stiff, and a quasi-steady state was assumed before numerical integration was performed.

A model describing the transient behaviour of biofilters and the details of diffusion processes within the biofilm was developed by Deshusses et al. (1995a, b). The rationale for this model was that traditional biofilter models showed that steady state should be obtained within a few seconds of operation, while it was observed experimentally that this usually takes several hours. This is because sorption affects biofilter dynamics (Devinny et al. 1999). The Deshusses et al. (1995a) model assumes that there exists a sorption volume made of water dispersed within the support matrix, and that no biological reaction occurs within this sorption volume. The biofilter is then split conceptually into well-mixed sections, with mass balances describing the fate of pollutants within each section. The pollutants simultaneously diffuse and are consumed by the microorganisms within the biofilm. Deshusses et al. (1995a) do not account for the liquid-solid boundary condition in their model. Deshusses (2000) claims that using numerical integration is a means of avoiding the boundary condition dilemma, and that the system will converge to a stable solution that automatically satisfies boundary conditions. In their model, the sorption volume is modelled as part of the biofilm, but with no reaction term and a different volume than the other biofilm divisions. Other important assumptions of the Deshusses et al. (1995a) model include no oxygen limitation, and Michaelis-Menten kinetics with competition to describe substrate kinetics. The two substrates under investigation were methyl ethyl ketone and methyl isobutyl

ketone. The dynamic mass balance equations were solved using finite differences, and simulated using a dynamic simulation program.

Most theoretical studies on biofilters are based on the idealised assumption of plug flow. Hodge and Devinny (1995) included a dispersion term in their biofilter model, but dispersion was never verified experimentally. In actual operation, deviations from plug flow can be caused by fluid channelling, stagnant regions arising due to non-uniformity in the size of the packing material, and a lack of adequate means for feed distribution. Zarook et al. (1998) presented evidence for axial dispersion in biofilters packed with porous media. A detailed analysis of the residence time distribution (RTD) of an abiotic biofilter showed that there was a significant amount of dispersion in the biofilter, which was packed with peat. One limitation, acknowledged by Zarook et al. (1998), is that the RTD studies may have been different had a biotic column been used in the tracer experiments. A steady state model accounting for axial dispersion was developed, and solved numerically. The effect of moisture content on the RTD was not reported in this model; work is underway and will appear in a future publication (Zarook et al. 1998).

An extremely comprehensive biofilter model was developed by Amanullah et al. (1999). This model incorporates convection and dispersion in the gas phase, partial biofilm coverage of the solid support, direct adsorption to the exposed uncovered solid medium, transfer between the biofilm and the solid support, and biological reactions in both the biofilm and the solid support. The model equations are solved numerically using the method of orthogonal collocation, for both transient and steady state operation. This study analyses the advantages and limitations of key biofilter models, and investigates the number of parameters needed to adequately capture biofilter dynamics. Parameter sensitivity analysis indicates that the biofilter performance is a strong function of specific surface area for mass transfer and biofilm thickness, but that these parameters are difficult to quantify. Media with higher adsorptive capacities seem to work best for all biofilter loads.

Many models exist for submerged biofilm or biotrickling reactors (Jennings et al. 1976; Ottengraf 1986). However, because of the absence of a free liquid phase in gas-phase bioreactors, major differences exist in the nature of the biofilm. Thus, these models cannot be applied directly for the simulation of biofilter operation.

2.7.2 Issues to consider in modelling

The main difficulty in modelling biofilters lies in the complexity of the underlying fundamental processes. Biofilters are living systems subject to dynamic changes, and as such are more difficult to model and control than traditional air pollution treatment technologies (Alonso et al. 2000). To accurately simulate a biofilter, a good model must be able to encompass many physical, chemical and microbiological phenomena. Many of these phenomena are still poorly understood. For example, little is known about the intrinsic microkinetics of biofilters, the physical geometry and physicochemical conditions of biofilms, and the boundary conditions that should be applied between the different phases within the filter (Devinny et al. 1999).

The time scale of biofilter operation makes it difficult to accurately model performance. Bacterial growth is a much slower process than the diffusion and chemical reaction of dissolved components in the biofilter (Alonso et al. 2000). Depending on the contaminant in the biofilter, and on the microbial population, the time scale for any model must be able to encompass changes happening on the order of minutes to months. This is a difficulty in numerical modelling, and can cause serious numerical instabilities such as stiffness. Often, quasi-steady state assumptions are made to overcome this difficulty (Alonso et al. 2000; Shareefdeen et al. 1993). Similar to those in all biological processes, the dynamics of a biofilter are intrinsically non-linear (Bourrel et al. 2000).

The output data for contaminant degradation in a biofilter are often quite simple; they are usually straight lines or exponential curves. This can make it quite difficult to validate a model, because there are many different mathematical models that can reproduce these simple forms.

3.0 Biofilter model

3.1 Model development

The goal of this model is to predict the performance of a biofilter designed to remediate air streams contaminated with H_2S gas, and to predict the formation of solids within the filter bed. The model describes the transport, physical, and biological processes that occur during biofiltration. As contaminated air passes through a biofilter, convection, dispersion, absorption, adsorption, diffusion, reaction, and characteristics of the biofilm affect the level of contaminant removal.

The main processes occurring in a biofilter are mass transport processes (diffusion and convection), interphase mass transfer, and biodegradation. These are shown in Figure 5. Chemical oxidation also occurs in H_2S biofilters, where there is air and water to catalyse the reaction.

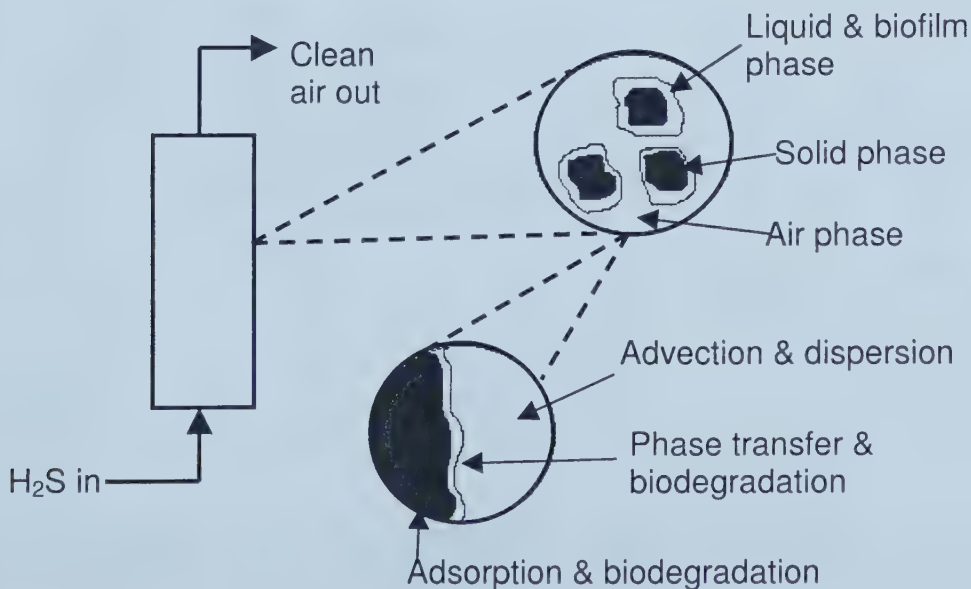


Figure 5: Transport processes occurring in a biofilter (after Hodge and Devinny 1995)

The biofilter has three phases: gas, liquid (biofilm), and solid (peat). The amount of free liquid phase is assumed to be negligible. For modelling, the biofilter height is divided into layers. There are 15 layers in total. Each layer has three main sections: the gas phase, biofilm, and solid phase. The layers themselves are discretised using planar (z , x) geometry. The biofilm, or liquid layer, is divided into eight subdivisions; each is assumed to be ideally mixed. The complete model has a total of 135 nodes. To account for dispersion effects and other boundary conditions, some of the variables have values outside of the nodes; these are hypothetical values that do not correspond to a particular location within the biofilter. This model is based largely on the paper of Deshusses et al. (1995a). It is constructed using a series of dynamic mass balances over subdivisions in the biofilter, as shown in Figure 6.

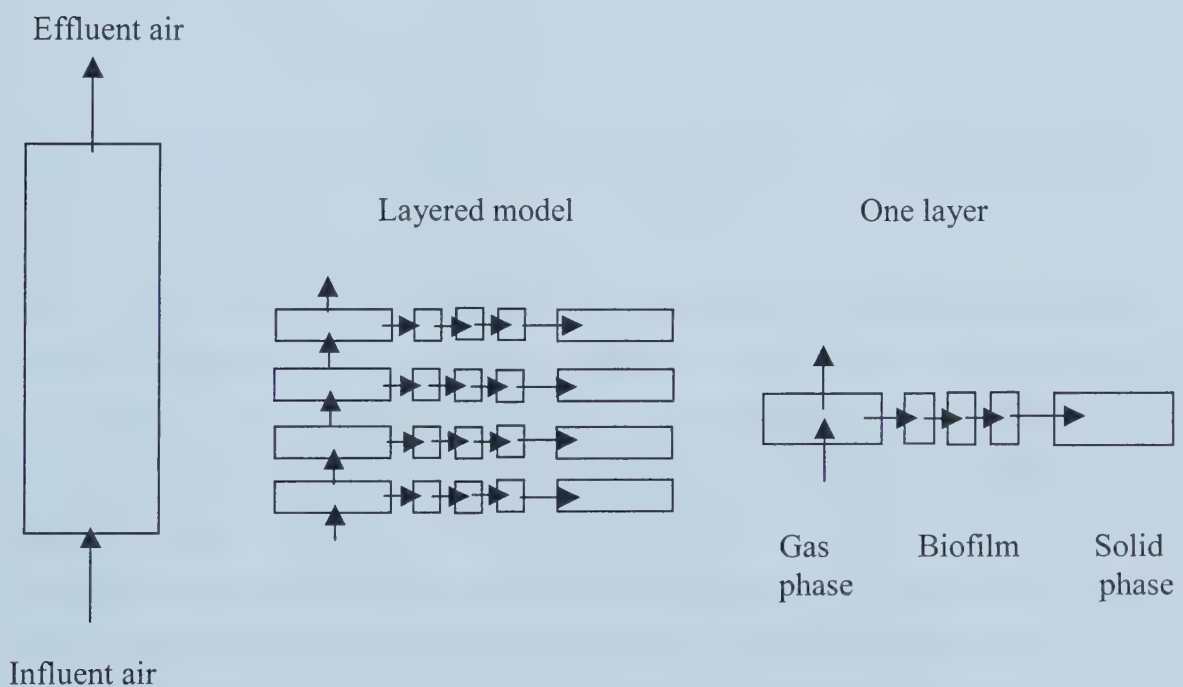


Figure 6: Schematic of biofilter subdivisions. Each subdivision is assumed to be ideally mixed (after Deshusses et al. 1995a).

Mass balances on H_2S in the biofilter give 135 partial differential equations, which comprise the model. The number of layers used to approximate the biofilter affects the

accuracy of the results. Discretisations using 10, 15, and 20 layers were tested, and 15 appears to give the best trade-off between accuracy and computational time. Similar tests were done for the biofilm, resulting in a total of 8 sub-divisions. The node structure for mass balances was shown in Figure 6; Figure 7 illustrates the modelling details for one section. For simplicity, only four of the eight biofilm sub-divisions are shown.

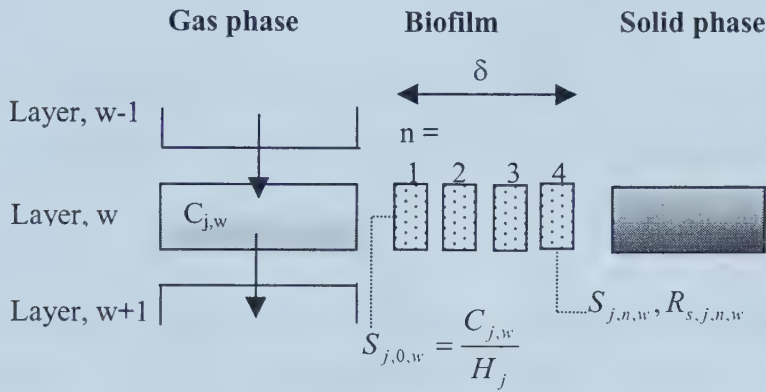


Figure 7: Schematic of the biofilter model for one layer (after Deshusses et al. 1995a).

Figure 7 describes the fate of the pollutant in any one section. The inlet waste air flows downward so that the vector of pollutant transport in the gas phase is convection, plus axial dispersion. The pollutant is in equilibrium at the gas-biofilm interface, as described by Henry's law. Once in the biofilm, the pollutant simultaneously diffuses and is degraded. Oxygen is transported in the biofilter by the same mechanisms, and it is needed for the degradation of the pollutant. It is assumed that no reaction occurs within the solid phase – it acts merely as a support and provides surface area for biofilm coverage.

There are two dimensions of integration in the biofilter: z (axial) and r (radial). In the literature, these directions are usually referred to as z and x (instead of r). The gas phase is integrated in the axial direction, along the length of the biofilter. The liquid phase is integrated radially.

3.2 Assumptions

The model is based on the following assumptions:

- 1) Each of the subdivisions defined in Figure 6 is ideally mixed (Deshusses et al. 1995a).
- 2) Gas flow through the packed column is described by an axially dispersed plug flow (no radial gradients). Axial dispersion was verified experimentally, as described in Section 5.1.
- 3) The interfacial resistance in the gas phase is negligible (Deshusses et al. 1995a). It is assumed that there is no resistance to mass transfer from the gas phase to the biofilm.
- 4) The biofilm is formed on the exterior surface of the peat particles, and its thickness (δ) is small when compared to the particle size. Hence, planar biofilm geometry can be used (Shareefdeen et al. 1993).
- 5) The extent of the biofilm coverage is much larger than its depth, so that any H_2S and O_2 transported into the biofilm through the side surfaces of the biolayer can be neglected, and the diffusion and reaction within the biofilm can be considered in a single direction only (Shareefdeen and Baltzis 1994).
- 6) The biofilm is formed uniformly around particles, leaving no direct contact between the surface of solids with the air stream. No adsorption occurs onto the solid phase.
- 7) The only substrates affecting the rate of biodegradation are H_2S and O_2 . Sufficient CO_2 is present to serve as a carbon source for *T. thiooxidans*. Diffusion and reaction of H_2S in the biofilm is considered; O_2 is considered to be present in excess.

- 8) Transport of H_2S and O_2 within the biofilm occurs by diffusion only, and is described by an effective diffusion coefficient, equal to the diffusion coefficient for the transport of that compound in water (Deshusses et al. 1995a).
- 9) After the initial transient stages of the process, biomass accumulation in the column occurs so slowly that it can be considered negligible, at least over substantial periods of time. This means that a steady state or more accurately, a quasi-steady state is established within the column, with no net biomass accumulation (Shareefdeen et al. 1993). This also ensures a constant specific biofilm surface area.
- 10) The biofilm density and thickness are constant throughout the column (Baltzis et al. 1997).
- 11) Nutrients and humidity are present in the required amounts within the biofilter. The filter is modelled as a classical gas phase filter, and not as a biotrickling filter. The moisture content of the peat is assumed to be at steady state, due to constant replenishment by the humidified inlet stream.
- 12) No degradation occurs within the sorption volume (peat), because the biolayer is formed on the exterior surface of the particles. Biomass does not grow in the pores of the peat fibres; thus, no reaction occurs in the pores and all activity is in the biofilm coating the peat support (Shareefdeen and Baltzis 1994).
- 13) Biodegradation of the H_2S occurs only aerobically. The biocatalyst (microbial biomass) is homogeneously distributed throughout the biofilm (Deshusses et al. 1995a).
- 14) The kinetics of H_2S degradation are described by a chemical H_2S degradation term, a microbial H_2S degradation term, and a microbial sulphur degradation term. Lumped kinetics are used to model the net biological sulphur deposition.

- 15) The H_2S and O_2 at the biofilm-air interface are always in equilibrium, as dictated by Henry's law. The Henry's law coefficients are the same as if the biofilm was made of water only. H_2S is extremely water soluble (Suzuki 1999), so this equilibrium is constantly maintained.
- 16) Temperature and pH variations along the bed are negligible. Wide ranges of pH and temperature would significantly affect the partition coefficients for absorptive equilibrium, biological growth rates, and final reaction products (McNevin et al. 1999).
- 17) The frictional pressure drop is assumed to be negligible (Amanullah et al. 1999).
- 18) The model is a lumped parameter model; there is no spatial variation in the parameters describing the system.
- 19) The gas phase H_2S removal assumed to be at steady-state. Sulphur deposition is a dynamic process. The modelling of these two processes was de-coupled.

Most authors make the additional assumption of plug flow in the gas phase, meaning that there is no axial dispersion (the d^2C/dz^2 term is negligible). According to Amanullah et al. (1999), axial dispersion effects are negligible if $300 < \text{Pe} < 600$, where $\text{Pe} = UL/D_L$ (interstitial gas velocity, bed height, dispersion coefficient). From the tracer studies (see Section 5.1), the Pe for this reactor is 17, so dispersion was incorporated into this model.

The biofilters operated at the ARC were subject to low liquid flow rates of approximately 3 L/d. This flow rate is considered low enough to assume that this biofilter operates as a classical biofilter. The moisture in the bed in classical biofilters is supplied by a humidified inlet stream, which results in low rates of condensed liquid trickling through the reactor. Traditional biotrickling filter models are valid as of hydraulic loading rates of approximately $1.2 \text{ m}^3/\text{m}^2\text{d}$ (Metcalf & Eddy 1991); this filter has a liquid loading rate of $0.05 \text{ m}^2/\text{m}^3\text{d}$.

The assumption of no resistance to interfacial mass transfer is often limiting in biofilter models (Deshusses 2000; Lobo et al. 1999). Especially at low residence times, the observed removal rates in a biofilter will be less than the maximum obtainable rates if the minimum residence time is not exceeded (McNevin and Barford 2000). If the substrate liquid concentration is close to zero, the rate-controlling step is mass transfer at the gas-liquid interface. However, when the substrate concentration in the liquid phase is close to the value in equilibrium with the gas phase, the rate-controlling step is the reaction occurring in the biofilm. H_2S has a very high solubility in water, so equilibrium at the gas-liquid interface is a valid assumption. Further, there is considerable uncertainty involved in experimentally obtaining the parameters needed to estimate the interfacial mass transfer, and to characterise the biofilm removal efficiency (Amanullah et al. 1999). To be completely rigorous, the interfacial mass transfer assumption should be evaluated at every point along the column, because the substrate concentration in the biofilm decreases along the length of the biofilter. Such an approach is beyond the scope of the model outlined here.

3.3 Parameters

Most of the parameters used in modelling the biofilter were taken from data obtained by the ARC, and from the literature. The physical operating parameters of the system (size, flow rates, etc.) are from the ARC where ever possible, since their experiments formed the basis of the system to be modelled. The kinetic constants for chemical H_2S oxidation were determined experimentally, and the remaining kinetic constants were estimated from data previously obtained by the ARC. Table 8 lists the parameters used in the biofilter model.

The value of biofilm thickness (δ) in the model was estimated by a numerical trial and error approach. This is commonly reported in the literature, because of uncertainties in quantifying this parameter (Amanullah et al. 1999). Sensitivity studies were performed to estimate the effect of δ on the overall removal predicted by the model.

Table 8: Parameters used in the biofilter model

Symbol	Parameter	Value	Source
A	interfacial area per unit volume, m^2/m^3	950	Trial and error
D_a	diffusivity of H_2S in air, m^2/s	0.3382	Amanullah et al. 1999
D_h	diffusivity of H_2S in water, m^2/s	1.36E-9	McNevin et al. 1999
D_i	dispersion coefficient, m^2/s	4.1E-3	Present study
E	porosity	0.45	Present study
EC	H_2S elimination capacity of the biofilter, $\text{kg}/\text{m}^3\text{s}$	5.9E-3	Budwill and Coleman 1999
H_h	Henry's law constant at $P = 1 \text{ atm.}$, $(\text{kg}/\text{m}^3)/(\text{kg}/\text{m}^3) - \text{strictly, } H'$	0.3886	National Research Council 1929
K_s	half saturation constant, kg/m^3	1.34E-4	Based on data from Budwill and Coleman 1999
k_s	chemical reaction rate constant, $(\text{kg}/\text{m}^3)^{0.38} \text{ s}^{-1}$	0.0058	Present study
N	number of biofilm subdivisions (x-dir.)	8	-
n_s	chemical reaction order	0.62	Present study
Pe	Peclet number	17	Present study
U	gas velocity, m/s	0.0679	Budwill and Coleman 1999
V	biofilter volume, m^3	2.0E-3	Budwill and Coleman 1999
V_m	maximum uptake rate, $\text{kg}/\text{m}^3\text{s}$	6.8E-6	Based on data from Budwill and Coleman 1999
W	number of z-direction subdivisions	15	-
Z	height of biofilter, m	1	Budwill and Coleman 1999
δ	biofilm thickness, m	175E-6	Trial and error
ρ	density of sulphur, kg/m^3	2000	Meyer 1977

Peat is often used as a solid support in biofiltration due to its high specific surface area (Wu et al. 1999). Biofilter simulation is very sensitive to the value of the interfacial area of the solid support, but this value is extremely difficult to quantify from independent

measurements (Amanullah et al. 1999). Estimates of the specific surface area for peat include 40 – 85 m²/m³ (Kennes and Thalasso 1998), 200 m²/m³ (Wu et al. 1999), and 1.6 m²/g (Zilli et al. 1996), which is approximately 60 000 m²/m³ for the biofilter modelled in this study. Due to the uncertainty in this parameter as compared with the remaining parameters used in the model, the specific surface area was determined numerically by trial and error until the model removal approximated the experimental removal. Sensitivity analysis was done to estimate the effect of the specific surface area on the overall H₂S removal predicted by the model.

3.4 Modelling details

The biofilter model is divided into two parts. The first describes the steady state H₂S removal in the gas and liquid phases of the biofilter, and the second describes the dynamic formation of a solid product. The modelling details for H₂S removal in the biofilter are presented in Section 3.4.1, and the modelling of sulphur accumulation is described in Section 3.4.2. Some interesting aspects of the ARC biofilter kinetics are discussed in Section 3.4.3. A copy of the complete model code is shown in Appendix B.

3.4.1 Overall H₂S removal

Mass balances are written for H₂S in each gas and biofilm subdivision. It is assumed that O₂ is present in excess, due to the high air flow rates used in the ARC experiments. In the following equations, C_h refers to gas phase H₂S concentrations, while S_h refers to liquid phase H₂S concentrations.

3.4.1.1 Mass balance over the gas phase

The general mass balance for the species in the gas phase can be described as follows:

change in time = flow by convection + flow by diffusion – mass flux into biofilm

Mathematically, this can be expressed as:

$$\frac{dC_h}{dt} = D_a \frac{d^2 C_h}{dz^2} - U \frac{dC_h}{dz} + D_h \frac{A}{E} \left(\frac{dS_h}{dx} \right)_{x=0} \quad (3-1)$$

where the mass flux term is inherently negative because of sign conventions.

Danckwerts boundary conditions (Danckwerts 1953) are used to account for dispersion in the gas phase. These boundary conditions state that the concentration of reactant entering the column is less than the concentration in the inlet stream, owing to diffusion just within the entrance of the reactor. Depending on the parameters in the equation, these boundary conditions may predict a jump in concentration within the region close to the reactor inlet, because of the circulation of the entrance stream (Kudrna et al. 1994). Such a jump is present in the current model. Danckwerts boundary conditions have been verified for use in tubular reactors (Aris 1999) and for biofilters (Zarook et al. 1998; Amanullah et al. 1999). The importance of dispersion within the column was verified experimentally with tracer tests. This is further discussed in Section 5.1. The boundary conditions are for the gas phase are:

$$\text{at } z = 0 \quad D_a \frac{dC_h}{dz} = U(C_h - C_{in}) \quad (3-2)$$

$$\text{at } z = Z \quad \frac{dC_h}{dz} = 0 \quad (3-3)$$

As noted in the assumptions, gas phase concentrations and interfacial concentrations are linked by the equilibrium dictated by Henry's law:

$$\text{at } x = 0 \quad S_h = \frac{C_h}{H_h} \quad (3-4)$$

In equation 3-4, H_h is actually H' , which is the Henry's law constant at a constant pressure of 1 atm. The pressure in the biofilter was assumed to be constant at atmospheric pressure. The Henry's law assumption is used here because H_2S is extremely soluble in water (Suzuki 1999), and therefore a constant state of equilibrium is attained at the gas-liquid interface. The rate of degradation in biofilters is often much lower than the rate of mass flux into the biofilm (Zilli et al. 1996), so that the microorganisms in the biofilm always "see" only the liquid saturated with H_2S . The Henry's law assumption is common in biofilter modelling; all biofilter papers cited in this thesis use this boundary condition.

3.4.1.2 Mass balances over the biofilm

The general equation describing the mass balance of pollutant over each subdivision in the biofilm can be described as follows:

$$\text{change in time} = \text{diffusion through biofilm} - \text{removal in biofilm}$$

Mathematically, this can be expressed as:

$$\frac{dS_h}{dt} = D_h \frac{d^2 S_h}{dx^2} - R \quad (3-5)$$

where R is the removal rate of H_2S in the biofilm and can be represented by:

$$R = \frac{V_m S_h}{K_s + S_h} + k_s S_h^{n_s} \quad (3-6)$$

3.4.1.3 System solution

The equations describing the mass balances in the biofilter are solved using numerical methods. Equations 3-1 to 3-7 are discretised using backward difference approximations, constructed using Newton backward difference polynomials. In the case of the second derivative in the biofilm (equation 3-5), a central difference is used because of the boundary constraints. The difference approximations are as follows (Mickens 1994):

$$\text{first-order:} \quad \frac{dC}{dz} \approx \frac{C_i - C_{i-1}}{\Delta z} \quad (3-8)$$

$$\text{second-order:} \quad \frac{d^2C}{dz^2} \approx \frac{C_{i+1} - 2C_i + C_{i-1}}{(\Delta z)^2} \quad (3-9)$$

The equations are inputted, simplified, and solved using Maple 6 (Waterloo Maple Inc. 2000), a commercially available mathematics package. The system is reduced to a set of algebraic equations, which is then solved exactly using a built-in solver package.

3.4.2 Formation of a solid phase

Solid sulphur is an intermediate product in the degradation of H_2S to SO_4^{2-} (Suzuki 1999; Wainwright 1984). It can be formed either chemically or as a result of microbial activity. At high loading rates, it is suspected that a significant amount of the influent H_2S in a biofilter is chemically converted to sulphur (Budwill 2000a).

No authors have yet modelled the formation of a solid degradation product or metabolite in biofilters. As sulphur forms in a biofilter, the properties of the filter bed will change. The most-affected parameter will be the porosity. The H_2S removal in the biofilter is assumed to be at steady state. Conversely, the build-up of solid sulphur is a dynamic process, and is dependent on the concentrations of H_2S in the gas and liquid phases.

3.4.1.3 System solution

The equations describing the mass balances in the biofilter are solved using numerical methods. Equations 3-1 to 3-7 are discretised using backward difference approximations, constructed using Newton backward difference polynomials. In the case of the second derivative in the biofilm (equation 3-5), a central difference is used because of the boundary constraints. The difference approximations are as follows (Mickens 1994):

first-order:
$$\frac{dC}{dz} \approx \frac{C_i - C_{i-1}}{\Delta z} \quad (3-8)$$

second-order:
$$\frac{d^2C}{dz^2} \approx \frac{C_{i+1} - 2C_i + C_{i-1}}{(\Delta z)^2} \quad (3-9)$$

The equations are inputted, simplified, and solved using Maple 6 (Waterloo Maple Inc. 2000), a commercially available mathematics package. The system is reduced to a set of algebraic equations, which is then solved exactly using a built-in solver package.

3.4.2 Formation of a solid phase

Solid sulphur is an intermediate product in the degradation of H_2S to SO_4^{2-} (Suzuki 1999; Wainwright 1984). It can be formed either chemically or as a result of microbial activity. At high loading rates, it is suspected that a significant amount of the influent H_2S in a biofilter is chemically converted to sulphur (Budwill 2000a).

No authors have yet modelled the formation of a solid degradation product or metabolite in biofilters. As sulphur forms in a biofilter, the properties of the filter bed will change. The most-affected parameter will be the porosity. The H_2S removal in the biofilter is assumed to be at steady state. Conversely, the build-up of solid sulphur is a dynamic process, and is dependent on the concentrations of H_2S in the gas and liquid phases.

Because the build-up of solid sulphur happens on a slower time scale than H₂S removal, the time scales for both processes were de-coupled, and the overall model remains at a pseudo-steady state. Embedded in this is the dynamic estimation of the solid product build-up. Extensive sulphur build-up will also affect the pressure drop; this was ignored in the current model because experimental observations at the ARC show that sulphur build-up necessitates shutdown and repacking long before excessive pressure drops become a problem (Budwill and Coleman 1999).

The following species were accounted for in the sulphur mass balance over the biofilter: H₂S in the gas phase, HS⁻, S²⁻ and SO₄²⁻ in the liquid phase, and S⁰ or S₈, either present as a solid or as a colloid in the liquid phase. All other sulphur species are assumed to be transient in nature. The rate balance for sulphur formation is expressed by the following equation:

$$r_s = r_{s,chem} + r_{biol} - r_{biol,SO_4} \quad (3-10)$$

Based on observations made both experimentally and from the literature, each of the terms on the right-hand side of equation 3-10 can be further broken down to the following kinetic expressions. These expressions are only theoretical; further experimentation is necessary to determine their exact forms.

$$r_{s,chem} = k_s (C_h)^{n_s} \quad (3-11)$$

$$r_{biol} = \frac{V_m C_h}{K_s + C_h} \quad (3-12)$$

$$r_{biol,SO_4} = k_{SO_4} (C_s)^{n_{SO_4}} \quad (3-13)$$

Because the biological conversion of sulphur to sulphate is the rate-limiting reaction in H₂S biodegradation, n_{SO4} is likely a value between 0 and 1. The reactions described by

equations 3-11 to 3-13 happen in or on the surface of the liquid phase. Because gas and liquid phase concentrations are linearly related by Henry's law, kinetic expressions 3-11 and 3-12 were modelled using gas phase concentrations, for ease of calculation. Reactions 3-11 and 3-13 also depend on O_2 , which is assumed to be present in excess. Thus, the rate constants shown are really pseudo rate constants, where $k_x = k_x' = k_x [O]^m$ (Fogler 1992). Values of the rate constants and reaction orders were shown in Table 8. Derivations of the rate expressions used in the model are shown in Appendix D; these are based on the experimental data shown in Appendix C.

The rate of chemical oxidation was determined experimentally, and estimates of the biological sulphur formation and degradation rates were obtained from the ARC data (Budwill and Coleman 1999; Coleman and Dombroski 1995). It was not possible to obtain individual estimates of r_{biol} and r_{biol,SO_4} from the ARC data, so a lumped biological parameter, expressing the net rate of biological sulphur deposition was used in the modelling. Chemically formed solid sulphur is less accessible and favourable to microbial attachment than biologically formed sulphur, although the microorganisms can use both as sources of energy (Knickerbocker et al. 2000; Tichý 1994). The rate of conversion of chemically deposited sulphur to sulphate appears to be the rate-limiting step in the H_2S degradation process, and further experimentation is required to obtain reliable estimates of this rate. Future sulphur deposition models should include independent estimates of r_{biol} and r_{biol,SO_4} . A more detailed discussion of H_2S biofilter kinetics is shown in Section 5.2.3.

In the model, the accumulation of solid sulphur is assumed to begin at the inlet and move towards the outlet of the biofilter. The deposition is also assumed to occur uniformly across the radius of the filter. It proceeds by plugging the pores of the solid support, either by filling the pores themselves, or by coating the support surface with a uniformly thin layer of sulphur. These assumptions have been verified experimentally (Allen and Yang 1992; Budwill and Coleman 1999). Scanning electron micrographs of sulphur-coated peat (see Section 5.2.1) revealed that the peat surface becomes uniformly coated with sulphur, and that there are occasional large sulphur particles stuck to the surface of

the solid support. With the regular addition of nutrient solution or water, it is expected that some of the solid sulphur will be washed to the bottom of the filter and out with the effluent. Experimentally, this amount was estimated by liquid-liquid extraction of the sulphur in the effluent with CS₂.

To model sulphur formation, the concentration of H₂S is calculated from the pollutant profile over the length of the biofilter. The rate of formation of sulphur is then calculated for each layer of the biofilter (assuming that the sulphur forms uniformly across each biofilter layer, with all subdivisions lumped into one). New values for the porosity and remaining volume for sulphur deposition are calculated according to:

$$E_{\text{new}} = \frac{EV - V_s}{V} \quad (3-14)$$

These calculations are repeated until the entire available volume of the biofilter is plugged.

4.0 Experimental

4.1 Overview of approach

The main focus of these experiments was to determine appropriate kinetic parameters for chemical H_2S degradation in a biofilter. There are three main reactive processes occurring in the filter: chemical sulphur formation, biological sulphur formation, and biological sulphur degradation (oxidation). An estimate of the biological conversion rates was obtained from the ARC data (Budwill and Coleman 1999; Coleman and Dombroski 1995), but no prolonged abiotic experiments were conducted at the ARC; the experiments focussed instead on biological conversion.

An estimate of the chemical sulphur formation rate was obtained by doing abiotic biofiltration experiments with high H_2S loading rates. All of the ARC data collected prior to biofilter inoculation (Coleman and Dombroski 1995) were collected using influent H_2S concentrations of less than 400 ppm; the current experiments were done with much higher H_2S loading (>1000 ppm) so as not to duplicate the existing data. A higher loading rate also more closely simulates conditions for the most recent ARC experiments (Budwill and Coleman 1999), which are closer to the range anticipated for field biofilter applications. The materials and methods used in these experiments are largely identical to those used at the ARC (Budwill and Coleman 1999; Coleman and Dombroski 1995).

The experimental effort described in this thesis is divided into two areas: 1) abiotic experiments to determine the chemical sulphur formation; and 2) tracer studies to obtain information regarding the residence time distribution in the column, and how it changes over time. Information related to experimental procedures and analytical techniques is presented in the following sections.

4.2 Column design and construction

4.2.1 Materials

The filter columns were constructed from black ABS plastic piping, following the method used at the ARC (Budwill and Coleman 1999; Coleman and Dombroski 1995).

The list of materials included:

- 1) Black ABS plastic piping, 5 cm (2") ID (for the main body)
- 2) Black ABS plastic piping, 4 cm (1.5") ID (for the side-arms)
- 3) Unions and fittings for the above
- 4) Stainless steel fittings for sampling ports and transmission tubing
- 5) Stainless steel tubing, 0.64 cm (0.25") OD
- 6) A rotameter to control the flow of air (Model 604, Matheson, Parsippany, NJ)
- 7) An air filter for the house air (MICROalescer®, Wilkerson Corporation, Engelwood, CO)
- 8) A stainless steel metering valve to control the flow of H₂S ("22" Series, Whitey, Highland Heights, OH)
- 9) Nalgene® carboy bottles
- 10) PFA plastic tubing, 0.64 cm (0.25") ID
- 11) A peristaltic pump for water addition (Model 7014, Cole-Parmer, Vernon Hills, IL)
- 12) Miscellaneous glassware
- 13) Plastic canvas exclusion mesh (3 mm mesh size)
- 14) Check valves to prevent the backflow of H₂S ("C" series, NUPRO, Willoughby, OH)

All piping was purchased in the plumbing section at The Home Depot®. Fittings and tubing were purchased from Swagelok®, through Edmonton Pipe and Fitting Ltd. All

tubing, valves and fittings that came into contact with H₂S were constructed of stainless steel, Teflon® and Aflon®, to prevent corrosion problems.

4.2.2 Column construction

Two filter columns were constructed: one for the tracer studies, and another for the H₂S experiments. The tracer study column was constructed according to the dimensions used at the ARC (Budwill and Coleman 1999). Due to space constraints in the fume hood, the H₂S biofilter was approximately half as large as the tracer column. The H₂S biofilter was operated in down-flow (co-current gas and water streams) mode to remove H₂S from an air stream.

The tracer study column consisted of a 5 cm (2") × 1 m black ABS plastic pipe with caps attached at both ends, clamped vertically onto a frame support structure. The H₂S biofilter, which had dimensions of 5 cm × 42 cm, was constructed with unions and side-arms on each end. An exclusion mesh, made of plastic canvas mesh (3 mm mesh size), was placed into the filters at both ends, to prevent the loss of matrix material. A water addition port was inserted at the top of the H₂S biofilter, to provide moisture for the chemical reaction. Edmonton tap water was used in the experiments. A summary of the major chemical, physical and microbiological parameters of the water can be found in Appendix E. The water flow rate was set to a nominal flow rate of 2.7 mL/min, or approximately 4 L/d.

Black 4 cm (1.5") × 20 cm ABS plastic tubes were connected to the top and bottom of the H₂S biofilter, at right angles to the upright section of the biofilter. These tubes were capped on one end, and served as an air emission mixing tube and disposal manifold connection, respectively. Air was directed downward into the biofilter and exhausted out the bottom. The mixing tube was connected to the house air supply, regulated to a delivery rate of 8.5 L/min. The air was filtered before use. The H₂S was provided from a cylinder (99.6 percent purity, Praxair, Edmonton) and was introduced to the air stream

at a mixing junction, using a tee fitting. A micro-metering valve was used to regulate the flow of H_2S . The gas delivery rate to the filter provided a nominal residence time of 22 s. Figure 8 shows a schematic diagram of the H_2S biofilter used in the experiments.

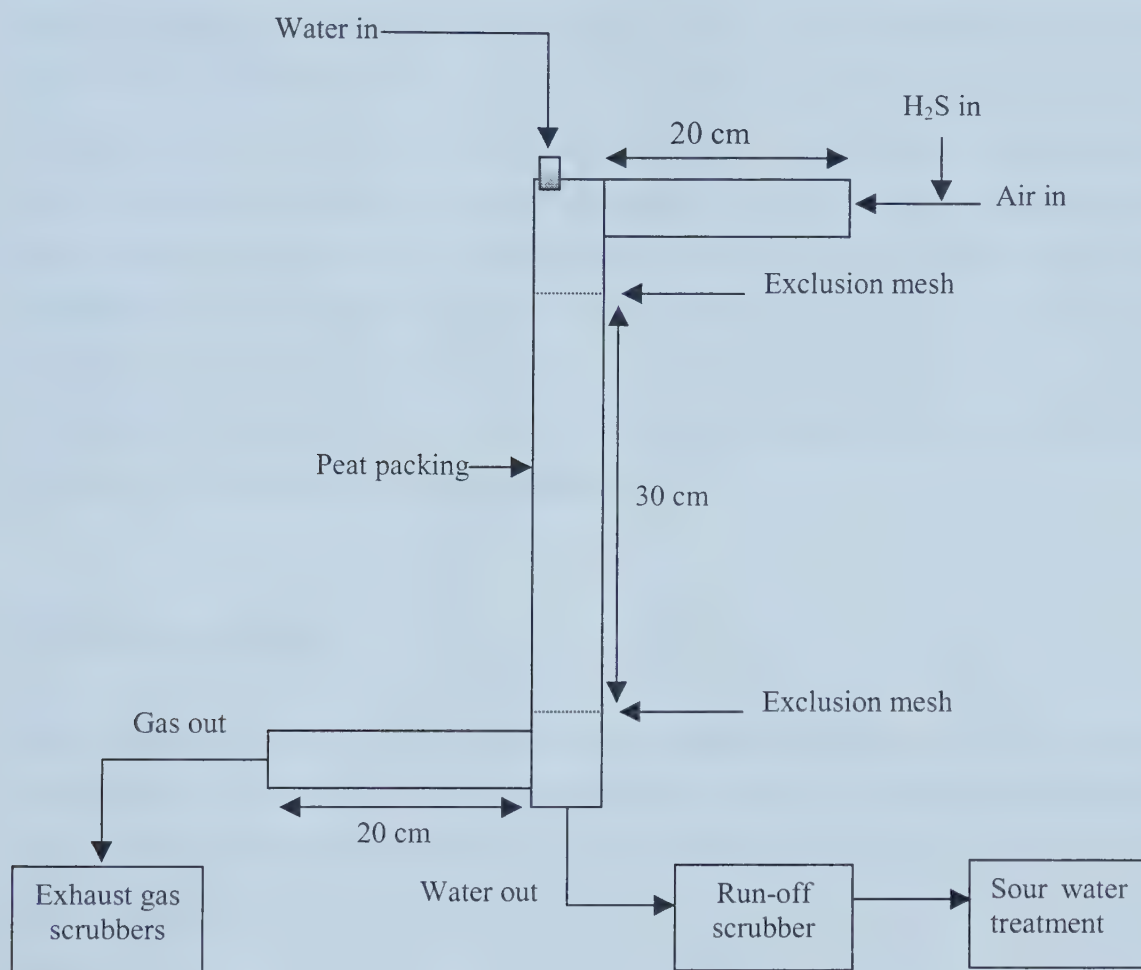


Figure 8: Schematic diagram of the H_2S biofilter used in the chemical oxidation experiments

The columns were packed with coarse Alberta sphagnum peat that had been screen rejected from an agricultural peat bagging operation. The peat was originally supplied by Lakeland Peat Moss of Edmonton, and donated to the University of Alberta by the ARC. All peat was sieved through a screen (13 mm mesh size) before use. Smaller sized particles were not used, in order to avoid large pressure drops due to less void space within the bed. Both columns were packed with approximately $70 \text{ mg peat/cm}^3 \text{ bed}$

volume. The final bed volumes were approximately 2030 cm³ and 850 cm³ for the tracer study column and the H₂S biofilter respectively.

H₂O₂ (30 percent w/w, Fisher Scientific, Fair Lawn, NJ) was used to treat both the gaseous emissions as well as the excess water eluting from the bottom of the H₂S biofilter. The scrubbers were constructed by drilling several venting holes into a Nalgene® carboy bottle filled with H₂O₂. For the gas scrubbers, four carboy bottles in series, each containing 500 mL of H₂O₂ were used. The liquid effluent drained into a small scrubber, to which 50 mL of H₂O₂ were added daily. The overflow from this scrubber drained into a large waste pail. The pail was replenished with 1.5 L of H₂O₂ at the beginning of each experiment. The absence of H₂S in the air stream leaving the final scrubber was checked using lead mercury strips (Fisher Scientific, Fair Lawn, NJ), which turn black in the presence of inorganic sulphides.

4.2.3 Substance delivery

Water was delivered to the H₂S biofilter using a peristaltic pump set to a flow rate of approximately 2.7 mL/min. The H₂S was diluted directly into the air stream and delivered to the biofilter. The influent volume of air was maintained by monitoring the rotameter and making adjustments as necessary.

4.3 Experimental procedure

4.3.1 Chemical oxidation studies

The biofilter experiments at the ARC involved the pre-moistening of the peat with culture before packing it into the biofilter column. This was followed by the pumping of up to 10 L of culture onto the top of the column as the air and H₂S delivery commenced (Budwill and Coleman 1999). To attain similar humidity levels in the peat used in these

experiments, the culture additions were simulated using water. Approximately 70 g of peat were pre-moistened by soaking in 3 L of water overnight. The column was then packed with 57 g (dry weight) of the pre-moistened peat. Water was added to the column during the experiments at a rate of approximately 4 L/d.

The air and H₂S flows were turned on to provide a concentration of approximately 1000 ppm, at a flow rate of 8.5 L/min. The water was provided right from the beginning of the experiment, to prevent drying out of the matrix material. The experiment was allowed to run for 1 week, before the H₂S flow was turned off and the system was purged with N₂ for 30 min. This procedure was repeated twice, for a total of three runs at 1000 ppm. The same procedure was followed for four runs at 3000 ppm, running for 2 d, 3 d, 5 d, and 1 week. The control run involved running only air and water through peat, for 1 week, to determine the background mass loss. This number was used in calculating the gravimetric peat balances.

An abiotic control, using plastic foam instead of peat, was performed in order to determine whether the H₂S removal observed in the biofilter was truly the result of chemical oxidation, and not due to indigenous microbial populations in the peat. Black plastic foam packing was autoclaved for three cycles of 15 min at 120°C, with at least 5 hours in between cycles. This ensured the killing of any spores that may have germinated as a result of the initial autoclaving. The column and side-arms were sterilised using 30 percent (w/w) H₂O₂, and the pump tubing was thoroughly flushed with H₂O₂ before use. All water used in the abiotic control experiment, including the water used to pre-soak the foam, was boiled for 10 min before use. The water reservoir was covered with aluminium foil to prevent contamination from the surrounding air. All influent air was filter sterilised. Otherwise, the experimental procedure was identical to the one outlined above, for an influent concentration of 1000 ppm H₂S, for the duration of 1 week.

For safety reasons, all H₂S experiments were done in a fume hood. The H₂S cylinder was placed directly into the fume hood, and all equipment was leak tested prior to use. Leak testing was done to a pressure of 20 psi using a helium sniffer gas leak detector (Model

21-250, Gow Mac Instrument Co., Bethlehem, PA). An H₂S detector (MiniH₂S®, Mine Safety Appliances Company, Pittsburgh, PA), set to alarm at 10 ppm, was placed at all times between the user and the H₂S cylinder.

4.3.2 Tracer studies

Tracer studies were performed for the 1 m tracer study column filled with Raschig rings, dry peat, and moist peat. The RTD for the 42 cm H₂S biofilter was also determined, both before and after a chemical oxidation experiment (1000 ppm H₂S for 1 week) had been completed. No water was flowing through the columns during the tracer studies.

Pulse injection tracer tests were conducted using methane (85 – 90 percent purity), from the house natural gas line as a tracer. The methane pulse injections were performed manually, using a 20 mL syringe. The methane was injected into a septum located in a tee junction before the inlet to the column. The outlet methane concentration was measured directly using a gas chromatograph equipped with a flame ionisation detector (Model 5890A, Hewlett Packard (Agilent), Palo Alto, CA) attached directly to the column tubing. In order to retrieve the measured concentrations in a computer system, the measurements were converted to ASCII files using Star chromatography software (Varian Systems, Walnut Creek, CA). The computer was connected to the gas chromatograph by means of an ADC adapter port.

The pulse injections were performed in triplicate, allowing just enough time between each injection for the outlet methane concentration to reach the background baseline of zero. This ensured both instantaneous methane concentration measurement and reproducibility of the samples.

4.4 Experimental methods

4.4.1 Scanning electron microscopy

Scanning electron microscopy (SEM) was used to observe the deposition of sulphur on the biofilter support matrix. The matrix support material (peat or foam) was removed as a core from the column. Samples were removed from various portions of the core. All samples were dried at 105°C for at least 24 h before analysis. Sub-samples were mounted on an SEM mounting stub using colloidal graphite. Mounted samples were coated with carbon using a carbon evaporator, and examined using a scanning electron microscope (Hitachi S-2700). Photographs were taken at 10 keV for secondary electron images, and 20 keV for back-scattered electron images. Digital images were collected using a Princeton Gamma Tech (PGT) IMIX system.

4.4.2 Energy dispersive x-ray spectroscopy

The scanning electron microscope (Hitachi S-2700) described above was also equipped with energy dispersive x-ray spectroscopy (EDX). Sub-samples of peat and foam from the biofilter matrix were prepared as outlined above. The samples were analysed by exposing selected locations of each sample to x-rays through focusing a beam spot of 1 µm in diameter on the matrix. Emission spectra were collected for 200 to 500 s at 20 keV in EDX mode, and detected with an x-ray detector (Prism Intrinsic Germanium, PGT). EDX was used to analyse qualitatively for the presence of sulphur, and also for iron and other metals, because these are known to catalyse the chemical oxidation of H₂S. All SEM and EDX work was performed by Tina Barker, the Chemical and Materials Engineering SEM technician.

4.4.3 Moisture content

Peat moisture content was determined gravimetrically by weighing triplicate sub-samples of 8 – 10 g of peat into tared aluminium pans. The samples were then dried in an oven with anhydrous calcium sulphate at 105°C for 48 h, and then re-weighed. The difference in weight before and after was considered to be the water content of the sample. Moisture content was reported as a fractional value.

4.4.4 Wet chemical methods

Sulphate was analysed using ion exchange chromatography, by Brian Rolseth in the Limnology Laboratory, Department of Biological Sciences, at the University of Alberta.

Solid sulphur was extracted from the biofilter effluent by means of liquid-liquid extraction with CS₂ (Spectranalyzed, Fisher Scientific, Fair Lawn, NJ). Well-mixed 50 mL samples of the effluent were extracted with an equal volume of CS₂. Multiple extractions did not improve the recovery. Due to the small amounts of sulphur recovered from the samples, the mass was determined by difference, after evaporation of the solvent. An estimate of the total sulphur present in the effluent was then obtained by multiplication.

4.4.5 Combustion analysis

Sulphur determination was done by combustion by Darlene Mahlow in Micro-analytical Services, Department of Chemistry, at the University of Alberta. Dried peat samples from the biofilter were manually homogenised with a mortar and pestle prior to submission for analysis.

4.4.6 Interparticle porosity

An estimation of the initial void space in the biofilter was attained by filling the biofilter with moist peat and then completing the volume with water. The amount of water used gave an indication of the amount of void space available. The interparticle porosity was calculated as the quotient of water volume over the total column volume.

5.0 Results and discussion

The results from the tracer studies are presented in Section 5.1, and the results of the chemical oxidation experiments are described in Section 5.2. The tracer study and chemical oxidation experiments provided parameters for the model; results of the modelling are presented in Section 5.3. The results from this thesis have implications for the use of H₂S biofilters in industry. These implications are presented in Section 5.4.

5.1 Tracer studies

5.1.1 Background

Tracer tests are used to obtain information about the flow characteristics in a reactor, and have been used in biofilters and biotrickling filters (MacFarlane 1998; Mysliwiec et al. 1996; Zarook et al. 1998). For packed beds, including biofilters, tracer studies are useful both to describe the air movement through the bed, and to calculate the effective interparticle porosity of the bed (Devinny et al. 1999).

Plug flow is an idealised flow pattern that would be observed in an ideal tubular reactor. When making the plug flow reactor (PFR) assumption, it is assumed that the fluid moves through the reactor as a plug, and spends an identical length of time in each part of the reactor. This results in a flat velocity profile and no axial mixing. By continuously monitoring the outlet concentration after the injection of a pulse of tracer, it is possible to obtain the concentration profile of the gas leaving the biofilter. Peak broadening of the concentration versus time profile occurs primarily as a result of two phenomena: axial diffusion and heterogeneous flow.

Deviations from plug flow in a biofilter occur because of channelling and short-circuiting. Short-circuiting occurs when the resistance to flow in a biofilter medium

varies strongly from place to place. This has the effect of drastically reducing the overall contact time and treatment efficiency. Significant tracer detection before the idealised (assuming plug flow) gas detection time is a clear indication of short-circuiting (Devinny et al. 1999). Channelling may cause the air path through the biofilter to be either longer or shorter than expected, depending on the types of fissures and channels present in the biofilter medium. A long peak tailing after the bulk of the tracer gas has been detected is an indication of channelling and dead zones within the biofilter bed (Devinny et al. 1999). Both short-circuiting and channelling result in regions of low permeability within a biofilter, and result in poor treatment efficiency.

Deviation from plug flow is commonly described by one of two models: the tanks-in-series (TIS) model and the dispersion model. Both of these models use one adjustable parameter to characterise non-ideal flow through a vessel. This parameter is the number of tanks in series for the TIS model and the dimensionless quotient of convective over diffusive flux for the dispersion model.

5.1.1.1 Tanks-in-series model

The TIS model is often used to describe non-ideal reactors. The TIS model treats the non-ideal reactor as a series of identically sized CSTRs. For a series of n equally sized CSTRs, the RTD is given by:

$$E(\Theta) = \frac{n(n\Theta)^{n-1}}{(n-1)!} e^{-n\Theta} \quad (5-1)$$

where $\Theta = t/t_m$ and t_m represents the mean residence time given by the RTD analysis.

The number of tanks in series for a particular system can be calculated from tracer experiments using the dimensionless variance, σ_Θ^2 :

$$n = \frac{1}{\sigma_{\Theta}^2} = \frac{t_m^2}{\sigma^2} \quad (5-2)$$

As n becomes large, the behaviour of the system approaches that of a plug flow reactor.

5.1.1.2 Dispersion model

The dispersion model involves a modification of the ideal reactor by imposing an axial dispersion term on plug flow. The dispersion term is governed by an analogy to Fick's law of diffusion and accounts for molecular and turbulent diffusion effects. This model compensates for axial mixing problems, as well as for effects caused by radial mixing and other nonflat velocity profiles (Levenspiel 1972). In dimensionless form, the basic equation representing the model describes a mass balance of the tracer is as follows:

$$\frac{dC}{d\Theta} = \frac{1}{Pe} \frac{d^2C}{dZ^2} - \frac{dC}{dZ} \quad (5-3)$$

where Pe is the reactor Peclet number, strictly called Pe_r , defined as UH/D_a . The reciprocal of Pe_r , D_a/UH is called the vessel dispersion number.

The dispersion model, shown in equation 5-3, has various solutions, depending on the type of boundary conditions chosen. Four common boundary conditions are often used: Gaussian, closed-closed, open-open, and closed-open. In a closed-closed vessel, it is assumed that there is no dispersion or radial variation in concentration either upstream (closed) or downstream (closed) of the reaction section. In an open-open vessel, dispersion occurs both upstream (open) and downstream (open) of the reaction section. A closed-open vessel boundary condition indicates that there is no dispersion in the entrance section, but that there is dispersion in the reaction and exit sections.

The calculation of the reactor Peclet number depends on the boundary conditions used when solving the transport equation for the dispersion model. Several solutions are as follows:

Gaussian solution:
$$Pe_r = \frac{2t_m^2}{\sigma_t^2} \quad (5-4)$$

Solution for an open-open system:
$$\frac{\sigma_t^2 Pe_r^2}{t_m^2} - 2Pe_r - 8 = 0 \quad (5-5)$$

Solution for a closed-closed system:
$$\frac{2}{Pe_r^2} (Pe_r - 1 + e^{-Pe_r}) - \frac{\sigma_t^2}{t_m^2} = 0 \quad (5-6)$$

Solution for a closed-open system:
$$\frac{2}{Pe_r} \left(1 + \frac{1.5}{Pe_r} \right) - \frac{\sigma_t^2}{t_m^2} = 0 \quad (5-7)$$

The boundary conditions most likely resembling the experimental set-up used in the laboratory are the ones used for an open-open vessel system. This boundary condition applies when the tracer is injected into a packed bed more than two or three particle diameters downstream from the entrance, and measured some distance upstream from the exit (Fogler 1992).

5.1.2 Tracer study results

To determine whether channelling was taking place, whether dispersion was important, and to estimate the bed porosity, tracer tests were conducted across the tracer study column (1 m column) and the H₂S biofilter (42 cm column). Methane pulse injection tests were performed across the empty tracer study column, as well as for packing with dry peat, wet peat, and Raschig rings. The injections were carried out in triplicate. For the H₂S biofilter, tracer studies were performed both before and after a chemical oxidation

experiment, wherein the originally fresh peat packing was subjected to 1 week of H₂S loading at 1000 ppm. Sample calculations for the RTD analyses are presented in Appendix F.

The RTD was calculated for each run; the results are shown in Table 9. The numbers presented are averages of at least three runs performed for each type of packing. Figures 9 and 10 show the RTDs in graphical form.

Table 9: Residence time distributions for tracer studies performed on two sizes of biofilter columns, using triplicate pulse injections of methane

Column	Bed material	t_m (min)	σ^2 (min ²)	σ (min)
Tracer study column	Empty column	0.43	0.01	0.12
	Dry peat	0.43	0.01	0.11
	Wet peat	0.34	0.01	0.11
	Raschig rings	0.33	0.004	0.06
H ₂ S biofilter	Fresh (wet) peat	0.37	0.03	0.18
	Sulphur-coated (wet) peat	0.36	0.04	0.19

For the tracer study column, at a flow rate of 8 L/min, the expected residence time for an ideally mixed reactor would be 0.30 min. For the H₂S biofilter, the ideal residence time would be 0.29 min. The data in Table 9 show that both biofilters exhibit non-ideal mixing behaviour; the observed residence times are higher than the predicted residence times. The shortest residence time was obtained when ceramic Raschig rings were used to pack the tracer study column. Raschig rings are easily characterised, and provide a large amount of free space (77 percent) in the column. The highest residence times were obtained using dry peat and an empty column. These two scenarios are similar, because both allow for significant amounts of vortexing and swirling within the column, due to the high linear velocity of the carrier gas.

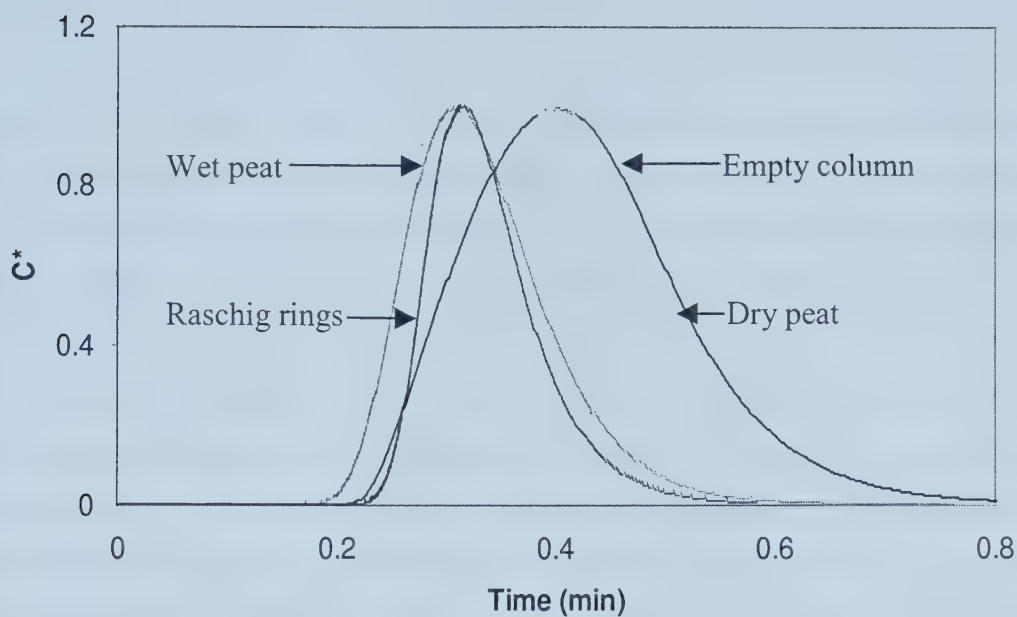


Figure 9: Normalised concentration profiles obtained for the 1 m tracer study column, using various different packings.

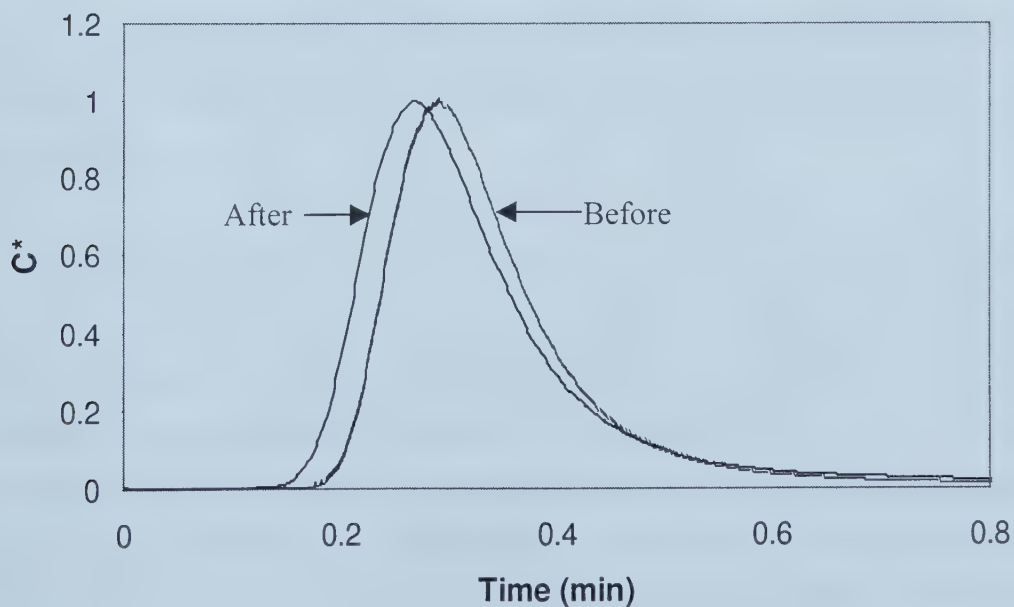


Figure 10: Normalised concentration profiles for tracer studies obtained for the 42 cm H_2S biofilter, before and after sulphur deposition (1000 ppm H_2S for 1 week).

The two tracer curves in Figure 10 are slightly different, with a shift to the left indicating a decrease in porosity in the sulphur-coated as compared with the fresh peat. This is consistent with the data shown in Table 10, which indicate that slight differences in porosity were present between the two columns. Sulphur deposition was observed to cause a decrease in apparent porosity from 1.7 to 1.6. However, despite these differences, the data in Table 9 show that no significant differences exist between the results of the tracer tests done before and after sulphur deposition on the column. This is because different methods of analysis have various sensitivities to experimental data. To obtain more accurate data, longer experiments should be run; 1 week at 1000 ppm is not long enough to observe significant drying out and sulphur deposition in the column. The biofilters operated at the ARC were exhibiting significant drying out and plugging only after several months of operation at high sulphur loading rates (Budwill and Coleman 1999). It is expected that a severely overloaded column would exhibit both channelling (bimodal curves) and a significant increase in the amount of dead space in the column (curves shifting towards the left).

The variations in residence times (σ^2) obtained within the column were very similar between runs. This indicates both the reliability of the experimental method and the reproducibility of the data.

The unimodal curves in Figures 9 and 10 show that there was no apparent channelling through the column at the time of the tracer studies. Channelling would have been indicated by bimodal curves. This was as expected, because channelling can be caused by water flowing through the filter, drying out due to the high air flow rate, or a change in porosity due to sulphur deposition. No water was flowing through the column during the tracer experiments, and there was no possibility of any additional sulphur deposition. Mysliwiec et al. (1996) studied channelling in biofilters and concluded that biofilters may operate for significant amounts of time with channels in formation, but that no symptoms of channelling are displayed until the channellised flow reaches a critical point. They also showed that it is possible to obtain unimodal curves even with significant channelling occurring, as long as there is a significantly high number of channels.

Experimentally, the only way to determine the presence of channels is to sample at different locations within the bed height and obtain residence time distribution curves for each section of the biofilter bed (Mysliwiec et al. 1996).

The earlier peak of the wet peat response curve in Figure 9 indicates the short mean residence time observed with this packing. For each peak, the effective volume is calculated by multiplying the volumetric flow rate by the residence time. Therefore, a shorter residence time indicates a lower effective volume. For example, in comparing the dry peat and the wet peat, the air flowing through the wet peat passes through a smaller effective volume and therefore exits faster. This indicates the existence of dead spaces within the bed. A decrease in porosity is shown by the displacement of the unimodal peaks towards the left, indicating lower retention times. The wet peat and Raschig ring-filled columns gave an effective volume of about 2.7 L, compared with 3.4 L for the dry peat-filled and empty columns.

The wider the peaks in the diagram, the more dispersion was present during the experiment for that particular column. Axial dispersion is the phenomenon primarily observed in this biofilter, as the peaks were broadened in a symmetrical manner (Devinny et al. 1999). High dispersion was expected in the peat columns, because of the variation in shape and size of the peat particles as compared with the uniform Raschig rings.

Even though the column for the H₂S biofilter was shorter than the tracer study column, the presence of side-arms on the smaller column increased the volume, which increased the residence time. In an ideal reactor (perfect mixing), the porosity can be determined from the tracer studies by multiplying the flow rate across the bed by the residence time measured in the bed. This gives the effective volume, which can be divided by the total volume to give an estimate of porosity. The results obtained using different packing materials and columns are shown in Table 10.

Clearly, the assumption of ideal mixing does not apply to these two columns. Calculating the porosity by the effective volume method, described above, results in physically

impossible porosity values of greater than one. These high values may have arisen from the high velocity of the nitrogen used in the tracer studies (8 L/min). MacFarlane (1998) found that the effective porosity found using tracer studies increased as the superficial gas velocity increased when conducting tracer tests in a compost- and wood chip-packed bed. These changes were explained on the basis of the dependence of the mean residence time on the coefficient of dispersion and linear velocity (MacFarlane 1998).

Table 10: Effective bed porosity for the two columns, as calculated assuming an ideal, perfectly mixed reactor

Column	Bed medium	Effective Porosity
Tracer study column	Empty bed	1.51
	Dry peat	1.52
	Wet peat	1.18
	Raschig rings	1.14
H ₂ S biofilter	Fresh (wet) peat	1.71
	Sulphur-coated (wet) peat	1.61

5.1.3 Flow pattern calculations and discussion

Two models are commonly used to account for non-idealities in mixing: number of tanks-in-series and the dispersion model.

5.1.3.1 TIS model

The number of tanks in series needed to give the same RTD as an ideal reactor was calculated for each type of packing. The results are summarised in Table 11.

Table 11: Average number of tanks-in-series needed to approximate ideal reactor RTD, for the two columns with various packing materials

Column	Packing	n
Tracer study column	Empty column	14
	Dry peat	16
	Wet peat	9
	Raschig rings	31
H ₂ S biofilter	Fresh (wet) peat	4
	Sulphur-coated (wet) peat	3

For the TIS model, the higher the number of tanks-in-series needed, the closer a reactor system approximates an ideal plug-flow reactor. At low values of n the reactor approximates mixed flow. Thus, $n=1$ corresponds to an ideal mixed flow reactor, while $n>30$ indicates that plug flow is achieved. The data in Table 11 show that the H₂S biofilter used in these experiments exhibits almost ideally mixed flow. For the tracer study column, the data in Table 11 show that the Raschig rings provide for plug flow within the column, whereas the peat packing and empty column have flow regimes that lie somewhere between mixed and plug flow. This is a further indication of dispersion occurring within the biofilter. Clearly, neither column is subject to the idealised plug flow pattern so commonly assumed for biofilters.

5.1.3.2 Dispersion model

The reactor Peclet number was calculated for the different types of packing used in the tracer experiments, using various different boundary conditions. The results are shown in Table 12.

Table 12: Reactor Peclet numbers calculated using different boundary conditions, in response to a pulse tracer input of methane

Column and packing	Gauss Pe	Open-open Pe	Closed-open Pe	Closed-closed Pe	Average Pe	Dispersion coefficient
Tracer study column						
Empty bed	27	31	28	26	28	0.04
Dry peat	31	35	33	30	32	0.03
Wet peat	18	21	7	17	17	0.06
Raschig rings	63	67	63	61	63	0.02
H₂S biofilter						
Fresh peat	8	11	10	7	9	0.11
Sulphur-coated peat	7	10	8	6	8	0.13

As seen in Table 12, the Peclet numbers calculated using different boundary conditions were mostly in close agreement with one another, except when using the closed-open boundary condition on the wet peat. For the dispersion model, $Pe \rightarrow 0$ approximates mixed flow, while $Pe \rightarrow \infty$ approximates plug flow. As expected, the Raschig rings gave the highest Peclet number, as they most closely resemble a well-defined and ideal system. The highest amounts of dispersion were seen in the H₂S biofilter, which is the column that also exhibits almost ideal mixed flow. The wet peat, in both of the columns, was the most non-ideal system, because of the channelling and short-circuiting that happens when water is present in a reactor system.

The inverse of the Peclet number, called the dispersion coefficient, can be used to predict the extent of backmixing occurring in a closed vessel, as shown in Figure 11.

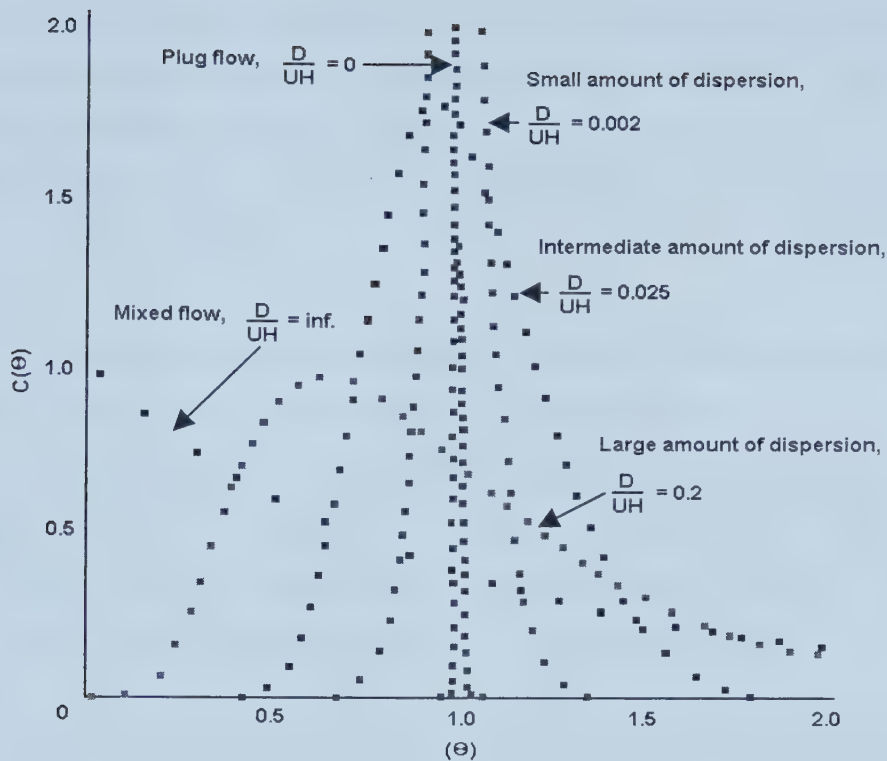


Figure 11: Concentration curves in closed vessels for various extents of backmixing, as predicted by the dispersion model (after Levenspiel 1972)

As $1/Pe \rightarrow \infty$, the system approximates mixed flow, while $1/Pe \rightarrow 0$ approximates plug flow. Systems undergoing plug flow have tracer study curves that resemble sharp spikes. As backmixing increases, the curves broaden to the point where the distribution is no longer bell-shaped and the maximum concentration is detected leaving the reactor right from time zero. This is characteristic of mixed flow.

Based on the data shown in Table 12 and Figure 11, a biofilter packed with moist peat can be classified as a reactor system subject to between medium and large amounts of dispersion.

5.1.4 Conclusions from the tracer studies

Both the TIS and the dispersion models indicated that the tracer study column and the H_2S biofilter exhibit non-ideal flow, somewhere between the mixed flow and plug flow

regimes. Both are subject to medium to large amounts of dispersion. This suggests that the assumption of plug flow in the gas phase is not valid for the biofilter used at the ARC, so boundary conditions incorporating dispersion were included in the model. Biofilters have been modelled using the dispersion model by incorporating Danckwerts boundary conditions (Zarook et al. 1998).

Because it is possible to obtain unimodal tracer curves even in the presence of significant channelling, further tests are recommended to fully characterise the flow within the biofilter. These could include the use of tracer step changes instead of pulse inputs, smoke tests, and radial measurements of the pollutant concentration at different levels within the biofilter bed. The use of a clear column, instead of the black ABS piping, would also help to reveal visible channelling occurring within the bed.

Different methods of flow pattern analysis can result in different conclusions about the significance of experimental data. Wherever possible, more than one method of analysis should be used to interpret data collected using tracer studies.

5.2 Chemical oxidation studies

5.2.1 SEM and EDX analyses

SEM analysis was used to obtain a qualitative picture of the distribution and extent of sulphur deposition on the peat and foam used in the H₂S experiments. Selected particles were then further analysed with EDX, for qualitative composition analysis. These were compared with control samples that had not been exposed to H₂S. The scanning electron micrographs of a peat sample taken from the biofilter inlet are shown in Figures 12 and 13. Figure 12 shows the matrix structure of peat, with sulphur particles (indicated by arrows) scattered throughout. Figure 13 shows a close-up of the sulphur particles; the large particle at the bottom of the picture is also seen in Figure 12.



Figure 12: SEM micrograph of sulphur-coated peat. The arrows indicate sulphur particles.



Figure 13: SEM micrograph of selected particles on sulphur-coated peat. The arrows indicate sulphur particles.

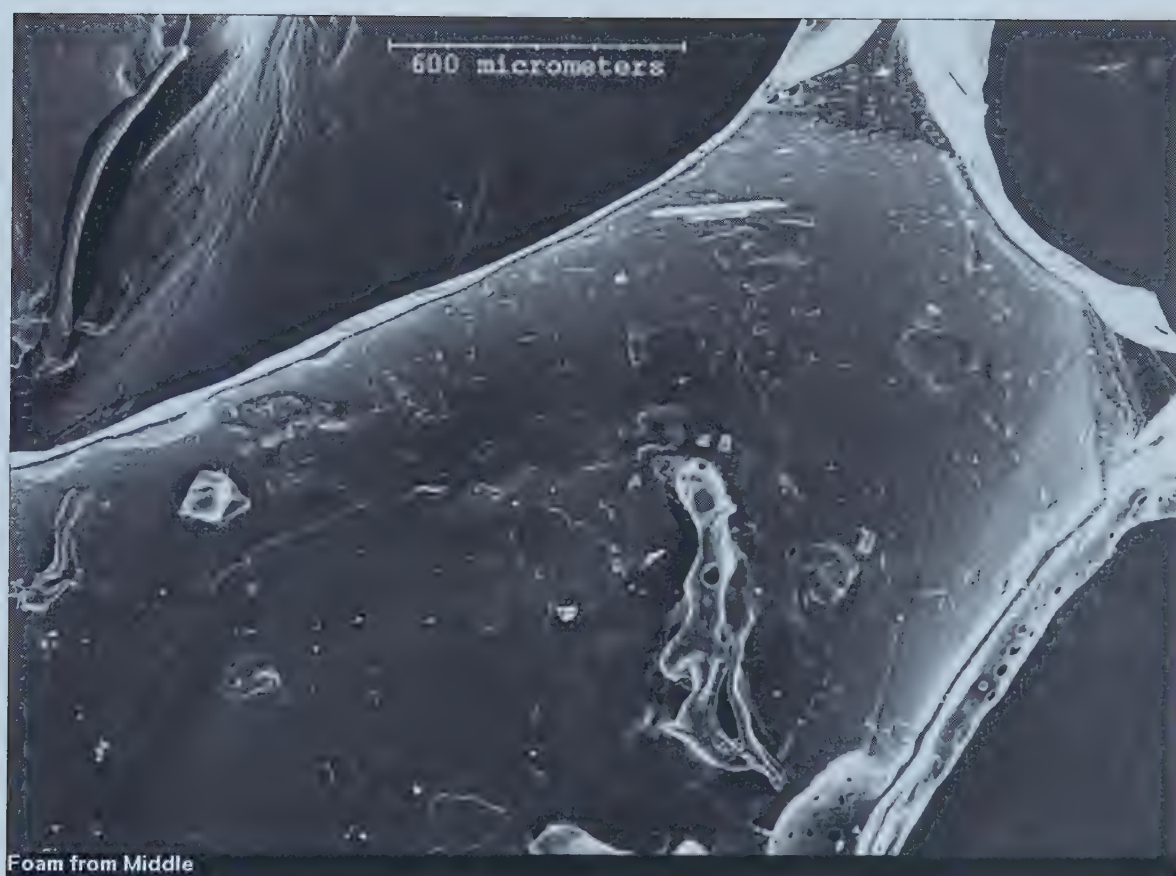


Figure 14: SEM micrograph of selected particles found on a webbed section of sulphur-coated foam

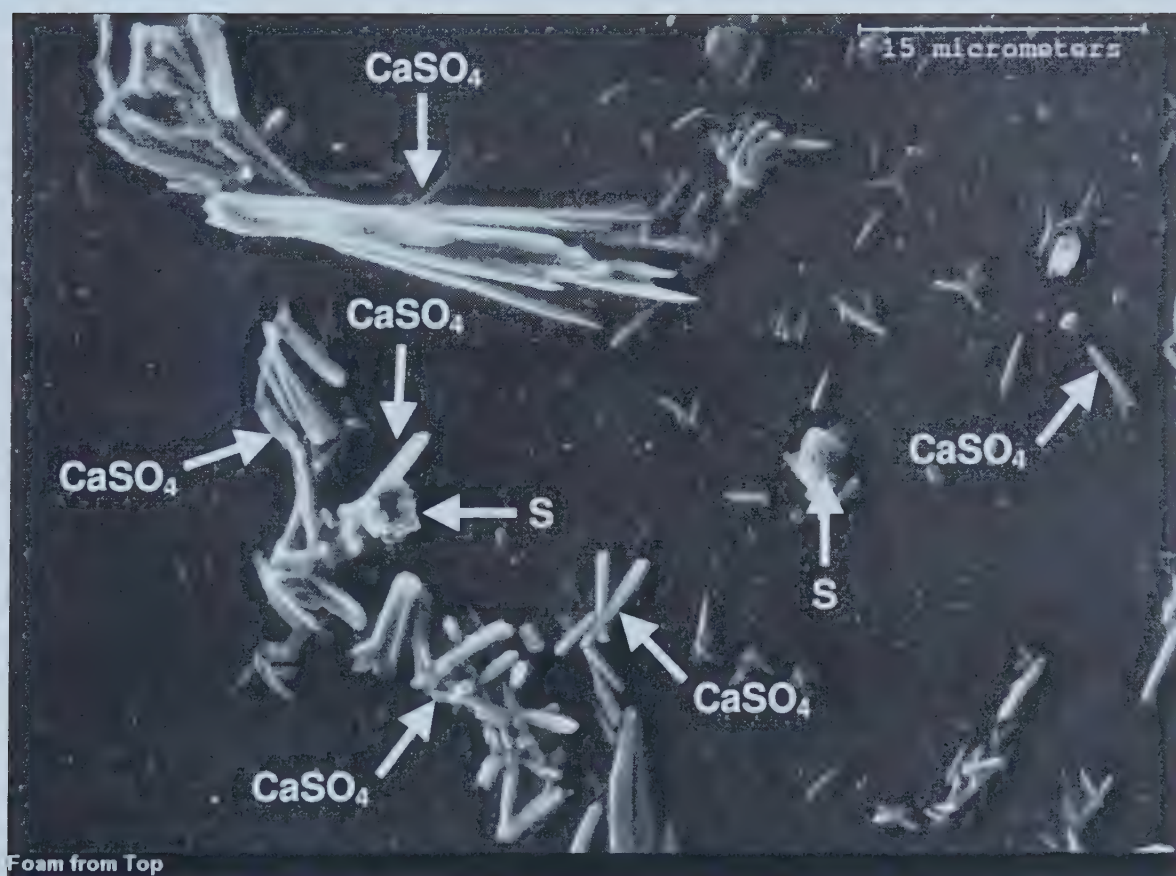


Figure 15: SEM micrograph, at higher magnification, of selected particles found on a webbed section of sulphur-coated foam. The arrows indicate H_2S oxidation products.

The photographs shown in Figures 12 and 13 were obtained using back-scattering electrons (BSE), which cause areas of differing composition to glow with various intensities. Because BSE images are obtained by collecting electrons reflected from the sample, the analysis is highly sensitive to the topography of the sample and is not usually recommended for non-flat samples. Peat has quite a varied topography; thus the lighter spots on the ribs of the sample may indicate either a thin film of sulphur deposition, or simply a height difference that is affecting the reflection of the beam. Irradiation is also destructive to the samples, and focussing the beam on any one spot for longer than approximately one minute causes thin layers of sulphur to vaporise before an SEM micrograph or EDX surface scan can be collected.

EDX analysis of the peat samples shows significantly higher sulphur contents in the samples taken from the column after the completion of the experiments, as compared with the control. However, this sulphur is not highly visible using the SEM. There are a few larger sulphur particles, seen in Figures 12 and 13, but the bulk of the deposition appears to be finely dispersed over the entire peat matrix. Peat is an extremely porous substance, and it is probable that sulphur is deposited in the pores, causing them to fill up. This is very difficult to detect with SEM, as the peat samples are not flat and uniform. This makes them difficult to analyse. EDX was used only as a qualitative measure of sulphur deposition; sulphur deposited on the peat support was quantified with combustion analysis (see Section 5.2.2).

Because the foam used as packing in one of the H_2S experiments was not suited for combustion analysis, SEM and EDX were used to qualitatively indicate the presence of sulphur. The micrographs shown in Figures 14 and 15, reveal that foam has much less surface area available for sulphur deposition than peat. The structure of foam consists of a network of ribs connected in some places by a “web.” Foam consists mainly of carbon and oxygen. The surface of the foam used in the H_2S experiment was covered with particles that were composed mostly of iron, aluminium and other metals. Some of the particles had relatively high sulphur contents. These were mainly irregular, shapeless particles scattered throughout the sample, adhering either to the ribs or web of the foam.

Figures 14 and 15 show the presence of crystalline deposits (indicated with arrows) that were identified with EDX analysis as containing both calcium and sulphur, possibly in the combination of CaSO_4 . These particles were not observed in the peat samples, but may have been difficult to detect due to the topography of the peat samples. The foam samples were mostly flatter than the peat samples, especially in the webbed portions. In one sample, the presence of sulphur was somewhat obscured by the presence of lead; lead and sulphur have overlapping emission spectra.

Tables 13 to 15 show composition analyses for peat and foam biofilter packing. The samples that are designated as ‘control’ in the tables below were never exposed to H_2S . EDX analysis cannot be used to analyse quantitatively for carbon or oxygen, which comprise the bulk of organic samples. As such, it is important to note that the numbers in Tables 13 to 15 are normalised concentration values, and not absolute percent composition values. The overall EDX scan of the foam control particle showed no elements other than carbon and oxygen.

Table 13: Composition analysis (normalised weight percent) determined by EDX scans of three isolated particles on a webbed sub-section of the foam control

Element	Particle 1	Particle 2	Particle 3
Na	0.5	-	4.0
Mg	3.4	0.9	3.7
Al	3.5	-	1.4
Si	46.4	10.0	2.0
P	-	-	0.8
S	4.7	-	4.8
Cl	3.5	0.7	38.9
K	4.7	0.5	24.6
Ca	29.5	1.9	12.4
Ti	0.6	-	-
Fe	3.2	85.1	2.7
Cu	-	0.9	2.5
Zn	-	-	2.2

Table 14: Composition analysis (normalised weight percent) determined by EDX scans for sulphur-coated foam from the top of the H₂S biofilter. The three particles were all found on webbed sub-sections of the foam.

Element	Overall	Particle 1	Particle 2	Particle 3 (CaSO ₄ crystal)
Na	-	0.8	-	2.2
Mg	8.1	2.3	5.6	4.7
Al	8.2	8.9	10.0	0.5
Si	20.3	28.8	22.4	0.2
S	9.5	6.0	14.1	47.0
Cl	-	0.7	-	-
Pb	-	-	18.6	-
K	0.2	0.3	1.6	0.9
Ca	5.1	3.1	9.9	43.9
Ti	3.2	16.0	1.5	-
Fe	40.2	14.1	9.9	0.6
Cu	5.2	1.1	3.6	-
Zn	-	1.7	2.8	-
Ba	-	16.2	-	-

Table 15: Composition analysis (normalised weight percent) based on EDX scans for control and sulphur-coated peat from the top of the biofilter. The two particles on the sulphur-coated peat were chosen at random, and appear to be composed largely of sulphur.

Element	Control	Sulphur-coated Overall	Particle 1	Particle 2
S	8.5	33.5	54.7	74.9
Ca	70.5	61.7	45.3	23.3
Mg	10.8	4.8	-	1.8
Al	5.1	-	-	-
Si	5.1	-	-	-

The data in Tables 13 and 14 show that there were many impurities present in the black packing foam used in these experiments. Visually, the main difference between the control and experimental samples was the presence of elongated crystals, also seen in Figures 14 and 15. These were identified as CaSO_4 on the basis of elemental analysis with EDX. Many trace metals and elements were also present, both in the experimental and control samples. This indicates that they are inherent to the foam itself, and are not artefacts of the experiment. It was thought originally that the calcium and magnesium observed in some of the samples may have come from the tap water used in the experiments, but significant amounts of both were observed in the control samples (that had not been wetted). There was no significant decrease in trace noble metals detected in the experimental over the control samples. This indicates that metal-catalysed H_2S oxidation was not occurring during the abiotic biofiltration experiments. The presence of noble metals, such as Fe, is known to catalyse the chemical oxidation of H_2S (Kuhn et al. 1983; Okabe et al. 1998).

The data in Table 15 show that there are fewer impurities and trace metals present in peat than in foam. The only difference between the control and sulphur-coated samples shown in Table 15 is the presence or absence of H_2S . Both samples came from biofilter experiments of 1 week in length, with continuous water washing at a rate of approximately 3 L/d. The composition of the peat samples shown agree with what has been reported in the literature. Heathwaite (1993) lists Si, Al, Ca, Na, K, and Mg to be major elements in peat. Peat samples are very heterogeneous; their composition depends on their peat bog of origin (Heathwaite 1993).

Significant amounts of calcium and magnesium were detected in both the peat and the foam packing; this provided cations for the formation of sulphate salts. However, no CaSO_4 crystals were observed during SEM analysis of the peat, and there is proportionately more sulphur in the particles analysed than would be present in CaSO_4 . This indicates that both sulphur and sulphate salts were formed during the chemical oxidation experiments. Sulphate salts have previously been observed in H_2S biofilters (Allen and Yang 1992). Because CaSO_4 crystals are quite small, relative to the sulphur

particles observed, and peat has a more highly varied topography than foam, it is possible that there were CaSO_4 crystals in the peat that could not be observed due to analytical limitations. Sulphur was observed, using SEM, mostly in big clusters, but EDX analysis revealed that it was likely also present as a fine film coating the entire sample.

EDX analysis of the peat revealed no significant presence of metals either before or after the oxidation studies, indicating that metal-catalysed H_2S oxidation was not a factor in the chemical oxidation experiments. Peat is known to contain low concentrations of metals, in comparison with other common biofilter packing materials (Degorce-Dumas et al. 1997).

5.2.2 Quantitative sulphur recovery

The H_2S biofilter was disassembled after the completion of each chemical oxidation experiment. When the peat was arranged as a core, yellow-green deposits were present towards the influent end of the matrix. The deposits had a sulphurous smell associated with them, especially upon drying in the oven. Combustion and EDX analyses confirmed that these deposits were composed mainly of sulphur, in the form of solid sulphur and SO_4^{2-} salts. These products have been previously observed as atmospheric sulphur oxidation products (Allen and Yang 1992; Wainwright 1984). A white-yellow powder was also present right at the inlet of the biofilter (prior to begin of the packing), where the influent H_2S first came into contact with the water trickling through the filter. This same powder was found coating the gas outlet of the effluent scrubber. It had a sulphurous smell associated with it. It is not known whether the sulphur (S) recovered in these experiments has the chemical designation of S^0 or S_8 , because analytical techniques were not available to distinguish between the two.

Some sulphur was also washed through the H_2S biofilter, because of the constant trickle of water downwards. This sulphur was quantified by extraction with CS_2 . Chemical analysis revealed the extracted compound to be composed of 53 percent O, 15 percent S, 2 percent C, and 3 percent H. The presence of high quantities of O indicates that the

sulphur recovered from the effluent may have contained sulphate salts in addition to elemental sulphur. A small fraction of the influent H_2S was chemically converted to SO_4^{2-} . The rest was assumed to pass through unchanged, and was determined by difference. Figure 16 shows the total sulphur recovery versus time for the H_2S biofilter at two different inlet concentrations. The total sulphur deposited is the sum of the sulphur deposited on the peat, detected in the effluent (as SO_4^{2-}), and extracted from the effluent (as S). The raw data are shown in Appendix C.

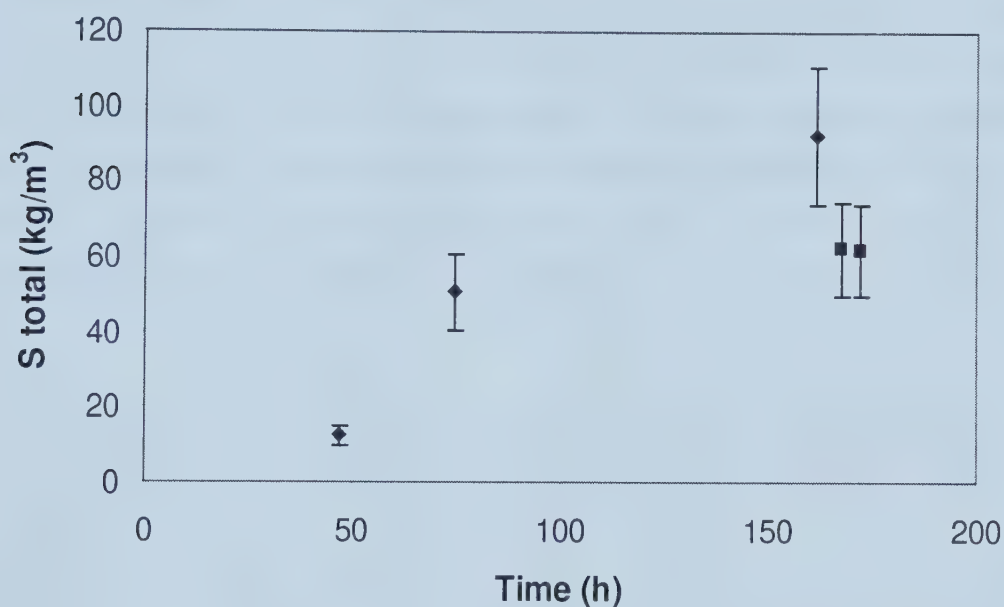


Figure 16: Chemical sulphur deposition over time in the H_2S biofilter, at 3000 (♦) and 1000 (■) ppm inlet H_2S concentration.

The data in Figure 16 show that chemical sulphur deposition follows a roughly linear trend. More sulphur was deposited at a higher inlet concentration of H_2S , with the final sulphur concentrations reaching 62 and 93 kg/m^3 for inlet concentrations of 1000 and 3000 ppm H_2S , respectively. These data were used to determine the kinetic rate constants for chemical sulphur formation, for input into the model.

The error on the data points shown in Figure 16 was calculated to be ± 20 percent. This was calculated by summing the percent contribution to the overall error of each analytical

method used. Most of the error came from the determination of the sulphur deposited on the peat. Homogenising the samples was extremely difficult, and the combustion analysis consistently gave variable results for the same samples. It would be instructive to complete a full sulphur balance on the columns, including measurements of the H_2S in the inlet and outlet streams and at various points along the length of the biofilter. However, the measurement of H_2S concentrations is not trivial, and suitable equipment was not available to perform this analysis during the time of experimentation.

Most of the H_2S oxidised in the H_2S biofilter was recovered as solid sulphur adhering to the peat matrix. Much of this sulphur was deposited near the inlet of the biofilter, but sulphur was detected all the way along the column. Prior to homogenising the peat samples, the matrix core was divided into four approximately equal parts. The parts were labelled BF-1 to BF-4, with BF-1 being the inlet section and BF-4 being the outlet section. Figure 17 shows the sulphur recovery from each section of the peat core.

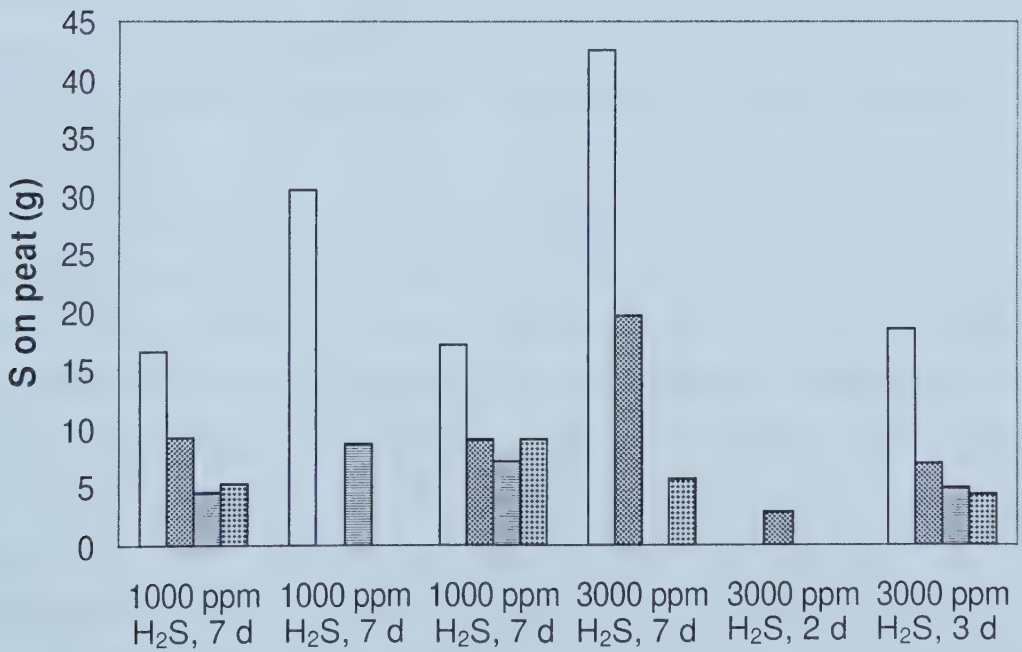


Figure 17: Sulphur recovery from the H_2S biofilter matrix after the completion of the chemical oxidation experiments. From inlet to outlet, the columns represent sections BF-1 (::), BF-2 (■), BF-3(≡), and BF-4(♦).

As seen in Figure 17, up to 43 g, or 63 percent of the total sulphur recovered was from the inlet section of the biofilter. Less sulphur was deposited on the remaining sections of the biofilter, though there are no consistent trends as to where the remaining sulphur was found, even under identical experimental conditions. The samples exhibited much heterogeneity. Part of the variation in sulphur deposition is due to the experimental error incurred in homogenising the core samples and determining sulphur by combustion analysis. It is also likely that some of the sulphur deposited in the inlet section of the biofilter was washed through the filter with the water trickling through the column. Any sulphur washed with the effluent may later have adhered to the peat at any point along the column, depending on the flow path of the water. This path was different for each experiment; it depends on how the peat was packed into the biofilter at the beginning of any one experiment.

The H₂S biofilter was run in co-current mode, with the polluted air and water flowing down through the column. This is in contrast to the ARC biofilter, which was run in counter-current mode. It is expected that more sulphur would have been washed out of the column in the ARC biofilter, because the influent H₂S oxidised to sulphur was immediately washed out of the column. For inlet H₂S concentrations of between 200 and 2500 ppm, the maximum amount of sulphur recovered from the peat in the ARC biofilters for experiments of 35 to 50 d was approximately 17 g (Budwill and Coleman 1999). This is significantly less sulphur than was observed during the current chemical oxidation experiments. One explanation for this is that in the H₂S biofilter used for this experiment, sulphur was only deposited, and never degraded. The difference in sulphur deposition between these two experiments suggests that microbial sulphur degradation plays a significant role in biotic H₂S biofilters. *T. thiooxidans* can grow on both chemically and biologically formed sulphur, although biological sulphur is preferred (Knickerbocker et al. 2000; Tichý 1994). This results in a prolonged life span of the filter bed, as sulphur blocking the biofilter void space is degraded. Microbial sulphur degradation also results in significant sulphate formation.

The majority of the influent sulphur in the ARC experiments was converted to sulphate (Budwill and Coleman 1999). Significantly less sulphate was detected in the effluent of the H₂S biofilter in these experiments, as shown in Table 16.

Table 16: Sulphur in the effluent of an H₂S biofilter. The sulphate in the effluent was measured and converted to the corresponding amount of sulphur.

Sample	Time (h)	Sulphate (mg/L)	Sulphur (g)
Expt. 1 (1000 ppm)	171	36	0.24
Expt. 2 (1000 ppm)	172	25	0.17
Expt. 3 (1000 ppm)	168	135	0.81
Expt. 5 (3000 ppm)	47	0	0
Expt. 7 (3000 ppm)	75	0	0
Expt. 4 (3000 ppm)	162	30	0.20
Peat control (no H ₂ S)	142	30	0.20
Abiotic (1000 ppm)	168	80	0.54

The amount of sulphur present in the biofilter effluent was calculated by multiplication from the sulphate measured in the effluent. The analytical error incurred in obtaining the sulphate data shown in Table 16 is less than 5 percent. The reference value for these measurements is the sulphate found in Edmonton tap water (62 mg/L), which was subtracted from each individual measurement. In general, the amount of sulphate detected in the H₂S biofilter effluent increased over time.

Sulphate is generally assumed to be an indicator of microbial activity in H₂S biofilters (Wainwright 1984). The final pH of the liquid effluent of the H₂S biofilter used in the chemical oxidation experiments was between 2.8 and 3.2. Peat is naturally acidic; the initial pH was approximately 4.5. This shows that a decrease in pH is not always indicative of microbial activity. To confirm that the data obtained from the chemical oxidation experiments were representative of chemical removal, and not microbiological activity, several controls were performed in addition to the regular chemical oxidation experiments with the H₂S biofilter. The first was a peat control, where the column was

operated with only air and water flowing through the peat bed, for a period of 1 week. The second was an abiotic control, where all equipment and materials were sterilised before use. The data in Table 16 show that there were no large differences in the sulphate detected in the peat control and chemical oxidation experiments (Experiments 1 – 7). The possible exception to this is Experiment 3, at 1000 ppm, where 135 mg/L of sulphate were detected. However, both of the other experiments conducted at 1000 ppm showed significantly less sulphate formation; the data point for Experiment 3 likely reflects experimental error rather than microbial sulphate generation. More sulphate was detected in the abiotic (foam) experiments than in the peat experiments; peat has more surface area than foam, so less of the sulphate would have been washed out with the effluent. It likely adhered to the peat instead, in the form of calcium sulphate.

The amount of sulphate detected in the *T. thiooxidans*-inoculated ARC biofilter effluent for an inlet H₂S concentration of 67 ppm was approximately 1700 mg/L (Coleman and Dombroski 1995). The data in Table 16 are all significantly lower than this value, which confirms that biological activity was not contributing to sulphate formation during the chemical oxidation experiments. Rather, a small fraction of the influent H₂S was being chemically converted to sulphate under the experimental conditions. This is supported by the observation that bubbling H₂S through a beaker of water also results in sulphate formation. A solution of pure H₂S bubbled through a beaker of tap water for approximately 1 minute resulted in the formation of 20 mg/L of sulphate. This sulphate must be chemical in origin, because the system was unlikely to contain significant numbers of bacteria, and the oxidation was instantaneous. Chen and Morris (1972) also concluded that solid sulphur was the main product of H₂S oxidation under conditions of high H₂S loading.

Comparing the values in Table 16 to those shown in Figure 16 indicates that the amount of sulphur chemically converted to sulphate represents less than 2 percent of the total sulphur recovered. For the model, the chemical oxidation of H₂S was assumed to proceed to solid sulphur and the chemical oxidation of H₂S to sulphate was assumed to be negligible.

One of the initial hypotheses of the chemical H₂S oxidation experiments was that a significant amount of the influent H₂S in an inoculated biofilter, such as the one operated by the ARC, was converted chemically rather than biologically. This was supported by the short lag times prior to high H₂S removal efficiency observed at the ARC, and also by the significant removal observed even at high gas flow rates (which do not allow much time for the microorganisms to degrade the H₂S). Generally, a lag time of a few minutes to days is observed in biofilters, as microorganisms acclimate to new substrates (Devinny et al. 1999). An extremely short lag time may therefore indicate either a pre-enriched culture or an alternate oxidation process, such as chemical oxidation. The overall percent recovery of sulphur in the chemical oxidation experiments is shown in Table 17. The percent chemical oxidation reported is the total amount of sulphur recovered on the peat (as S), in the effluent (as S), and in the effluent (as SO₄²⁻), divided by the total amount of influent sulphur.

Table 17: Chemical oxidation in the H₂S biofilter

Sample	Concentration of H ₂ S (ppm)	Total time (h)	% Chemical Oxidation
Expt. 2	1000	172	49
Expt. 3	1000	168	51
Expt. 5	3000	47	13
Expt. 7	3000	75	32
Expt. 4	3000	162	27

The data in Table 17 show that between 13 and 51 percent of the influent sulphur (as H₂S) was recovered (as S or SO₄²⁻) in these experiments. As discussed in relation to Figure 16, these data are subject to an experimental error of up to 20 percent. When this is added to the data shown in Table 17, up to 70 percent of the influent sulphur was chemically oxidised in the H₂S biofilter. More sulphur was apparently recovered at a lower inlet concentration of H₂S, but this may be indicative of experimental error equally as much as of a trend. Degorce-Dumas et al. (1997) observed an initial efficiency of 60 to

65 percent in a sterilised H₂S biofilter, which was attributed to physicochemical phenomena including adsorption, absorption, and chemical H₂S oxidation. A rigorous sulphur balance, incorporating gas phase concentration data at various points along the biofilter column, as well as more experiments at different concentrations, are needed to draw further conclusions about trends in the data shown in Table 17.

The data shown in Table 17 provide evidence that chemical removal plays an important role in the contaminant removal observed in H₂S biofilters, contributing up to 70 percent of the overall H₂S removal. The chemical H₂S oxidation experiments were only a few days to a week long, whereas the ARC experiments ran for up to 50 d. The differences in overall sulphur deposition in these experiments as compared to the ARC experiments suggest that some of the initially (chemically) deposited sulphur is later oxidised to sulphate by the microbial culture present in an inoculated H₂S biofilter. Almost no acclimation phase was ever observed at the ARC (Budwill 2000b). This was thought to be due to the high density of culture inoculation and the extreme activity of the culture on H₂S (Budwill 2000b). The data collected during the chemical H₂S oxidation experiments suggest that it was chemical, and not biological removal that was responsible for the short acclimation phase and high initial removal efficiency. The high chemical removal in the H₂S biofilter was also aided by the high surface area and adsorptive capacity of peat (McNevin et al. 1999).

5.2.3 Kinetics of H₂S removal

The model predictions are based on the H₂S removal kinetics observed in the ARC biofilter. The net rate of H₂S elimination in the ARC biofilters was linear over the range of concentrations used. This is shown in Figure 18. The rate of H₂S elimination from the gas phase, plotted on the y-axis, was calculated as:

$$r = \frac{Q}{V} (C_{h,in} - C_{h,out}) \quad (5-8)$$

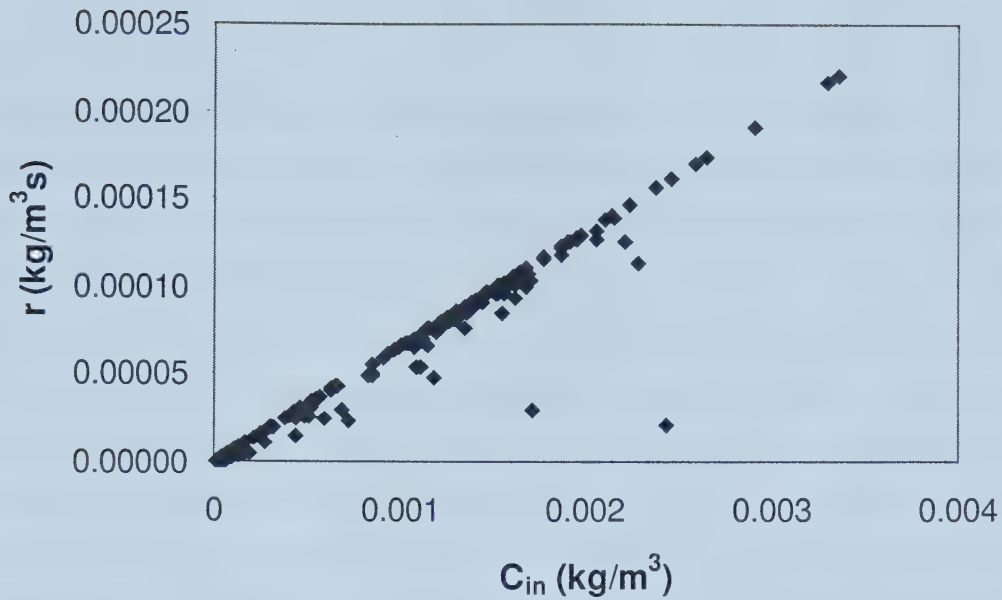


Figure 18: Observed removal rate in a 1 m laboratory-scale H₂S biofilter, inoculated with *T. thiooxidans*. Data are shown are from experiments conducted at the ARC in 1995 and 1999 (Budwill and Coleman 1999; Coleman and Dombroski 1995).

The data shown in Figure 18 follow a trend that is linear. This indicates that the kinetics in the biofilter are first-order over the range of H₂S concentrations shown. Many biofilters display apparent zero-order kinetics, especially at high concentrations, where the elimination capacity of the biofilter is usually constant over a certain range of inlet pollutant concentrations (Deshusses et al. 1995a). Figure 18 shows that the elimination capacity of the ARC biofilter did not level off over the range of concentrations tested, even though these concentrations were higher than those in most previously published H₂S biofilter experiments (Budwill and Coleman 1999). A levelling off of the elimination capacity would indicate local overloading of H₂S (Yang and Allen 1994b), but this was clearly not a problem during the ARC experiments.

Because there are three kinetic processes operating in the biofilter, the rate described by equation 5-8 can also be expressed as:

$$r = r_{\text{chem}} + r_{\text{biol}} - r_{\text{biol,SO}_4} \quad (5-9)$$

It is important to note the distinction between equations 5-9 and equation 3-10. The rate of H₂S depletion from the gas phase (r) during biofilter operation does not equal the rate of sulphur formation in an H₂S biofilter (r_s). The rate of H₂S depletion from the gas phase during the chemical oxidation experiments (r_{chem}) is not equivalent to the rate of sulphur formation due to chemical oxidation ($r_{s,\text{chem}}$), because the protons in H₂S are converted to water (see equation 2-3), and some H₂S passes through the biofilter unchanged. The kinetic calculations for $r_{s,\text{chem}}$ and r_{chem} are shown in Appendix D. The value of the last two terms on the right hand side of equation 5-9, $r_{\text{biol}} - r_{\text{biol,SO}_4}$, is indicative of the net sulphur deposition by the microbial culture in an H₂S biofilter, and is hereafter referred to as the total biological activity. Solid sulphur begins to accumulate in H₂S biofilters when the sum of the biological and chemical sulphur deposition rates surpasses the rate of biological sulphur degradation.

The observed rate of H₂S depletion in a biofilter, denoted as r in equation 5-9, is the sum total of the chemical and biological activity rates. An estimate of the total biological degradation activity can therefore be obtained by subtracting the chemical degradation rate, determined by experimentation, from the observed total H₂S removal rate. For microbial sulphur deposition, the breakthrough or balance point in an H₂S biofilter happens when the culture is depositing solid sulphur faster than it is being degraded. At the balance point, the biological sulphur degradation rate and the biological sulphur deposition rate are equal but opposite. Microbially produced sulphur will be deposited in the biofilter when the total biological activity, denoted by $r - r_{\text{chem}}$, or $r_{\text{biol}} - r_{\text{biol,SO}_4}$, is greater than zero, and no additional sulphur will be deposited when $r_{\text{biol}} - r_{\text{biol,SO}_4}$ is less than zero. Therefore, a plot of $r - r_{\text{chem}}$ can be used to determine the balance point for an H₂S biofilter. For a microbial culture following Michaelis-Menten kinetics, the balance point is indicated by the x-intercept of a plot of $r - r_{\text{chem}}$ versus inlet concentration. Such a plot is shown in Figure 19.

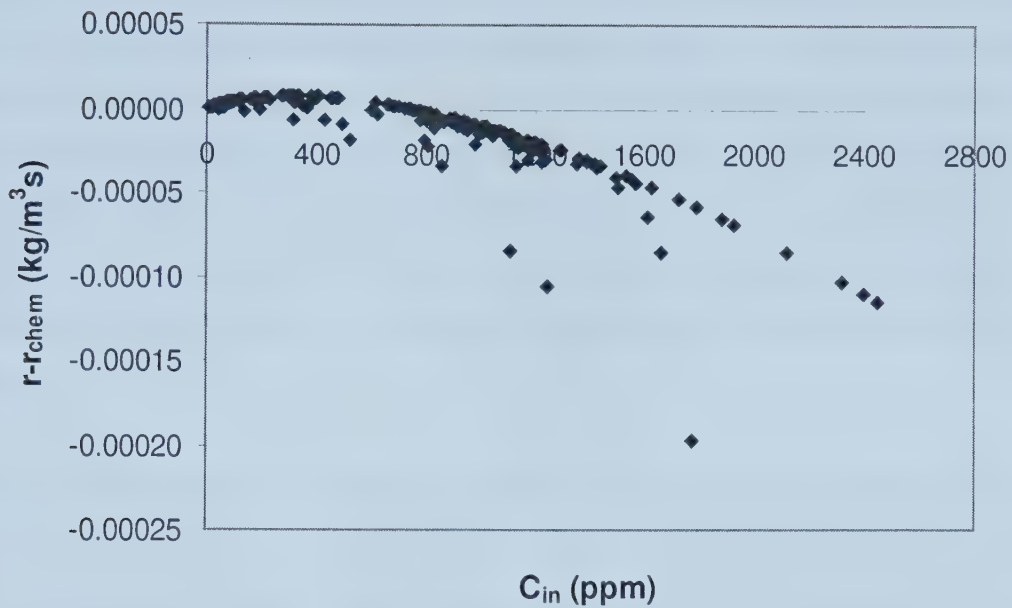


Figure 19: Total biological activity versus inlet concentration in an H₂S biofilter. Values of r were calculated from ARC data (Budwill and Coleman 1999; Coleman and Dombroski 1995), and r_{chem} was calculated with kinetic constants derived from experimental data.

Chemical sulphur deposition is independent of biological sulphur deposition, but the presence of chemically produced sulphur lowers the balance point because it significantly increases the amount of solid sulphur in the biofilter bed. Further experimentation is required to accurately predict the true balance point of the biofilter, incorporating both chemical and microbial sulphur deposition. Once independent estimates of r_{biol,SO_4} and r_{biol} are obtained, the sum of the biological and chemical deposition rates can be subtracted from the total rate of H₂S removal to predict the point at which sulphur first begins to accumulate in H₂S biofilters. Chemical sulphur deposition happens at all H₂S concentrations, but increasing the amount of sulphur present in the biofilter bed will lower the balance point because the microbial culture can degrade both chemically and biologically formed sulphur.

As shown in Figure 19, when the rate of chemical oxidation is subtracted from the overall rate, plotted in Figure 18, the data no longer fall on a straight line. The differences

between Figures 18 and 19 suggest that it is the combination of chemical and biological processes in the biofilter, and not solely the biological oxidation process that provides the apparent first-order rate that was shown in Figure 18. Biological H_2S degradation at high concentrations is generally thought to be zero-order (Yang and Allen 1994b). The apparent switch from zero- to first-order removal kinetics is thus a unique feature of H_2S biofilters, and occurs because H_2S can be oxidised both chemically and biologically. The differences in Figures 18 and 19 highlight the importance of chemical oxidation in H_2S biofilters.

The data in Figure 19 also show that the microbial culture in the H_2S biofilter at the ARC was not following simple Michaelis-Menten kinetics. The Michaelis-Menten model breaks down once the data begin to slope downwards. The presence of two roots indicates that this culture is exhibiting inhibition kinetics. Various sulphur compounds, including H_2S , HS^- , S^{2-} , SO_4^{2-} , and S are known to be inhibitory to microbial cultures (Buisman et al. 1990b; Cheng et al. 1999; Janssen et al. 1995; Wani et al. 1998a; Yang and Allen 1994b). The two roots (where the curve crosses the x-axis) in Figure 19 are at approximately 40 ppm and 800 ppm. The first root likely indicates the breakthrough point, above which microbially produced sulphur begins to accumulate in the biofilter. The second root likely denotes the point at which H_2S or SO_4^{2-} begins to become inhibitory to the microbial culture in the biofilter. At gas phase H_2S concentrations of higher than 800 ppm the apparent activity becomes negative, as the activity of the culture decreases due to inhibition. Wani et al. (1999) observed a similar tapering off of H_2S elimination capacity in their biofilters, at H_2S concentrations of greater than 140 ppm, but they did not acknowledge this to be the result of inhibition. Chung et al. (1997) found that H_2S concentrations above 140 ppm were inhibitory to *T. novellus*.

Attempts were made to fit the data shown in Figure 19 to an inhibition model. The model that provided the best fit was a modified form of an expression that is commonly employed to describe the effect of product inhibition on the growth of microbial cells. The model is as follows (Blanch and Clark 1997):

$$r_{\text{inhib}} = V_m \left(1 - \frac{C}{K_i} \right) \left(\frac{C}{K_s + C} \right) \quad (5-10)$$

where K_i is inhibition constant, or the value above which the growth of cells is inhibited. All inhibition models are empirical models; they do not describe the fundamental processes of inhibition. As such, it is possible to use a product inhibition model to model inhibition that may arise from any component present in the system, not only from products.

The values of V_m and K_s that were calculated from the ARC data and used in the model to describe the lumped, total biological activity are not the true values of V_m and K_s for this culture. Rather, they represent the apparent kinetics of a culture exhibiting inhibition kinetics. The effect of inhibition is to change both of these parameters from their “true” values. To find the true values of V_m and K_s a series of experiments designed to determine inhibition are needed. In the absence of rigorous experimentation, curve fitting can be used to determine plausible values of V_m , K_s for use in equation 5-10. It was assumed that H_2S is self-inhibiting in the biofilter, so that C in equation 5-10 is equal to C_{in} , the inlet concentration of H_2S . The value of K_i used was the value of the second root in Figure 19, above which the microbial culture in the biofilter was severely inhibited. The resulting plot is shown in Figure 20.

The curve in Figure 20 shows that microbially produced sulphur accumulates in the biofilter at concentrations of up to 800 ppm. Between 40 and 800 ppm, $r_{\text{biol}} > r_{\text{biol,SO}_4}$ and the culture is depositing sulphur faster than it can be degraded. Above 800 ppm, the culture becomes inhibited, and no additional (microbial) sulphur is deposited in the biofilter. In terms of chemical oxidation, above 800 ppm H_2S , $r_{\text{chem}} > r$ and chemical sulphur deposition becomes the dominant mechanism of solid sulphur deposition in the biofilter. However, it is important to note that the chemical oxidation of H_2S results in solid sulphur formation at all influent concentrations of H_2S ; it does not have breakthrough points analogous to those found in microbial sulphur deposition.

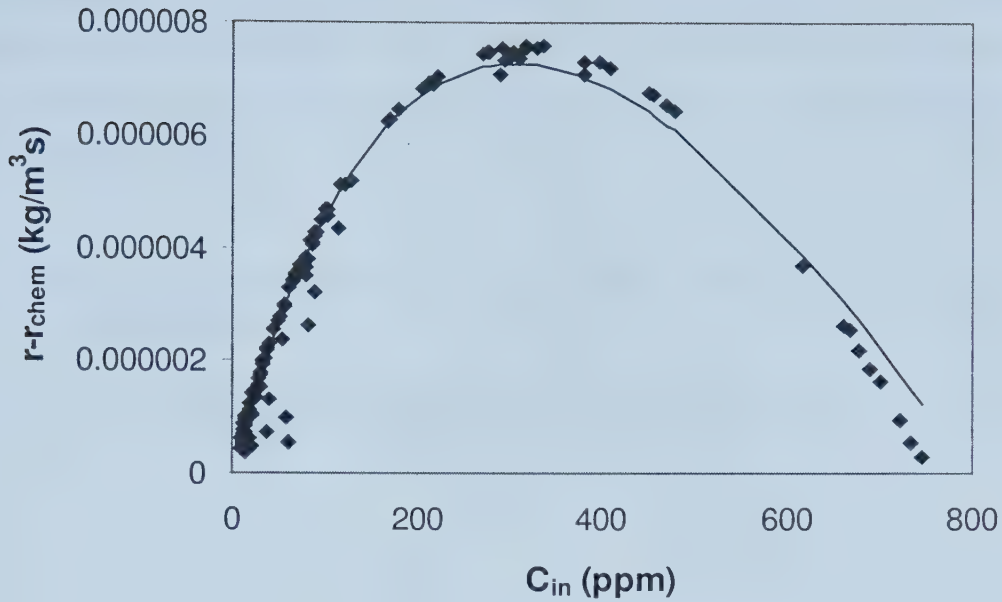


Figure 20: Modelling inhibition kinetics for H₂S self-inhibition in an H₂S biofilter. The curve shown is the model prediction obtained using a product inhibition model. Values of r and r_{chem} were calculated from ARC data (Budwill and Coleman 1999; Coleman and Dombroski 1995).

Even though the inhibition curve shown in Figure 20 provides an adequate fit to the biofilter data, there are many situations where multiple substrates and/or products may simultaneously limit the growth rate and activity of a microbial culture (Blanch and Clark 1997). As mentioned previously, H₂S, SO₄²⁻, and S, in their various oxidation states, have all been shown to be inhibitory to microbial systems. Inhibitors may act on a microbial system in numerous ways, including modifying chemical potential of reactants and products, altering cell permeability, altering enzyme activity, influencing the functional activity of a cell, and affecting enzyme synthesis (Blanch and Clark 1997). As such, further experimentation is needed to rigorously determine which components are truly inhibitory in an H₂S biofiltration system.

The effect of inhibition is to change the values of the kinetic parameters in a system, from true to apparent values. The “true” values of V_m and K_s were determined in this case by curve-fitting, to produce the curve shown in Figure 20. The curve fitting procedure used

was least squares analysis. Table 18 shows the effect of inhibition on the kinetic parameters in the ARC biofilter. The apparent values of the kinetic parameters shown in Table 18 are the original constants calculated from the ARC data, assuming linear Michaelis-Menten kinetics.

Table 18: Effect of inhibition on the apparent kinetic parameters in H₂S biofiltration

Parameter	Apparent value	Curve-fit value
V _m	6.81E-06	3.09E-05
K _s	0.000134	0.000682
K _i	-	3.95E-04

The values in Table 18 show that inhibition causes a decrease in both V_m and K_s for this system, which is usual in cases of substrate inhibition. The apparent kinetic parameters shown in Table 18 are the ones used in the model to describe the lumped biological activity in the system; they describe the apparent kinetic parameters of the system while under the effects of inhibition. The inhibition model shown in Figure 20 is a curve-fit only; it does not describe the fundamental processes occurring in the biofilter. As such, it is recommended that further inhibition studies be performed to determine more accurate inhibition parameters. These parameters should then be incorporated into the model.

5.2.4 Conclusions from the chemical oxidation studies

The results from the chemical H₂S oxidation experiments show that chemical oxidation plays a significant role in H₂S oxidation. Microbial H₂S oxidation, which is slower than chemical H₂S oxidation, becomes more important over time, as the microbes have time to “catch up” to the abiotic processes occurring in the biofilter. This agrees well with the results of McNevin et al. (1999), who observed a two-stage H₂S removal in biofilters and biotrickling filters: an initial chemical oxidation to elemental sulphur followed by a slower biological oxidation to sulphate.

It is important to note that although a significant amount of the H_2S removal in a biofilter is chemical in nature, the presence of microorganisms is vital to obtain 100 percent H_2S removal. Complete H_2S removal was not observed during the chemical oxidation experiments, but was consistently observed during the ARC experiments (Budwill and Coleman 1999; Coleman and Dombroski 1995). The presence of microbial cultures able to degrade H_2S is necessary for optimal biofilter operation. As noted previously, the presence of microorganisms in the biofilter also helps to prolong the life span of the filter bed, by oxidising much of the chemically deposited sulphur to sulphate. Sulphate is washed out of the biofilter with the biofilter effluent.

5.3 Model predictions

Because the kinetic processes occurring in the biofilter were de-coupled, the model is composed of two largely distinct parts. The first is concerned with the overall H_2S removal in the biofilter, which is discussed in Section 5.3.1. The second is the solid sulphur formation and subsequent biofilter plugging, as discussed in Section 5.3.2. The model proposed in this study was validated by predicting the performance of the 1 metre laboratory-scale ARC biofilter, inoculated with *T. thiooxidans*, that was capable of removing up to 2500 ppm H_2S (Budwill and Coleman 1999).

5.3.1 Modelling H_2S removal

5.3.1.1 Concentration profiles

Figure 21 shows the model predicted concentration profiles at steady state, for the gas phase of an H_2S biofilter operating at various inlet concentrations. The nearly linear shape of the curves agrees well with previously reported model predictions (Baltzis et al. 1997; Shareefdeen et al. 1993). The points shown in Figures 21 and 23 to 25 are for clarity, to distinguish between the curves; they do not represent experimental data points.

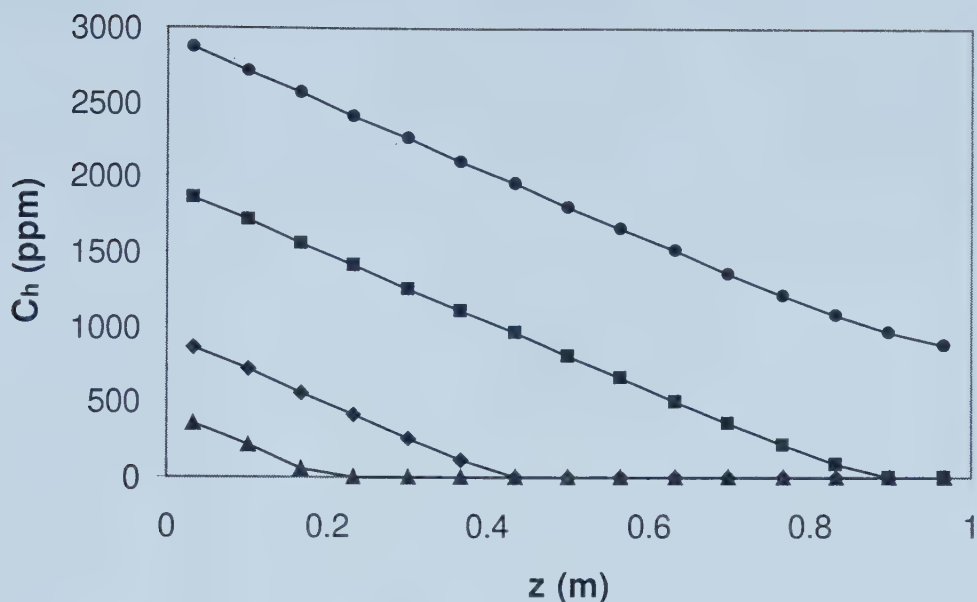


Figure 21: H₂S removal profiles in the gas phase, along the length of the biofilter, as predicted by the model. The curves are for inlet concentrations of 3000 (●), 2000 (■), 1000 (◆), and 500 (▲) ppm. All model parameters are as reported in Table 8.

Experimentally, the ARC biofilter was capable of completely removing H₂S to a maximum value of approximately 2500 ppm. The data in Figure 21 show that, at lower concentrations, the entire length of the biofilter is not needed to attain complete H₂S removal. For example, 500 ppm H₂S is completely removed 20 cm downstream of the biofilter inlet. This confirms the hypothesis that the biofilter at the ARC was over-designed. Every H₂S biofilter has a (unique) maximum loading capacity that depends on the microbial community, operating conditions, and physical parameters of the system (Allen and Yang 1991). The data in Figure 21 show that the maximum loading capacity for this particular H₂S biofilter occurs between 2000 and 3000 ppm inlet H₂S concentration, because the model predicts that 3000 ppm is not completely removed over the length of the biofilter. The removal rate of H₂S in the biofilter, as indicated by the slope of curves shown in Figure 21, is roughly independent of the inlet H₂S concentration.

The concentration of H_2S at the gas-biofilm interface in the biofilter is dictated by Henry's law. Because the concentration of H_2S in the gas phase decreases along the length of the column, so does the equilibrium concentration in the biofilm. Figure 22 shows the concentration profiles of H_2S in the biofilm, as predicted by the model for an inlet H_2S concentration of 2000 ppm.

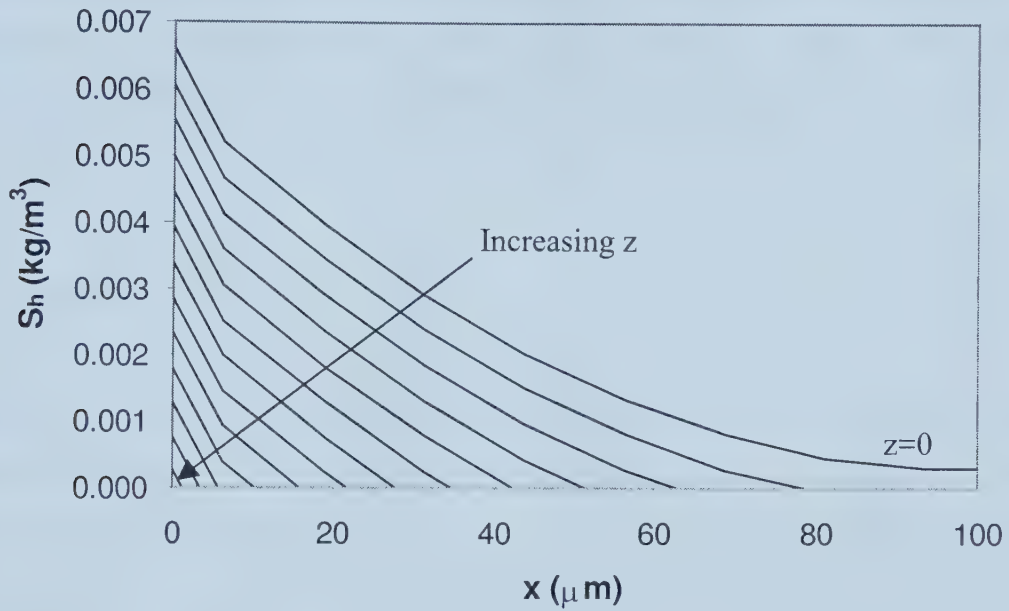


Figure 22: H_2S removal profiles in the biofilm, as predicted by the biofilter model. The inlet H_2S concentration is 2000 ppm, and all other parameters are those found in Table 8.

The data in Figure 22 show that complete H_2S removal in the biofilm is attained in all layers except at the column inlet ($z=0$). The H_2S concentrations in the biofilm decrease steadily along the length of the column, with the final curves indicating complete removal. It is clear that the substrate concentration varies nonlinearly along the biofilm. This agrees with the results presented by other authors (Amanullah et al. 1999; Baltzis et al. 1997; Shareefdeen and Baltzis 1994). The discontinuities in Figure 22 arise from the grid size used to approximate the biofilm. A finer grid gives smoother curves, but at the expense of increased computation time.

The depletion of H_2S in a fraction of the biofilm indicates that the maximum H_2S removal rate, by biodegradation and chemical oxidation, exceeds the maximum diffusion rate. This is characteristic of processes operating under diffusion control, where the diffusion coefficient is very low (Deshusses et al. 1995a). This is intuitive for this biofilter, because the pollutant is being degraded by both chemical and biological processes. *T. thiooxidans* has a high affinity for H_2S , and the chemical oxidation of H_2S is spontaneous under the operating conditions, so it is reasonable to assume that it is diffusion and not degradation that is limiting in this biofilter. In many other biofilters, where biological degradation is only method of pollutant removal, this assumption may not be valid.

5.3.1.2 Sensitivity to Pe

The shape of the curves shown in Figure 21 is determined in part by the value of the dispersion coefficient in the column. Dispersion is responsible for deviations from the idealised plug flow pattern, which are caused by channelling, the existence of stagnant regions because of non-uniformity in packing, and by a lack of adequate feed distribution. When there is much dispersion in a biofilter, the concentration profile is more curved from inlet to exit. The importance of dispersion in the H_2S biofilter was verified experimentally with tracer studies. The dispersion coefficient is inversely related to the experimentally determined Peclet number. The model sensitivity to the value of Pe is shown in Figure 23.

The curves in Figure 23 have increasing, or less negative, slopes as the Pe number in the biofilter is decreased. At lower Pe, less of the column is active in effecting the removal of H_2S . More of the influent gas is being dispersed (or channelled) through the column, and therefore is passing through without being degraded. This is reflected in Figure 23 by the decreasing apparent inlet concentrations seen at lower Pe. Changes in the Peclet number have a very pronounced effect in the low Peclet number regime (<100), as seen in Figure 23. The Peclet number typically encountered in biofilter operations is in the

range of 300 to 600, where axial dispersion has a limited effect on the removal efficiency (Amanullah et al. 1999). This is why most biofilter models do not account for axial dispersion within the column.

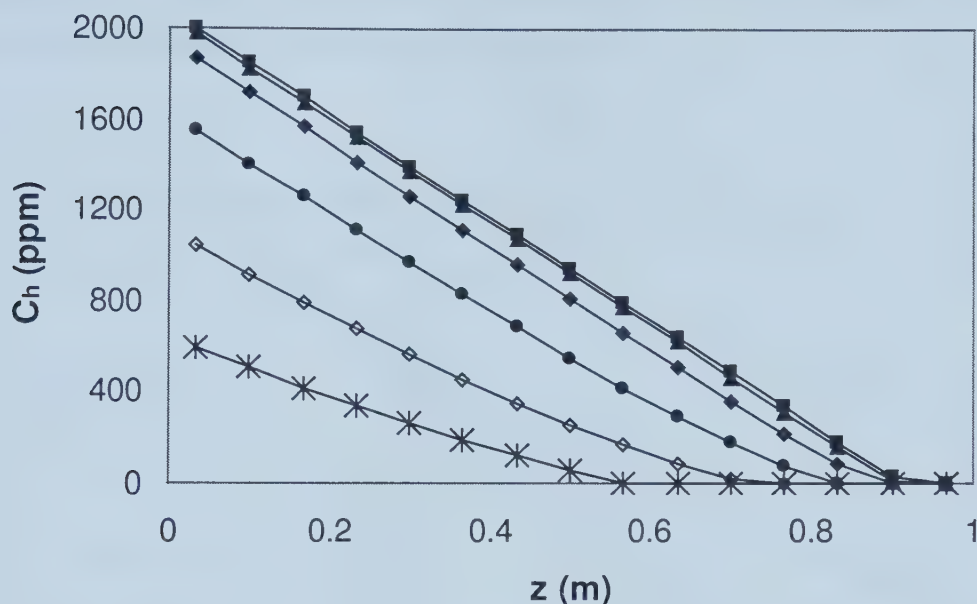


Figure 23: Effect of Peclet number on gas phase H_2S concentration profiles along the length of the biofilter. Peclet numbers of 1000 (\blacksquare), 100 (\blacktriangle), 17 (\blacklozenge), 5 (\bullet), 2 (\diamond) and 1 (\star) are shown. The inlet concentration is 2000 ppm, and the remaining parameters are those reported in Table 8.

The curves shown in Figure 23 highlight the importance of experimentally determining the Peclet number for each individual biofilter before making the assumption that axial dispersion is negligible. In biofilters where axial dispersion due to severe channelling is decreasing the removal in the column, the feed distribution can be improved by such means as adding a bulking agent, such as glass beads, to the packing (Zilli et al. 1996).

5.3.1.3 Sensitivity to A and δ

The proposed model replicates the H_2S removal obtained at the ARC by setting the specific surface area (A) to $950 \text{ m}^2/\text{m}^3$, and the biofilm thickness (δ) to $175 \text{ }\mu\text{m}$. This

approach is common in the literature; when parameters are difficult to measure directly, they are either assumed, or determined numerically by trial and error. The values used for A and δ in this model are within the range of values reported for A and δ in the literature. Biofilter models are extremely sensitive to the values for these two parameters (Amanullah et al. 1999). The effect of changing A or δ on the extent of removal predicted by the model is shown in Figures 24 and 25.

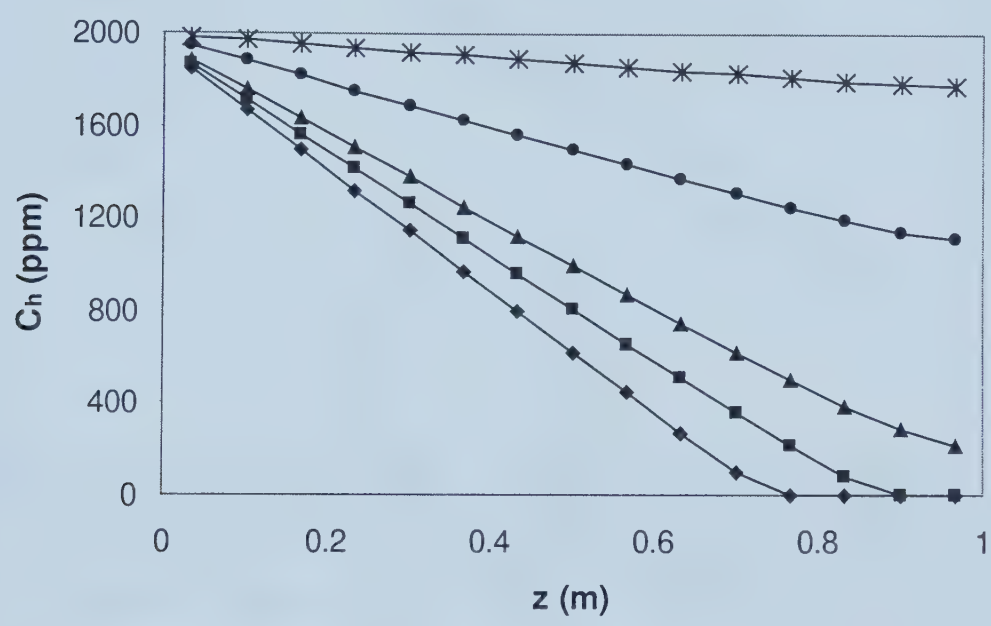


Figure 24: Effect of the specific surface area (A) on the H_2S gas phase concentration profile along the biofilter. The curves are for surface areas of 1100 (♦), 950 (■), 800 (▲), 400 (●) and 100 (★) m^2/m^3 . The inlet concentration is 2000 ppm; all other parameters are those reported in Table 8.

The curves in Figure 24 clearly show that a higher specific surface area increases the H_2S removal in the biofilter. The linear relationship shown in Figure 24 is intuitively expected, since a larger surface area provides an increased reaction volume and area for mass transfer, especially when complete biofilm coverage is assumed. Thus, a larger area results in increased H_2S conversion. Even though this model assumes that there is no reaction in the solid support, this linear trend will hold irrespective of the place of reaction (Amanullah et al. 1999). If the rate of reaction is controlled by reactions in the

solid phase, then the increase in removal at higher surface areas is due to an increased area for mass transfer.

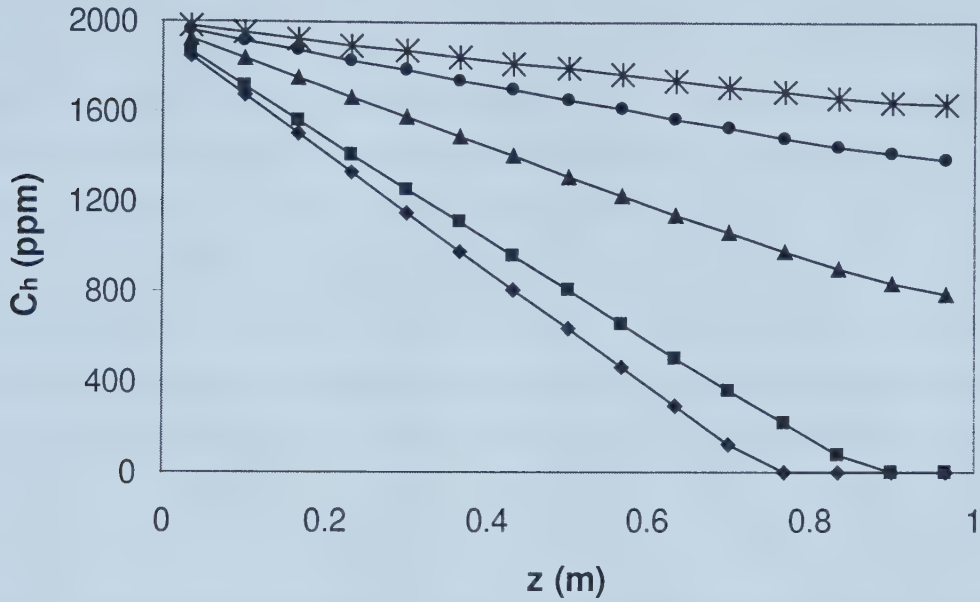


Figure 25: Effect of the biofilm thickness on the gas phase H₂S removal profiles in the biofilter. Biofilm thicknesses of 200 (♦), 175 (■), 100 (▲), 50 (●) and 30 (*) μm are shown. The inlet concentration is 2000 ppm, and the remaining parameters are those reported in Table 8.

The curves in Figure 25 display a linear relationship. This relationship is unexpected, as most biofilter literature indicates that there is an effective biofilm thickness (δ^*), beyond which the concentration of either the contaminant or oxygen is zero (Baltzis et al. 1997; Shareefdeen et al. 1993). The current model predicts that the effective biofilm thickness is very high at high concentrations of H₂S. This was also shown in Figure 22, where the concentration of H₂S in the biofilm was not depleted in the inlet section of the biofilter. This is likely a function of the high solubility of H₂S. Most studies on biofilter modelling are verified using compounds such as toluene, which is much less water soluble than H₂S. The trends shown in Figure 25 are valid only for this particular column under the experimental conditions used at the ARC, and conclusions cannot be drawn from this model regarding the biofiltration of other compounds. Further studies are recommended

to investigate the observed linear relationship between biofilm thickness and H_2S removal.

The curves in Figure 25 show clearly that biofilm thickness is one of the most crucial parameters affecting the gas phase H_2S removal in a biofilter. A higher biofilm thickness increases the level of substrate removal, because of the larger volume available for the reaction. All of the biological removal in a biofilter happens in the biofilm. There are two common situations for the biofilm: diffusion-controlled and reaction-controlled. Amanullah et al. (1999) suggest that for low values of biofilm thickness ($5 - 20 \mu\text{m}$), the biofiltration process is reaction-controlled. For biofilm thicknesses of greater than $30 \mu\text{m}$, the process becomes diffusion-controlled, with either the contaminant or oxygen failing to reach the depths of the biofilm. Therefore, an additional biofilm thickness is not beneficial (Amanullah et al. 1999). This does not seem to be the case with this model, as evidenced by the greater removal seen in Figure 25 for biofilm thicknesses of 175 and $200 \mu\text{m}$ as compared with $100 \mu\text{m}$. It is possible that oxygen may be limiting in the H_2S biofilter; experiments to determine this are recommended.

Values for biofilm thickness used in biofilter models reported in the literature vary between 25 and $2700 \mu\text{m}$ (Amanullah et al. 1999). However, none of the investigators measured δ directly from experiments. The specific surface area depends on the material used as a solid support. For peat, reported values of A range from 40 to $60\,000 \text{ m}^{-1}$, as discussed in Section 3.3. Values of A are also seldom measured experimentally. The difficulty in determining A and δ is one of the major obstacles to be overcome in biofilter modelling.

5.3.1.4 Overall parametric sensitivity studies

Biofilter models are undoubtedly useful in visualising pollutant removal in a biofilter, but much biofilter design is still based on laboratory-scale tests and extrapolation from published material (Devinny et al. 1999). The trend in the literature is shifting towards

more rigorous modelling approaches, to predict scenarios such as adsorption and degradation in the support media. However, the value of these more rigorous approaches is questionable when considering the practical insufficiency in quantifying key model parameters from independent experiments (Amanullah et al. 1999; Devinny et al. 1999).

Of all the parameters in the model, Pe , A , and δ have the most significant effects on the predicted concentration profiles. Figure 26 illustrates the model sensitivity to these parameters. The relative value of the parameter, plotted on the x-axis, is the assumed parameter value divided by the value of the same parameter as reported in Table 8. The relative value of the midpoint concentration, indicated on the y-axis, is defined as the predicted H_2S concentration under the assumed new value of the model parameter, divided by the model predicted H_2S concentration for a set of reference conditions. The reference conditions are the gas phase H_2S concentration at the midpoint of the biofilter ($z=0.5$) when the inlet H_2S concentration is 2000 ppm and the model parameters are those reported in Table 8.

Figure 26 shows the nearly linear dependence of pollutant removal predicted by the model on A and δ . Both parameters have exactly the same effect on the relative removal capacity of the biofilter. As discussed previously, both of these parameters were estimated by a numerical fitting approach. Increasing the value of A and δ above their reference values results in increased removal in the biofilter, as was seen in Figures 24 and 25. The error in predicting the removal rate of H_2S at any assumed value of A and δ can be quite significant. This agrees with previously published results, in which the authors concluded that the parameters that need the most care in estimations are the specific surface area (Shareefdeen and Baltzis 1994) and the biofilm thickness (Amanullah et al. 1999).

By contrast, the effect of small changes in Pe do not have as great an effect on the relative removal capacity predicted by the model. Increasing Pe has a greater effect than decreasing Pe ; for relative values of Pe larger than 0.9, the predicted removal rate is relatively insensitive to the actual value of Pe . This was also seen in Figure 23. Thus,

even though the value of Pe should be experimentally determined where possible, for values of Pe between 10 and 30, the error in the predicted removal rate due to estimating Pe is less than 10 percent.

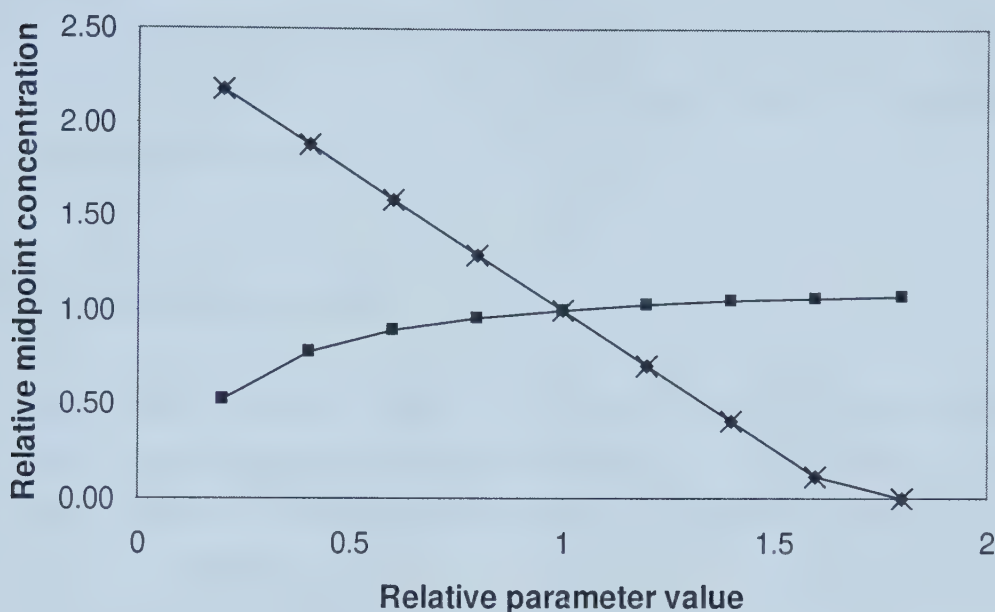


Figure 26: Sensitivity of the model to the values of parameters A (♦), Pe (■), and δ (×). The reference value for the midpoint concentration is the H_2S concentration predicted at the midpoint of the biofilter ($z=0.5$), when the inlet concentration is 2000 ppm. The reference values for the parameters are those reported in Table 8.

Experimentally, the percentage of H_2S removal at the ARC was observed to be constant over time (Budwill and Coleman 1999; Coleman and Dombroski 1995). Problems with biofilter plugging were encountered before the H_2S removal in the gas phase began to decrease (Budwill and Coleman 1999). The chemical oxidation experiments also showed constant H_2S removal with time, as seen by the last two entries in Table 17, where roughly 30 percent of the influent 3000 ppm H_2S were oxidised over time, both at 75 and 162 h. These observations justify the assumption of steady state removal in the gas phase. The biofilm concentration profiles are linked to the gas phase concentrations by Henry's law, so they can also be assumed to be constant. Shareefdeen and Baltzis (1994) also observed steady state removal in the biofilm during transient biofiltration.

The main focus of the modelling effort in this thesis was on modelling sulphur deposition, and not gas phase removal. Time is an important variable in sulphur deposition, so the two processes were de-coupled and solved using different time scales. It should be noted that the gas phase model presented here should be viewed primarily as a means of obtaining the axial H₂S concentration profiles that are needed to model sulphur formation. This model, which serves to effectively capture the important features of the H₂S removal obtained at the ARC, can be used as a basis for designing more elaborate experiments in the future.

5.3.2 Modelling sulphur formation

The complete model incorporates parameters characterising both the chemical sulphur deposition rate and the net biological sulphur deposition rate. The model predictions of sulphur deposition were verified by setting the biological sulphur deposition rate to zero, and comparing the model results with the experimentally determined sulphur deposition. The results are shown in Figure 27.

The data in Figure 27 show that there is good agreement between the model predictions and experimental observations of sulphur deposition. The sulphur deposition was linear over the concentration range of H₂S used in the experiments. An increased rate of sulphur formation was observed at higher concentrations of H₂S, as expected. Sulphur formation due to chemical oxidation is modelled according to the equation:

$$r_{s,chem} = 0.0058C_h^{0.62} \quad (5-11)$$

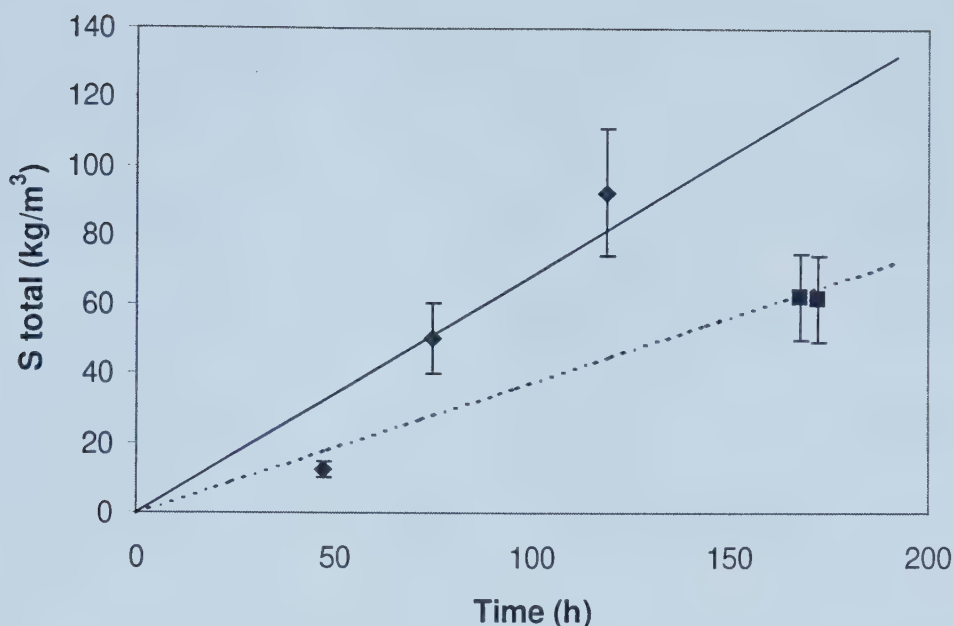


Figure 27: Sulphur deposition over time at 1000 (■) and 3000 (◆) ppm inlet H₂S concentrations. The lines represent model predictions at 1000 (---) and 3000 (—) ppm. The points represent the data from the chemical oxidation experiments. The error bars are ± 20 percent, as in Figure 16.

Over time, sulphur deposition in a biofilter results in a decrease in porosity, as the void space available for plugging is gradually filled by sulphur deposits. A model of sulphur deposition is thus very useful in predicting the life span of a biofilter bed being used to treat H₂S-contaminated air streams. Figure 28 shows the model predictions of porosity decrease in an H₂S biofilter, due to chemical oxidation only. This replicates the situation in the laboratory, where the H₂S biofilter was not inoculated with microorganisms.

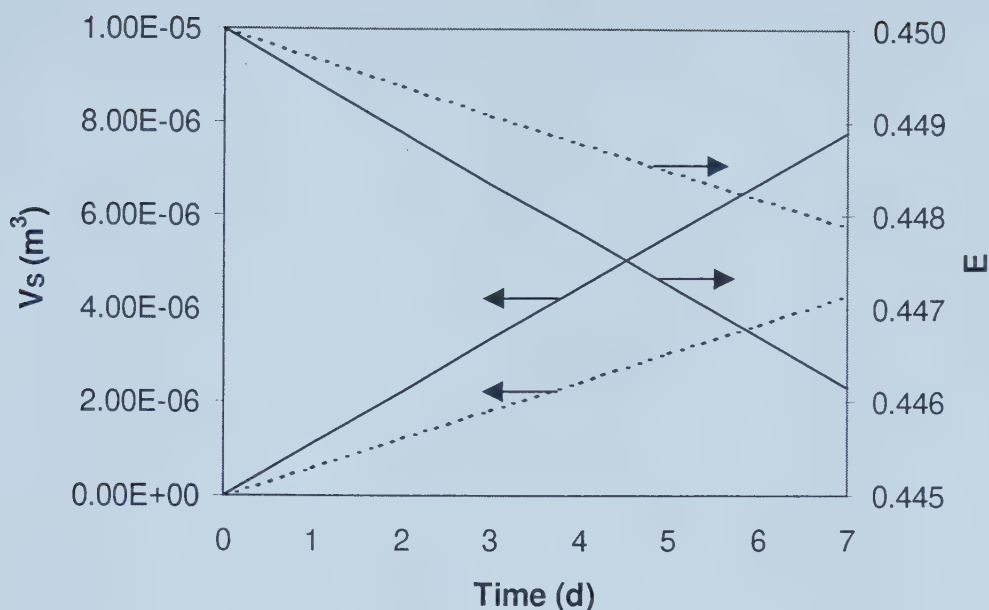


Figure 28: Model predictions of the changes in the volume of sulphur formed (V_s) and porosity (E) over time, due to chemical oxidation at influent H_2S concentrations of 1000 (---) and 3000 (—) ppm.

As the volume of solid sulphur accumulated in a biofilter increases, the porosity decreases correspondingly. Based on linear extrapolations of the curves shown in Figure 28, it would take approximately 1500 and 800 d, respectively, to completely plug a 0.42 m column in which influent concentrations of 1000 and 3000 ppm H_2S were being chemically oxidised. These numbers are purely hypothetical in nature, as removing H_2S by chemical oxidation only results in significantly lower removal than when both biological and chemical oxidation are taking place; it would not be feasible to operate such a column industrially.

Figure 29 shows the model predictions for biofilter plugging when both the chemical and biological oxidation processes are taken into account. The slopes of the curves in Figure 29 are steeper than those in Figure 28, indicating a faster overall rate of plugging, as expected. In 7 d, the porosity in the inoculated biofilter decreases to 0.447 and 0.444 for 1000 and 3000 ppm, respectively, as compared with 0.448 and 0.446 when only chemical oxidation is occurring. The times for complete biofilter plugging are predicted to be

approximately 1100 and 500 d, respectively. These values differ by 400 and 300 d from the predictions where only chemical oxidation is modelled.

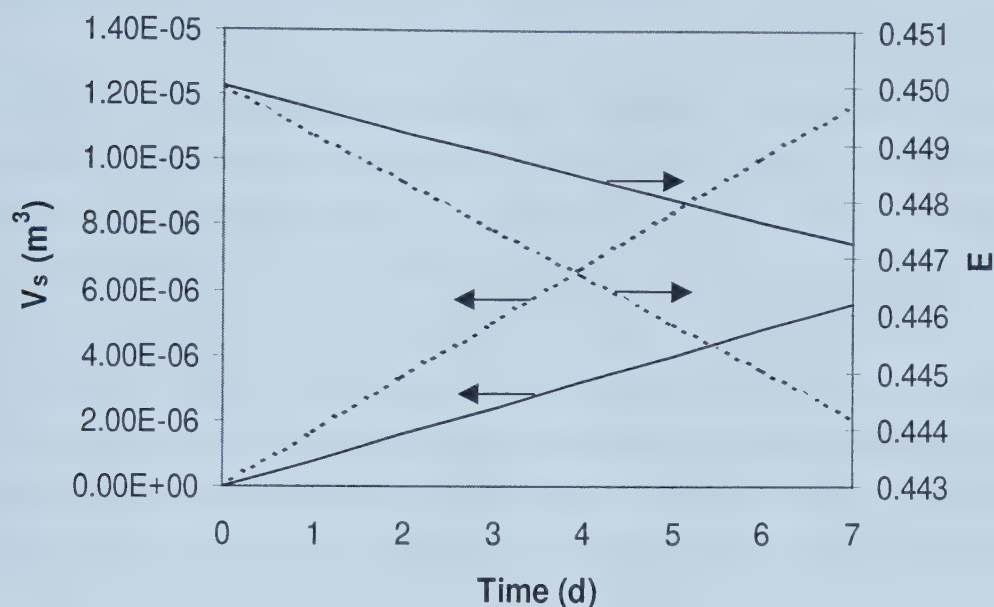


Figure 29: Model predictions of the changes in the volume of sulphur formed (V_s) and porosity (E) over time, due to chemical and biological oxidation at influent H_2S concentrations of 1000 (---) and 3000 (—) ppm.

The life span of the peat biofilter bed at the ARC was approximately 50 d, for influent H_2S concentrations of up to 2500 ppm (Budwill and Coleman 1999). This observation cannot be predicted by the model in its current state, because of the fluctuating inlet concentrations of H_2S incurred during the ARC experiments. A future step in modelling solids formation in a biofilter would be to include dynamic changes in the gas phase, so that such fluctuations and their effect on sulphur plugging can be modelled.

The model predictions shown in Figures 28 and 29 are linear over time. This is both a function of the inlet H_2S concentrations and a consequence of the lumped biological sulphur deposition parameter. Sulphur build-up is a dynamic process, that changes in response to the conditions in the biofilter. For example, microbial sulphur oxidation is likely a non-linear function of the amount of solid sulphur in the biofilter bed at any one

time. A model incorporating the biological sulphur deposition term could more effectively simulate column plugging, and the resulting curves would no longer be linear. This was verified by inputting dummy variables for biological sulphur deposition and degradation into the model and examining the resulting curves.

The next step in modelling H_2S biofiltration with solids formation is to separate the net biological oxidation rate into its constituent parts. This requires a two-step experiment. The first step is chemical oxidation experiments, similar to the ones described in Section 3, to plug a biofilter column with sulphur. The rate of biological sulphur oxidation can then be determined by inoculating the column and measuring the rate of sulphate evolution, or sulphur disappearance. This rate likely depends on the concentration of solid sulphur in the filter bed, which will fluctuate depending on the inlet concentration of H_2S . A more comprehensive study of the relative rates of biological sulphur deposition and oxidation is necessary to accurately predict the dynamic process of sulphur plugging.

5.4 Biofilter applications

5.4.1 Replacement for flaring

Based on an extrapolation of the biofiltration results obtained at the ARC, Budwill and Coleman (1999) suggested that biofiltration might be a safe, low-cost alternative to the flaring of sour solution gases. The application of a publicly accepted “natural” process to remediate sour solution gases is quite an attractive option, especially given the ongoing negative publicity surrounding sour gas wells. However, a few simple calculations can be used to show that H_2S biofilters in the oilfield would not be a widely applicable technology.

The size of biofilters needed to remediate high volumes of solution gases rapidly becomes prohibitive, even at relatively low concentrations of H_2S . Based on an elimination capacity of $400 \text{ g H}_2\text{S/m}^3/\text{h}$ (Budwill and Coleman 1999), a biofilter designed

to remediate a flare gas stream of 1.5 percent H_2S , which is approximately the average concentration in Alberta, would need to be 1 m in diameter and 2 m in height. A sample calculation is shown in Appendix G. To handle a load of 80 percent H_2S , the same biofilter would need to be 111 m high. Clearly, treating high concentrations of H_2S in the field is infeasible. Also prohibitive are the high volumes of peat or other solid supports needed to pack large biofilters.

Biofiltration is a biological process, so a biofilter requires sources of both water and heat. This does not generally pose a problem in warmer climates, indeed, (outdoor) biofilters are used successfully in the southern United States and in Europe (Devlin et al. 1999). However, freezing of the H_2S biofilter matrix would almost be guaranteed in the colder climates of Alberta and British Columbia, where most of oil and gas production in Canada takes place. This is not an insurmountable problem, and with some engineering work it would be possible to provide both heat and water at oilfield battery sites. For instance, some of the effluent gas stream from the biofilter could be diverted to heat the system. Practically, these biological needs imply that any biofiltration system is not maintenance free, and requires occasional operator intervention to function smoothly. By contrast, flare stacks do not require extensive maintenance or upkeep. Many flare locations are extremely remote, and are only occasionally serviced by oilfield personnel.

By far the biggest obstacle to the widespread use of biofilters in the oilfield is the problem of sulphur deposition and plugging at high H_2S loading rates. Chemical sulphur deposition increases with increasing H_2S concentrations. It is also likely that sour solution gas streams contain H_2S_x compounds, that would result in further sulphur deposits in the biofilter. Influent H_2S concentrations of greater than 40 ppm result in microbial sulphur deposition, and chemical sulphur deposition is a problem at all inlet H_2S concentrations, as discussed in Section 5.2.3. The concentration of H_2S in sour gas wells around Alberta can range from 0 to over 90 percent (PCF 2000a); 0.1 percent corresponds to 1000 ppm, while 1 percent is equivalent to 10 000 ppm. Sulphur plugging necessitates frequent changing of the biofilter matrix material, adding to both capital costs and maintenance time. Research by Webster et al. (1996) has shown that biofilters

are effective treatment technologies for processes with low and variable contaminant concentrations. Clearly, the composition of flare gas streams is highly variable, but predominantly not very low.

The ARC proposed that biofiltration would be effective for H₂S loading rates of up to 1 tonne per day (Budwill and Coleman 1999). This would require a biofilter volume of 104 m³. Current commercial biofilters have volumes of up to 2500 m³ (Devinny et al. 1999), but these are all fixed beds in industrial or plant settings. This size of biofilter is not feasible for all field applications. The maximum size of biofilter appropriate to a single lease must be calculated on an individual basis, to determine whether this technology is applicable to a particular site. For biofilters to be both cost-effective and feasible in the oilfield, only wells containing low concentrations of H₂S should be considered as candidates for biofiltration treatment.

There remains the question of what to do with the spent biofilter matrix material, in this case, sulphur-coated peat. Many soils in arid and semiarid regions of the world are unproductive because they are saline, or alkaline (Wainwright 1984). Moser and Olson, cited in Smith and Strohl (1991), have suggested that soils which are highly alkaline can be acidified by the application of elemental sulphur, or in this case, the spent peat, which is then oxidised by the resident thiobacilli. The oxidation of S⁰ to H₂SO₄ in soils reduces pH, supplies SO₄²⁻ to plants, makes phosphorus and other micronutrients more available, and acts to reclaim soils (Burns, cited in Lindemann et al. 1991; López-Aguirre et al. 1999). Most of the soils in Alberta are in the acidic to neutral pH range (Najda 1997), and as such there is not likely to be a market for this type of sulphur application in the oilfield regions of Canada.

5.4.2 Pre-treatment alternative to flaring

To account for operational upsets and variability in the flow rates of solution gases, it would be safer and more feasible to implement H₂S biofilters as pre-treatment alternatives to solution gas flaring, rather than as flare replacements. Natural gas is

composed largely of CH_4 . Upon flaring, most of this CH_4 is converted to CO_2 . Since thiobacilli are not known to degrade methane, and the acidic conditions in the biofilter are not conducive to the growth of methanotrophs (Topp and Pattey 1997), all methane in the inlet biofilter stream would emerge unchanged. This results in the question of whether it is better, from an environmental standpoint, to release methane or carbon dioxide into the atmosphere. Both carbon dioxide and methane are greenhouse gases, and contribute to global warming. Since 1800, the concentrations of CO_2 and CH_4 in the atmosphere have increased by 150 and 23 percent, respectively (Pearman and Fraser 1988). Rodhe (1990) has made estimates as to the relative contributions of individual gases to the greenhouse effect, based on the increases of those compounds in the atmosphere. With some variation, it is generally accepted that the relative contributions of CO_2 and CH_4 are in the vicinity of 60 and 15 percent, respectively (Rodhe 1990).

After CO_2 , CH_4 is the second most important greenhouse gas. On a molecular basis, CH_4 is about 25 – 30 times more effective in absorbing infrared radiation in the atmosphere than CO_2 , but since there is less of it, CH_4 is still second to CO_2 (Alexander 1999). However, the global warming potential of CH_4 , on a mass basis, is estimated to be between 25 to 62 times that of CO_2 , on a 20 year time horizon (PCF 2000b; Topp and Pattey 1997). CH_4 reacts in the troposphere and lower stratosphere to form ozone (O_3), whereas it destroys O_3 in the upper stratosphere. Increasing the CH_4 concentration in the atmosphere leads to a decrease in OH^\cdot radicals, which are major participants in a number of processes important to atmospheric chemistry (Alexander 1999). Photochemical reactions of CH_4 in the upper atmosphere produce O_3 , water vapour and CO_2 . It is estimated that every emitted mole of CH_4 reacts to produce 1 mole of CO_2 , about 0.7 moles of O_3 , and a certain (unknown) amount of water vapour (Rodhe 1990). CH_4 also breaks down to form CO, which is also an important pollutant, in the troposphere. Flaring CH_4 to produce CO_2 therefore results in fewer net greenhouse gas emissions than would result from releasing CH_4 directly into the atmosphere (PCF 2000b). Thus, the products of H_2S oilfield biofilters (H_2S -free solution gases) should be directed to a flare stack for combustion before release into the atmosphere.

5.4.3 Microbially soured wells

It is difficult to obtain reliable estimates of the composition of flare gas streams in Alberta, because of a lack of regulation surrounding the collection and analysis of gas samples (Johnson et al. 2001). To try to pinpoint wells that may be candidates for successful biofiltration treatments, one place to start looking would be to evaluate wells that have recently become sour, due to the action of sulphate-reducing bacteria (SRB).

There are three main sources of H₂S in hydrocarbon reservoirs: 1) bacterial or microbial sulphate reduction; 2) thermal decomposition of organic sulphur compounds in kerogen or oil; and 3) thermochemical sulphate reduction (Worden et al. 1995). A 1977 study by Orr, cited in Worden et al. (1995) suggests that the thermal decomposition of organic sulphur occurring during kerogen maturation and oil cracking contributes less than 5 percent of the total H₂S to a gas, because of the limited levels of sulphur in kerogen and oils. According to Orr, this leaves thermochemical sulphate reduction as being the only H₂S source contributing high levels, or greater than 10 percent H₂S to gases in underground reservoirs. Wells that have always been sour, which account for approximately 30 percent of Canadian wells (PCF 2000a), are sour as a result of abiotic processes. However, in oil and gas reservoirs with moderate temperatures (up to 110°C), or in those formed from recent sediments, bacterial sulphate reduction is believed to be the primary cause of souring (Jenneman et al. 1999; McInerney et al. 1997; Worden et al. 1995). The souring of reservoirs due to microbial hydrogen sulphide production is termed microbial souring. Microbially soured reservoirs are thought to contain only low levels of H₂S (<5 percent) (Worden et al. 1995). As opposed to wells in which H₂S is formed by chemical reactions within the sedimentary rocks, the microbially formed H₂S is pure; thus, reservoirs soured by bacteria will not contain any H₂S_x compounds, which would cause significant sulphur deposition and operational problems in oilfield H₂S biofilters.

Microbial well souring is believed to be mediated primarily by SRB, as well as other sulphide-producing bacteria, such as *Shewanella putrefaciens* (McInerney et al. 1997). SRB are bacteria that gain energy for growth by coupling the oxidation of organic

compounds or H_2 to the reduction of sulphate. These bacteria accumulate in biofilms on reservoir rock and reduce SO_4^{2-} to H_2S . For microbial sulphide production to occur, active microorganisms must be present, along with an oxidised sulphur species, suitable organic electron donors, and inorganic nutrients such as nitrogen and phosphorus. The electron donors most favourable for thermophilic sulphate reduction are hydrogen, lactate, formate, propionate, butyrate and longer-chain fatty acids up to C_7 (Mueller and Nielsen 1996).

Although it is likely that sulphide-producing populations already exist in many petroleum reservoirs, they can also be introduced into the formation as a consequence of drilling or enhanced oil recovery processes. Any change in the environmental conditions downhole may be enough to stimulate microbial life, which can in turn lead to sulphide production. Microbial souring is generally observed in wells into which water has been injected, as part of the secondary recovery process. The injected water is generally water which has been produced by the well, supplemented by water from an external source such as a nearby river or body of water. The injection of sea water into oil reservoirs for secondary recovery is common in the British and Norwegian sectors of the North Sea oilfields, as well as in the coastal United States (Mueller and Nielsen 1996; Rosnes et al. 1991). Seawater contains sulphate, an electron acceptor, as well as other nutrients essential for bacterial growth.

There are two ways in which waterflooding can stimulate hydrogen sulphide production: microbial sulphide production and the nonoxidative dissolution of pyrite (McInerney et al. 1997). The produced water that is reinjected into a well is rich in organic carbon, which provides both carbon and energy sources for microorganisms (Chen et al. 1993; Mueller and Nielsen 1996). The growth requirements of SRB are eventually met, and this is followed by the production of hydrogen sulphide in reservoirs. Drilling mud and fluids can also carry large numbers of bacteria, which may also contribute to microbial souring (Pankhurst 1968). One example of a microbially soured field is the Coleville field in Western Saskatchewan, which has been receiving water injections since 1958

(Jenneman et al. 1997). Many wells which are currently receiving water injections are becoming increasingly sour, due to the action of SRB.

5.4.4 Microbial column regeneration

One way to prolong the life of sulphur-plugged biofilter beds is to take advantage of the process of microbial sulphur degradation. Microorganisms are capable of degrading solid sulphur, both of chemical and biological origin (Tichý 1994; Suzuki 1999). Microbial sulphur degradation is the rate-limiting step in H_2S degradation. By using a bank of biofilter columns, with each biofilter operated periodically, it would be possible to give the microbes sufficient time to effect the sulphur degradation, while not hindering the overall biotreatment process. When running several biofilters in parallel, the influent H_2S -containing gas stream could be switched between columns, depending on their stage of sulphur deposition. Once the first column becomes severely overloaded, the influent stream would switch to the second filter, and so forth. All columns would still receive air and water, ideally as humidified air. Air is necessary to prevent the columns from becoming anaerobic, so as to prevent the development of a completely different microbial system (Devinny et al. 1999). The addition of water will prevent drying, which would kill many of the microorganisms present in the biofilter matrix (Devinny et al. 1999). A banked biofiltration system was proposed for the treatment of VOCs by Moe and Irvine (2000).

Allen and Yang (1992) observed the decrease of yellow-white deposits on compost in a biofilter system in which the H_2S loading was decreased. They speculated that under these conditions, the microbial population was using the accumulated intermediate or partially oxidised sulphur compounds as a supplemental energy source, by oxidising these materials to sulphate. As a result, the observed sulphur deposits in the biofilter bed disappeared within a few days of prolonged underloading (Yang and Allen 1994b). Experimental observations at the ARC showed that biofilter performance after overloading was enhanced with the addition of a nutrient solution (Budwill 2000c). However, if a biofilter is continuously overloaded (days to weeks) the resulting

deterioration in biofilter performance cannot be reversed by reducing the H_2S loading rate (Allen and Yang 1992). Careful study of the biofilters is required to determine the optimal point at which the feed should be switched to another column in the bank.

A solution of dilute H_2SO_4 will trickle out of the biofilter columns because of the oxidation of solid sulphur to SO_4^{2-} . This solution must be collected in a corrosion-proof vessel and disposed of accordingly. The production of a mildly corrosive effluent is an engineering challenge, but it is one that is also present during normal biofilter operation. Any biofilter treating H_2S will produce a mildly corrosive effluent.

The process described above is a self-regeneration process, requiring no external inputs beyond the air and water, which must be supplied regardless during biofilter operation. Running a bank of biofilters is simply a way of allowing sufficient time for microbial sulphur degradation to take place. By extending the life of the biofilter bed, both capital costs and maintenance time are reduced. Running a bank of H_2S biofilters instead of a single biofilter makes H_2S biofiltration more attractive for use in remote locations.

6.0 Conclusions and recommendations

The treatment of H_2S -contaminated air streams in a biofilter under pseudo-steady state conditions was described with a general mathematical model. The model accounts for chemical oxidation, net biological oxidation, and dispersion in the filter bed, in order to successfully model the formation of a solid phase. The resulting model predicts chemical sulphur formation and the resulting porosity decrease over time, in an H_2S biofilter. The two parameters most affecting the removal predicted by the biofilter model are the surface area and biofilm thickness. Care must be taken when estimating these parameters, and they should be determined experimentally whenever possible.

A series of experiments showed that chemical oxidation is responsible for up to 70 percent of the H_2S removal in a biofilter. Microbial inoculation is necessary to effect complete removal. Chemical oxidation results in sulphur deposition, in the form of elemental sulphur and sulphate salts. Most of the sulphur was deposited near the inlet of the biofilter. Microbial H_2S oxidation happens in two steps: an initial oxidation to solid sulphur, followed by the rate-limiting oxidation of solid sulphur to sulphate. Microbes can oxidise both chemically and biologically formed sulphur. At low concentrations, the end product of microbial H_2S oxidation is sulphate. Sulphur build up occurs when the rate of biological sulphur utilisation is less than the rate of sulphur formation by both chemical and biological means. Further studies are recommended to obtain reliable estimates of the rates of microbial H_2S and sulphur oxidation in H_2S biofilter. From these, the true balance point, at which solid sulphur begins to accumulate in an H_2S biofilter, can be determined.

The biofilter used in these experiments, which was built according to the specifications of the biofilters used at the ARC, was subject to large amounts of dispersion and channelling. Many biofilter models assume plug flow in the gas phase; it is recommended that tracer studies be performed on individual biofilters prior to making this assumption.

Microbial sulphur deposition occurs in H₂S biofilters for inlet concentrations of greater than 40 ppm. Inhibition was observed for H₂S concentrations of greater than 800 ppm. A model for product inhibition was fitted to the microbial H₂S removal data. H₂S is self-inhibiting at high concentrations; sulphur and sulphate have also been reported to have inhibitory effects on H₂S degradation. Further inhibition studies are recommended to gain a more comprehensive knowledge of the upper concentration limit for H₂S biofiltration.

The next stage in modelling solids formation in a biofilter is to account for transient removal and fluctuating inlet concentrations by extending the steady state model to a dynamic one. Reliable estimates of the rates of microbial H₂S and sulphur oxidation will give a more comprehensive picture of the changes in sulphur deposition with time in H₂S biofilters. This knowledge can then be used in determining the feasibility of using biofiltration to treat high concentrations of H₂S.

Based on the results of the current study, H₂S biofilters are not recommended to completely replace flares on sour gas wells. Rather, this technology may be appropriate as a pre-treatment alternative to flaring, for solution gas streams containing low levels of H₂S. One class of potential candidates for H₂S biofiltration are microbially soured wells, which are often sour in lower concentrations than long-term sour wells. The biggest obstacle to the implementation of H₂S biofilters in the oilfield is sulphur plugging at high concentrations of H₂S. In order to extend the life of the biofilter bed, and to minimise problems with sulphur deposition, it is recommended that a bank of H₂S biofilters be used instead of a single column. By switching the feed to another filter bed when one becomes overloaded, sufficient time is allowed for the microbial oxidation of solid sulphur to sulphate. This is a self-regeneration process.

Biofiltration has been shown to be an effective treatment technology for H₂S. Further work in the area of modelling sulphur deposition in H₂S biofilters will lead to an increased understanding of the fundamental processes leading to plugging, which will in turn lead to further suggestions for process optimisation.

7.0 References

- Alexander, M., 1999, *Biodegradation and Bioremediation*, 2nd Ed., Academic Press, California, USA.
- Allen, E., and Yang, Y., 1991, Biofiltration control of hydrogen sulfide emissions, presented at the *Air & Waste Management Association's 84th Annual Meeting*, June 16-21, Vancouver, British Columbia, Canada.
- Allen, E., and Yang, Y., 1992, Operational parameters for the control of hydrogen sulfide emissions using biofiltration, presented at the *Air & Waste Management Association's 85th Annual Meeting*, June 21-26, Kansas City, Missouri, USA.
- Alonso, C., Zhu, X., and Suidan, M., 2000, Parameter estimation in biofilter systems, *Environ. Sci. Technol.* **34**: 2318-2323.
- Amanullah, M., Farooq, S., and Viswanathan, S., 1999, Modeling and simulation of a biofilter, *Ind. Eng. Chem. Res.* **38**: 2765-2774.
- Aris, R., 1999, *Mathematical Modeling: A Chemical Engineer's Perspective*, Process Systems in Engineering, Vol. 1, Academic Press, USA.
- Arvin, E., Pedersen, A., Jacobsen, M., and Rosenørn, J., 1993, Biological removal of hydrogen sulfide from waste gases, presented at the *Sixth Annual IGT-Symposium on Gas, Oil and Environmental Biotechnology*, Nov. 29-Dec. 3, Colorado Springs, USA.
- Baltzis, B., Wojdyla, S., and Zarook, S., 1997, Modeling biofiltration of VOC mixtures under steady-state conditions, *J. Environ. Eng. (ASCE)* **123**: 599-605.
- Beauchamp, R., Bus, J., Popp, J., Boreiko, C., and Andjelkovich, D., 1984, A critical review of the literature on hydrogen sulfide toxicity, *CRC Critical Reviews in Toxicology* **13**: 25-97.
- Blanch, H., and Clark, D., 1997, *Biochemical Engineering*, Marcel Dekker, Inc., New York, USA.
- Bourrel, S., Dochain, D., Babary, J., and Queinnec, I., 2000, Modeling, identification and control of a denitrifying biofilter, *J. Process Contr.* **10**: 73-91.
- Bryant, R., Costerton, J., and Laishley, E., 1983, The role of *Thiobacillus albertis* glycocalyx in the adhesion of cells to elemental sulphur, *Can. J. Microbiol.* **30**: 81-90.

- Budwill, K., 2000a, Alberta Research Council, Vegreville, Alberta, Personal communication via email, June 27, 2000.
- Budwill, K., 2000b, Alberta Research Council, Vegreville, Alberta, Personal communication via email, August 1, 2000.
- Budwill, K., 2000c, Alberta Research Council, Vegreville, Alberta, Personal communication via email, May 8, 2001.
- Budwill, K., and Coleman, R., 1999, Effect of carbon dioxide levels on hydrogen sulphide oxidation by *Thiobacillus* species in a trickling biofilter, prepared for CANMET, Natural Resources Canada, Contract #23440-8-1015/001/SQ, Alberta Research Council, Vegreville, Alberta, Canada.
- Buisman, C., Geraats, B., Ijspeet, P., and Lettinga, G., 1990a, Optimization of sulphur production in a biotechnological sulphide-removing reactor, *Biotechnol. Bioeng.* **35**: 50-56.
- Buisman, C., Ijspeert, P., Janssen, A., and Lettinga, G., 1990b, Kinetics of chemical and biological sulphide oxidation in aqueous solutions, *Water Res.* **24**: 667-671.
- Chan, C., and Suzuki, I., 1993, Quantitative extraction and determination of elemental sulfur and stoichiometric oxidation of sulfide to elemental sulfur by *Thiobacillus thiooxidans*, *Can. J. Microbiol.* **39**: 1166-1168.
- Chen, C.-I., Reinsel, M., and Mueller, R., 1993, Kinetic investigation of microbial souring in porous media using microbial consortia from oil reservoirs, *Biotechnol. Bioeng.* **44**: 263-269.
- Chen, K., and Morris, J., 1972, Kinetics of oxidation of aqueous sulphide by O₂, *Environ. Sci. Technol.* **6**: 529-537.
- Cheng, Y., Peng, R., Su, J., and Lo, D., 1999, Mechanisms and kinetics of elemental sulfur oxidation by *Thiobacillus thiooxidans* in batch fermenter, *Environ. Technol.* **20**: 933-942.
- Cho, K.-S., Zhang, L., Hirai, M., and Shoda, M., 1991a, Removal characteristics of hydrogen sulphide and methanethiol by *Thiobacillus* sp. isolated from peat in biological degradation, *J. Ferment. Bioeng.* **71**: 44-49.
- Cho, K.-S., Kuniyoshi, I., Hirai, M., and Shoda, M., 1991b, A newly isolated heterotrophic bacterium, *Xanthomonas* sp. DY44, to oxidize hydrogen sulfide to polysulfide, *Biotechnol. Lett.* **13**: 923-928.

- Chung, Y.-C., Huang, C., and Li, C., 1997, Removal characteristics of H₂S by *Thiobacillus novellus* CH 3 biofilter in autotrophic and mixotrophic environments, *J. Environ. Sci. Health* **A32**:1435-1450.
- Chung, Y.-C., Huang, C., Pan, J., and Tseng, C.-P., 1998, Comparison of autotrophic and mixotrophic biofilters for H₂S removal, *J. Environ. Eng. (ASCE)* **124**: 362-367.
- Clark, P., Fitzpatrick, E., and Lesage, K., 1994, The H₂S/H₂S_x/Liquid Sulfur system: Application to sulfur degassing and removing low levels of H₂S from sour gas streams, *ASRL Quarterly Bulletin* **31**: 1-15.
- Coleman, R., 1993, Removal of organic carbon and sulphur compounds from process and fugitive emissions: Phase I, Results from laboratory studies, In: *Proceedings of the BIOMINET 10th Annual General Meeting*, Oct. 28, Mississauga, Ontario, pp. 119-145.
- Coleman, R., 1994, Development of biofilters for hydrogen sulphide and organic sulphide oxidation, presented at the *Industrial & Engineering Chemistry Special Symposium of the American Chemical Society*, Sept. 17-20, Atlanta, Georgia, USA.
- Coleman, R., and Dombroski, E., 1995, Removal of organic carbon and sulphur containing compounds from process and fugitive gaseous emissions using biofilters, prepared for *CANMET, Natural Resources Canada*, D.S.S. Requisition #23440-2-9232, Vegreville, Alberta, Canada.
- Dalla Lana, I., 2001, University of Alberta, Edmonton, Alberta, Personal communication via email, April 30, 2001.
- Danckwerts, P., 1953, Continuous flow systems – Distribution of residence times, *Chem. Eng. Sci.* **2**: 1-13.
- Degorce-Dumas, J., Kowal, S., and Le Cloirec, P., 1997, Microbiological oxidation of hydrogen sulphide in a biofilter, *Can. J. Microbiol.* **43**: 264-271.
- Deshusses, M., 2000, University of California, Riverside, CA, Personal communication via email, September 8, 2000.
- Deshusses, M., Hamer, G., and Dunn, I., 1995a, Behaviour of biofilters for waste air biotreatment. 1. Dynamic model development, *Environ. Sci. Technol.* **29**: 1048-1058.
- Deshusses, M., Hamer, G., and Dunn, I., 1995b, Behaviour of biofilters for waste air biotreatment. 2. Experimental evaluation of a dynamic model, *Environ. Sci. Technol.* **29**: 1059-1068.

- Devinny, J., Deshusses, M., and Webster, T., 1999, *Biofiltration for Air Pollution Control*, CRC Press LLC, USA.
- Dombroski, E., Gaudet, I., and Coleman, R., 1995, Reduction of odorous and toxic emissions from kraft pulp mills using biofilters, *In: Proceedings of the 1995 Conference on Biofiltration*, Eds. D. Hodge and E. Reynolds, Oct. 5-6, University of Southern California, Los Angeles, California, USA, pp. 287-294.
- EUB, 1997, *Policy Review of Solution Gas Flaring and Conservation in Alberta*, Alberta Energy and Utilities Board, Calgary, Alberta.
- Fehér, F., and Winkhaus, G., 1956, Über die Darstellung der Sulfane H_2S_5 , H_2S_6 , H_2S_7 , und H_2S_8 , *Z. anorg. allg. Chem.* **288**: 123-130.
- Fehér, F. and Hitzemann, G., 1958, Verdampfungsenthalpien, Dampfdrucke, Siedepunkte, kritische Temperaturen und Drucke sowie Troutonsche Konstanten von Sulfanen, *Z. anorg. allg. Chem.* **294**: 50-62.
- Fogler, H., 1992, *Elements of Chemical Reaction Engineering*, Prentice-Hall, New Jersey, pp. 708-795.
- Flakstad, N., 2000, U of A flaring research examines a burning issue, *the PEGG*, Association of Professional Engineers, Geologists and Geophysicists of Alberta, June 2000, p. 13.
- Furusawa, N., Togashi, I., Hirai, M., Shoda, M., and Kubota, H., 1984, Removal of hydrogen sulfide by a biofilter with fibrous peat, *J. Ferment. Technol.* **62**: 589-594.
- Gadre, R., 1989, Removal of hydrogen sulfide from biogas by chemoautotrophic fixed-film bioreactor, *Biotechnol. Bioeng.* **34**: 410-414.
- Giggenbach, W., 1971, Optical spectra and equilibrium dissolution of polysulphide ions in aqueous solution at 20°, *Inorg. Chem.* **11**: 1201-1207.
- Hazeau, W., Batenburg-van der Vegte, W., Bos, P., van der Pas, R., and Kuenen, J., 1988, The production and utilization of intermediary elemental sulfur during the oxidation of reduced sulfur compounds by *Thiobacillus ferrooxidans*, *Arch. Microbiol.* **150**: 574-579.
- Heathwaite, A., Ed., 1993, *Mires: Process, Exploitation and Conservation*, John Wiley & Sons Ltd., Chichester, Great Britain.
- Hirai, M., Ohtake, M., and Shoda, M., 1990, Removal kinetics of hydrogen sulfide, methanethiol and dimethyl sulphide by peat biofilters, *J. Ferment. Bioeng.* **70**: 334-339.

- Hodge, D., and Devinny, J., 1995, Modeling removal of air contaminants by biofiltration, *J. Environ. Eng. (ASCE)* **121**: 21-32.
- Hyne, J., and Wassink, B., 1991, Degassing liquid sulphur, *ASRL Quarterly Bulletin* **27**: 14-42.
- Janssen, A., Sleyster, R., van der Kaa, C., Jochemsen, A., Bontsema, J., and Lettinga, G., 1995, Biological sulphide oxidation in a fed-batch reactor, *Biotechnol. Bioeng.* **47**: 327-333.
- Jenneman, G., Bala, G., Clement, R., Fox, S., Gevertz, D., Sublette, K., and Ward, T., 1999, Characterization of novel sulphide-oxidizing bacteria for use in desulphurization of produced water and gas, *In: Proceedings of the 6th International Petroleum Environmental Conference*, Ed. Kerry Sublette, Nov. 16-18, Houston, Texas, pp. 366-376.
- Jenneman, G., Moffit, P., Bala, G., and Webb, R., 1997, Field demonstration of sulfide removal in reservoir brine by bacteria indigenous to a Canadian reservoir, SPE 38768, presented at the 1997 SPE Annual Technical Conference and Exhibition, Oct. 5-8, San Antonio, Texas.
- Jennings, P., Snoeyink, V., and Chian, E., 1976, Theoretical model for a submerged biological filter, *Biotechnol. Bioeng.* **18**: 1249.
- Jensen, A., and Webb, C., 1995, Treatment of H₂S-containing gases: a review of microbiological alternatives, *Enzyme Microb. Technol.* **17**: 2-10.
- Johnson, M., 1999, Flare Research Project Homepage, Department of Mechanical Engineering, University of Alberta, <http://www.mece.ualberta.ca/groups/combustion/flare/index.html>.
- Johnson, M., Spangelo, J., and Kostiuk, L., 2001, A characterization of solution gas flaring in Alberta, *J. Air Waste Manage. Assoc.* (in press).
- Jolley, R., and Forster, C., 1985, The kinetics of sulphide oxidation, *Environ. Technol. Lett.* **6**: 1-10.
- Kennes, C., and Thalasso, F., 1998, Waste gas biotreatment technology, *J. Chem. Technol. Biotechnol.* **72**: 303-319.
- Knickerbocker, C., Nordstrom, D., and Southam, G., 2000, The role of "blebbing" in overcoming the hydrophobic barrier during biooxidation of elemental sulfur by *Thiobacillus thiooxidans*, *Chem. Geol.* **169**: 425-433.

- Kudrna, V., Vejmolá, L., and Hasal, P., 1994, Certain problems associated with the application of stochastic diffusion processes for the description of chemical engineering phenomena. Stochastic model of isothermal continuous flow chemical reactor, *Collect. Czech. Chem. Commun.* **59**: 1772-1787.
- Kuenen, J., 1975, Colorless sulphur bacteria and their role in the sulphur cycle, *Plant Soil* **43**: 49-76.
- Kuenen, J., 1989, Colorless Sulfur Bacteria, In: *Bergey's Manual of Systematic Bacteriology*, Vol. 3, Eds. J. Staley, M. Bryant, N. Pfennig, and J. Holt, Williams and Wilkins, Baltimore, USA, pp. 1834-1837.
- Kuhn, A., Kelsall, G., and Chana, M., 1983, A review of the air oxidation of aqueous sulphide solutions, *J. Chem. Technol. Biotechnol.* **33A**: 406-414.
- LeBeau, A., and Milligan, D., 1994, Control of hydrogen sulfide gas from a wastewater lift station using biofiltration, In: *Proceedings of the Water Environmental Federation Conference on Odor and Volatile Organic Compound Emission Control for Municipal and Industrial Wastewater Treatment & Facilities*, Apr. 24-27, Jacksonville, Florida, USA, pp. 6-49-6-60.
- Levenspiel, O., 1972, *Chemical Reaction Engineering*, 2nd Ed., Wiley, New York, USA, pp. 290-293.
- Lindemann, W., Aburto, J., Haffner, W., and Bono, A., 1991, Effects of sulfur source on sulfur oxidation, *Soil Sci. Soc. Am. J.* **55**: 85-90.
- Lobo, R., Revah, S., Viveros-Garcia, T., 1999, An analysis of a trickle-bed bioreactor: carbon disulfide removal, *Biotechnol. Bioeng.* **63**: 98-109.
- López-Aguirre, J., Farias-Larios, J., Guzman-Gonzalez, A., and de Freitas, J., 1999, Effect of sulphur application on chemical properties and microbial populations in a tropical alkaline soil, *Pedobiologia* **43**: 183-191.
- MacFarlane, S., 1998, *Investigation of airflow through compost-based biofilters*, Ph.D. thesis, Department of Civil Engineering, University of Toronto, Toronto, Canada.
- McInerney, M., Sublette, K., Bhupathiraju, V., Coates, J., and Knapp, R., 1997, Causes and control of microbially induced souring, In: *Manual of Environmental Microbiology*, Ed. C.J. Hurst, American Society for Microbiology, Washington, DC, USA, pp. 363-371.
- McNevin, D., and Barford, J., 1998, Modeling adsorption and biological degradation of nutrients on peat, *Biochem. Eng. J.* **2**: 217-228.

- McNevin, D., and Barford, J., 2000, Biofiltration as an odour abatement strategy, *Biochem. Eng. J.* **5**: 231-242.
- McNevin, D., Barford, J., and Hage, J., 1999, Adsorption and biological degradation of ammonium and sulfide on peat, *Water Res.* **33**: 1449-1459.
- Metcalf & Eddy, Inc., 1991, *Wastewater Engineering: Treatment, Disposal and Reuse*, 3rd Ed., Eds. G. Tchobanoglous and F. Burton, McGraw-Hill, Inc., New York, USA.
- Meyer, B., 1977, *Sulfur, Energy, and Environment*, Elsevier Scientific Publishing Company, Amsterdam, The Netherlands.
- Mickens, R., 1994, *Nonstandard Finite Difference Models of Differential Equations*, World Scientific Ltd., Singapore.
- Moe, W., and Irvine, R., 2000, Performance of periodically operated gas phase biofilters during transient loading conditions, *Water Sci. Technol.* **41**: 441-444.
- Mueller, R. and Nielsen, P., 1996, Characterization of thermophilic consortia from two souring oil reservoirs, *Appl. Environ. Microbiol.* **62**: 3083-3087.
- Mysliwiec, M., Shroeder, E., and Kavvas, M., 1996, Flow characterization of biofilters, *In: Proceedings of the 89th AWMA Annual Meeting and Exhibition*, June 23-28, Nashville, Tennessee, USA.
- Najda, H., 1997, Forage soil and climatic zones of Alberta, Alberta Agriculture, Food, and Rural Development, Government of Alberta, <http://www.agric.gov.ab.ca/crops/forage/species/forsoil.html>.
- National Research Council, 1929, *International Critical Tables*, Vol. III, McGraw Hill Book Company, New York, USA.
- Nelson, D., 1989, Physiology and biochemistry of filamentous sulfur bacteria, *In: Autotrophic Bacteria*, Eds. H.G. Schlegel and B. Bowien, Springer Verlag, Berlin, Germany, pp. 219-238.
- New Paradigm, 2001, The Technology: description of the Shell-Paque Process, New Paradigm Gas Processing Ltd., <http://www.npgas.ca/tech-dev.htm>.
- O'Brien, D., and Birkner, F., 1977, Kinetics of oxygenation of reduced sulfur species in aqueous solution, *Environ. Sci. Technol.* **11**: 1114-1120.
- Okabe, S., Matsuda, T., Satoh, H., Itoh, T., and Watanabe, Y., 1998, Sulfate reduction and sulfide oxidation in aerobic mixed population biofilms, *Water. Sci. Technol.* **37**: 131-138.

- Ottengraf, S., 1977, Theoretical model for a submerged biofilter, *Biotechnol. Bioeng.* **19**: 1411-1417.
- Ottengraf, S., 1986, Exhaust gas purification, *In: Biotechnology*, Vol. 8, Eds. H. Rehm and G. Reed, VCH Verlagsgesellschaft, Weinheim, Germany, pp. 425-452.
- Ottengraf, S. and van Den Oever, A., 1983, Kinetics of organic compound removal from waste gases with a biological filter, *Biotechnol. Bioeng.* **25**: 3089-3102.
- Pankhurst, E., 1968, Bacteriological aspects of the storage of gas underground, *J. Appl. Bacteriol.* **31**: 311-322.
- PCF, 2000a, *Sour Gas Questions + Answers*, Petroleum Communication Foundation, Canada.
- PCF, 2000b, *Flaring Questions + Answers*, Petroleum Communication Foundation, Canada.
- Pearman, G., and Fraser, P., 1988, Sources of increased methane, *Nature* **332**: 489-490.
- PITS, 1997, *H₂S Alive®*, Hydrogen sulphide training manual, Petroleum Industry Training Service, Calgary, Alberta, Canada.
- Prescott, L., Harley, J., and Klein, D., 1993, *Microbiology*, 2nd Edition, Ed. K. Kane, Wm. C. Brown Communications, Inc., Dubuque, IA, USA.
- Pronk, J., Meulenbergh, R., Hazeu, W., Bos, P., and Kuenen, J., 1990, Oxidation of reduced inorganic sulfur compounds by acidophilic thiobacilli, *FEMS Microbiol. Rev.* **75**: 293-306.
- Raymont, M., 1975, Make hydrogen from hydrogen sulfide, *Hydrocarbon Process.* **54(7)**: 139-142.
- Rodhe, H., 1990, A comparison of the contribution of various gases to the greenhouse effect, *Science* **248**: 1217-1219.
- Rosnes, J., Torsvik, T., and Lien, T., 1991, Spore-forming thermophilic sulfate-reducing bacteria isolated from North Sea oil field waters, *Appl. Environ. Microbiol.* **57**: 2302-2307.
- Schmidbaur, H., Schmidt, M., and Siebert, W., 1964, Die Protonenresonanzspektren der Sulfane, II, *Chem. Ber.* **97(Part III)**: 3374-3380.
- Scott, H., 1998, *Effects of air emissions from sour gas plants on the health and productivity of beef and dairy herds in Alberta, Canada*, Ph.D. Thesis, University of Guelph, Guelph, Canada.

- Shareefdeen, Z., and Baltzis, B., 1994, Biofiltration of toluene vapor under steady-state and transient conditions: theory and experimental methods, *Chem. Eng. Sci.* **49**: 4347-4360.
- Shareefdeen, Z., Baltzis, B., Young-Sook, O., and Bartha, R., 1993, Biofiltration of methanol vapor, *Biotechnol. Bioeng.* **41**: 512-524.
- Smet, E., Lens, P., and van Langenhove, H., 1998, Treatment of waste gases contaminated with odorous sulfur compounds, *Crit. Rev. Environ. Sci. Technol.* **28**: 89-117.
- Smith, D., and Strohl, W., 1991, Sulfur-oxidizing bacteria, *In: Variations in Autotrophic Life*, Eds. J. M. Shively and L.L. Barton, Academic Press, USA, pp. 121-147.
- Steudel, R., 1989, On the nature of “elemental sulfur” (S^0) produced by sulfur-oxidizing bacteria – a nature of S^0 globules, *In: Autotrophic Bacteria*, Eds. H. Schlegel and B. Bowien, Springer Verlag, Berlin, Germany, pp. 289-304.
- Strosher, M., 1996, *Investigations of flare gas emissions in Alberta*, Alberta Research Council, Calgary, Alberta.
- Strosher, M., Chambers, A., and Kovacik, G., 1998, *Removal of liquid from solution gas streams directed to flare and development of a method to establish the relationship between liquids and flare combustion efficiency*, Alberta Research Council, Edmonton, Alberta.
- Sublette, K., 1989, Immobilization of *Thiobacillus denitrificans* for the oxidation of hydrogen sulfide in sour water, *Appl. Biochem. Biotechnol.* **20/21**: 675-686.
- Sublette, K., and Sylvester, N., 1987a, Oxidation of hydrogen sulfide by *Thiobacillus denitrificans*: desulfurization of natural gas, *Biotechnol. Bioeng.* **29**: 249-257.
- Sublette, K., and Sylvester, N., 1987b, Oxidation of hydrogen sulfide by continuous cultures of *Thiobacillus denitrificans*, *Biotechnol. Bioeng.* **29**: 753-758.
- Sublette, K., Kolhatkar, R. and Ratterman, K., 1998, Technological aspects of the microbial treatment of sulfide-rich wastewaters: a case study, *Biodegradation* **9**: 259-271.
- Suzuki, I., 1965, Oxidation of elemental sulfur by an enzyme system of *Thiobacillus thiooxidans*, *Biochim. Biophys. Acta* **104**: 359-371.
- Suzuki, I., 1999, Oxidation of inorganic sulfur compounds: chemical and enzymatic reactions, *Can. J. Microbiol.* **45**: 97-105.

- Suzuki, I., Chan, C., and Takeuchi, T., 1994, Oxidation of inorganic sulfur compounds by thiobacilli, *In: Environmental Geochemistry of Sulfide Oxidation*, Eds. C. Alpers and D. Blowes, American Chemical Society, Washington, USA, pp. 60-67.
- Suzuki, I., Chan, C., Vilar, R., and Takeuchi, T., 1993, Sulfur and sulfide oxidation by *Thiobacillus thiooxidans*, *In: Biohydrometallurgical Technologies*, Eds. A. Torma, J. Wey and V. Lakshmanan, TMS, Warrendale, Pennsylvania, USA, pp. 109-116.
- Tichý, R., 1994, Possibilities for using biologically-produced sulphur for cultivation of *Thiobacilli* with respect to bioleaching processes, *Bioresour. Technol.* **48**: 221-227.
- Topp, E., and Pattey, E., 1997, Soils as sources and sinks for atmospheric methane, *Can. J. Soil Sci.* **77**: 167-178.
- van Groenestijn, J., and Hesselink, P., 1993, Biotechniques for air pollution control, *Biodegradation* **4**: 283-301.
- Wainwright, M., 1984, Sulfur oxidation, *Adv. Agron.* **37**: 358-396.
- Waldner, C., Ribble, C., and Janzen, D., 1998, Evaluation of the impact of a natural gas leak from a pipeline on productivity of beef cattle, *J. Am. Vet. Med. Assoc.* **212**: 41-48.
- Wani, A., Lau, A., and Branion, R., 1999, Biofiltration control of pulping odors – hydrogen sulfide: performance, macrokinetics and coexistence effects of organo-sulfur species, *J. Chem. Technol. Biotechnol.* **74**: 9-16.
- Wani, A., Lau, A., and Branion, R., 1997, Biofiltration: A promising and cost-effective control technology for odors, VOCs and air toxics, *J. Environ. Sci. Health* **A32**: 2027-2055.
- Wani, A., Lau, A., and Branion, R., 1998a, Effects of periods of starvation and fluctuating hydrogen sulfide concentration on biofilter dynamics and performance, *J. Hazard. Mater.* **60**: 287-303.
- Wani, A., Lau, A., and Branion, R., 1998b, Dynamic behavior of biofilters degrading reduced sulfur odorous gases, presented at the *Air & Waste Management Association's 91st Annual Meeting & Exhibition*, June 14-18, San Diego, California, USA.
- Wani, A., Lau, A., and Branion, R., 1998c, Dynamic behavior of biofilters degrading pulping odors and VOCs: hydrogen sulfide, presented at the *TAPPI 1998 International Environmental Conference and Exhibit*, April 5-8, Vancouver, British Columbia, Canada.

- Wani, A., Lau, A., and Branion, R., 1998d, Bio-elimination kinetics of hydrogen sulfide in compost and wood-waste based biofilters: effects of coexistence of organo-sulfur compounds, *In: Conferences Proceedings of Environmental Strategies for the 21st Century – An Asia Pacific Conference*, April 8-10, Singapore, pp. 383-390.
- Waterloo Maple Inc., 2000, Maple 6, Copyright © 1981-2000.
- Webster, T., Devanny J., Torres, E., and Basrai, S., 1996, Biofiltration of odors, toxics and volatile organic compounds from publicly owned treatment works, *Environ. Prog.* **15**: 141-147.
- Wilmot, P., Cadee, K., Katinic, J., and Kavanah, B., 1988, Kinetics of sulphide oxidation by dissolved oxygen, *J.—Water Pollut. Control Fed.* **60**: 1264-1270.
- Worden, R., Smalley, P., and Oxtoby, N., 1995, Gas souring by thermochemical sulfate reduction at 140°C, *AAPG Bulletin* **79**: 854-863.
- Wu, G., Dupuy, A., Leroux, A., Brzezinski, R., and Heitz, M., 1999, Peat-based toluene biofiltration: a new approach to the control of nutrients and pH, *Environ. Technol.* **20**: 367-376.
- Yang, Y., and Allen, E., 1994a, Biofiltration control of hydrogen sulfide 1. Design and operational parameters, *J. Air Waste Manage. Assoc.* **44**: 863-868.
- Yang, Y., and Allen, E., 1994b, Biofiltration control of hydrogen sulfide 2. Kinetics, biofilter performance, and maintenance, *J. Air Waste Manage. Assoc.* **44**: 1315-1321.
- Zarook, S., Shaikh, A., and Azam, S., 1998, Axial dispersion in biofilters, *Biochem. Eng. J.* **1**: 77-84.
- Zhang, J.-Z., and Millero, F., 1994, Kinetics of oxidation of hydrogen sulfide in natural waters, *In: Environmental Geochemistry of Sulfide Oxidation*, Eds. C. Alpers and D. Blowes, American Chemical Society, Washington, USA, pp. 393-409.
- Zilli, M., Fabiano, B., Ferraiolog, A., and Converti, A., 1996, Macrokinetic investigation on phenol uptake from air by biofiltration: influence of superficial gas flow rate and inlet pollutant concentration, *Biotechnol. Bioeng.* **49**: 391-398.

Appendix A – ARC raw data

Table A1: Hydrogen sulphide profile for laboratory-scale Biofilter 1 - Dec. 1992 to March 1993 (Source: Coleman and Dombroski 1995)

Date	Time (24 h)	H ₂ S (ppm)				
		Inlet	Bottom	Middle	Top	Outlet
De 7 ^a	-	ND ^l	ND	ND	ND	ND
De 9 ^b	1415	11.61	10.72	9.59	10.91	10.83
De 10	1350	7.03	7.69	3.35	8.45	8.66
De 10	1540	12.78	12.44	11.14	12.29	12.46
De 11	1115	11.02	11.37	9.94	11.34	11.91
De 15	1045	12.53	12.36	11.36	12.16	12.1
De 15 ^c	1330	13.33	11.55	10.28	11.59	11.83
De 15	1540	12.25	7.54	9.94	9.92	8.61
De 16	1045	11.69	7.02	10.86	11.64	9.56
De 16	1105	10.07	6.79	10.59	11.53	7.55
De 17	1105	11.16	8.00	6.74	6.95	6.58
De 17	1455	5.33	8.85	6.9	7.44	7.91
De 21	1115	10.12	6.56	6.46	4.8	4.57
De 22	1045	10.08	7.11	7.25	6.64	5.61
Fe 3	1440	9.29	9.43	7.34	6.82	4.51
Fe 4	1640	12.22	12.38	13.36	11.33	3.86
Fe 5 ^d	940	12.97	9.45	9.77	7.96	6.01
Fe 8	1350	11.89	10.99	8.57	8.71	7.04
Fe 10	1555	13.67	11.74	11.19	8.54	3.54
Fe 12	1220	12.00	11.10	9.93	8.54	4.42
Fe 17	1525	13.48	3.19	ND	0.023	0.008
Fe 18 ^e	1030	12.74	5.17	0.06	0.022	0.016
Fe 18	1047	31.38	21.40	1.25	ND	ND
Fe 18	1425	33.60	13.87	ND	ND	0.51
Fe 22	1335	37.22	30.66	14.88	1.99	0.139
Fe 24 ^f	1100	26.91	25.82	26.26	ND	0.041
Fe 26 ^g	1345	39.12	41.88	28.07	25.41	11
Fe 27 ^h	-	ND	ND	ND	ND	ND
Fe 28 ⁱ	-	ND	ND	ND	ND	ND
Mr 1 ^j	1055	11.99	ND	ND	ND	4.19
Mr 1	1115	17.90	ND	ND	ND	0.61
Mr 1 ^k	1325	19.67	ND	ND	ND	7.44

^a Biofilter packed with 2.1 L (196 g) of coarse peat. Air turned on.

^b H₂S turned on at 1100h December 9.

^c Water turned on at 1350h December 15.

^d Inoculate with seed bacteria 1400h February 5.

^e H₂S flow increased 1045h February 18

^f H₂S flow terminated

^g H₂S flow re-started.

^h H₂S flow turned off 2000h February 27 due to safety sensor system shutdown

ⁱ H₂S flow turned back on 1330h February 28.

^j H₂S flow increased slowly March 1.

^k H₂S flow turned off 1345h March 1 due to safety sensor system shutdown

^l ND – not determined

Table A2: Sulphate and pH profile for laboratory-scale Biofilter 1 - Dec. 1992 to March 1993 (Source: Coleman and Dombroski 1995)

Date	Day Number	Volume (mL)	pH	SO ₄ ²⁻ (mg/L)	SO ₄ ²⁻ (mg/d)	Cumulative SO ₄ ²⁻ (mg)
Dec 7 ^a	0	ND ⁱ	ND	ND	ND	ND
Dec 9 ^b	1	ND	ND	ND	ND	ND
Dec 15 ^c	6	ND	ND	27.7	166.5	166.5
Dec 17	8	305	3.67	221.9	27.7	221.9
Dec 18	9	535	4.72	29.4	29.4	251.3
Dec 22	13	425	4.66	131.3	32.8	382.6
Dec 26	17	1250	4.82	223.8	56	606.4
Jan 4	26	1075	3.8	669.7	74.4	1276.1
Jan 5	32 ⁷	1930	4.15	100.67	1005.7	2281.8
Jan 8	30	740	4.12	380.9	127	2662.7
Jan 14	36	230	3.37	488.3	81.4	3151
Jan 22	44	2300	3.78	1227.7	153.5	4378.7
Jan 27	49	2300	3.95	949.4	189.9	5328.1
Feb 3	56	1770	3.89	719.3	102.8	6047.4
Feb 5 ^d	58	70	2.46	27.4	13.7	6074.8
Feb 8	61	120	3.59	187.1	62.4	6261.8
Feb 10	63	780	4.22	1125.6	562.8	7387.4
Feb 12	65	470	3.49	528.5	264.2	7916
Feb 17	70	585	2.17	1618.3	323.7	9534.2
Feb 18 ^e	71	1100	1.94	3159.8	3159.8	12694
Feb 27 ^f	80	ND	ND	ND	466.3	16890.2
Feb 28 ^g	81	ND	ND	ND	466.3	17356.6
Mar 1 ^h	82	ND	ND	ND	466.3	17822.8
Mar 3	84	1085	1.73	6061.4	466.3	18755.4
Mar 5	86	915	2.06	757.8	378.9	19513.2
Mar 12	93	2300	2.09	1269.4	181.3	20782.6

^a Biofilter packed with 2.1 L (196 g) coarse peat. Air turned on.

^b H₂S turned on at 1100h December 9.

^c Water turned on at 1350h December 15.

^d Inoculate with seed bacteria 1400h February 5.

^e H₂S flow increased 1045h February 18.

^f H₂S flow turned off 2000h February 27 due to safety sensor system shutdown.

^g H₂S flow turned back on 1330h February 28.

^h H₂S flow increased slowly March 1. H₂S flow turned off 1345 March 1 due to safety sensor system shutdown.

ⁱ ND – not determined

Table A3: Sulphur mass balance for laboratory-scale Biofilter 1 - Dec. 1992 to March 1993 (Source: Coleman and Dombroski 1995)

Date	IN			OUT					
	H ₂ S ppm	H ₂ S mmoles/d	Cum. H ₂ S mmoles	H ₂ S ppm	H ₂ S mmoles/d	Cum. H ₂ S mmoles	SO ₄ ²⁻ mg/d	SO ₄ ²⁻ mmoles/d	Cum. SO ₄ ²⁻ mmoles
Dec 7 ^a	NA ^j	0	0	NA	0	0	NA	0	0
Dec 8	NA	0	0	NA	0	0	NA	0	0
Dec 9 ^b	11.61	4.18	4.18	10.83	3.899	3.899	27.7	0.289	0.289
Dec 10	9.74	3.506	7.686	10.56	3.802	7.701	27.7	0.289	0.578
Dec 11	12.53	4.511	12.197	11.91	4.288	11.989	27.7	0.289	0.867
Dec 12	12.53	4.511	16.708	12.1	4.356	16.345	27.7	0.289	1.156
Dec 13	12.53	4.511	21.219	12.1	4.356	20.701	27.7	0.289	1.445
Dec 14	12.53	4.511	25.73	12.1	4.356	25.057	27.7	0.289	1.734
Dec 15 ^c	12.39	4.46	30.19	10.36	3.73	28.787	27.7	0.289	2.023
Dec 16	10.88	3.917	34.107	8.56	3.082	31.869	27.7	0.289	2.312
Dec 17	8.24	2.966	37.073	7.24	2.606	34.475	27.7	0.289	2.601
Dec 18	10.12	3.643	40.716	4.57	1.645	36.12	29.4	0.306	2.907
Dec 19	10.12	3.643	44.359	4.57	1.645	37.765	32.8	0.342	3.249
Dec 20	10.12	3.643	48.002	4.57	1.645	39.41	32.8	0.342	3.591
Dec 21	10.12	3.643	51.645	4.57	1.645	41.055	32.8	0.342	3.933
Dec 22	10.08	3.629	55.274	5.61	2.02	43.075	32.8	0.342	4.275
Dec 23	9.29	3.344	58.618	4.51	1.624	44.699	56	0.583	4.858
Dec 24	9.29	3.344	61.962	4.51	1.624	46.323	56	0.583	5.441
Dec 25	9.29	3.344	65.306	4.51	1.624	47.947	56	0.583	6.024
Dec 26	9.29	3.344	68.65	4.51	1.624	49.571	56	0.583	6.607
Dec 27	9.29	3.344	71.994	4.51	1.624	51.195	74.4	0.775	7.382
Dec 28	9.29	3.344	75.338	4.51	1.624	52.819	74.4	0.775	8.157
Dec 29	9.29	3.344	78.682	4.51	1.624	54.443	74.4	0.775	8.932
Dec 30	9.29	3.344	82.026	4.51	1.624	56.067	74.4	0.775	9.707
Dec 31	9.29	3.344	85.37	4.51	1.624	57.691	74.4	0.775	10.482
Jan 1	9.29	3.344	88.714	4.51	1.624	59.315	74.4	0.775	11.257
Jan 2	9.29	3.344	92.058	4.51	1.624	60.939	74.4	0.775	12.032
Jan 3	9.29	3.344	95.402	4.51	1.624	62.563	74.4	0.775	12.807
Jan 4	9.29	3.344	98.746	4.51	1.624	64.187	74.4	0.775	13.582
Jan 5	9.29	3.344	102.09	4.51	1.624	65.811	100.6	1.047	14.617
Jan 6	9.29	3.344	105.434	4.51	1.624	67.435	127	1.322	15.939
Jan 7	9.29	3.344	108.778	4.51	1.624	69.059	127	1.322	17.262
Jan 8	9.29	3.344	112.122	4.51	1.624	70.683	127	1.322	18.584
Jan 9	9.29	3.344	115.466	4.51	1.624	72.307	81.4	0.847	19.431
Jan 10	9.29	3.344	118.81	4.51	1.624	73.931	81.4	0.847	20.278
Jan 11	9.29	3.344	122.154	4.51	1.624	75.555	81.4	0.847	21.126
Jan 12	9.29	3.344	125.498	4.51	1.624	77.179	81.4	0.847	21.973
Jan 13	9.29	3.344	128.842	4.51	1.624	78.803	81.4	0.847	22.821
Jan 14	9.29	3.344	132.186	4.51	1.624	80.427	81.4	0.847	23.668
Jan 15	9.29	3.344	135.53	4.51	1.624	82.051	153.5	1.598	25.266
Jan 16	9.29	3.344	138.874	4.51	1.624	83.675	153.5	1.598	26.864
Jan 17	9.29	3.344	142.218	4.51	1.624	85.299	153.5	1.598	28.462

Table A3 (continued): Sulphur mass balance for laboratory-scale Biofilter 1 - Dec. 1992 to March 1993 (Source: Coleman and Dombroski 1995)

Date	IN			OUT					
	H ₂ S ppm	H ₂ S mmoles/d	Cum. H ₂ S mmoles	H ₂ S ppm	H ₂ S mmoles/d	Cum. H ₂ S mmoles	SO ₄ ²⁻ mg/d	SO ₄ ²⁻ mmoles/d	Cum. SO ₄ ²⁻ mmoles
Jan 18	9.29	3.344	145.562	4.51	1.624	86.923	153.5	1.598	30.06
Jan 19	9.29	3.344	148.906	4.51	1.624	88.547	153.5	1.598	31.658
Jan 20	9.29	3.344	152.25	4.51	1.624	90.171	153.5	1.598	33.256
Jan 21	9.29	3.344	155.594	4.51	1.624	91.795	153.5	1.598	34.854
Jan 22	9.29	3.344	158.938	4.51	1.624	93.419	153.5	1.598	36.452
Jan 23	9.29	3.344	162.282	4.51	1.624	95.043	189.9	1.977	38.429
Jan 24	9.29	3.344	165.626	4.51	1.624	96.667	189.9	1.977	40.406
Jan 25	9.29	3.344	168.97	4.51	1.624	98.291	189.9	1.977	42.383
Jan 26	9.29	3.344	172.314	4.51	1.624	99.915	189.9	1.977	44.36
Jan 27	9.29	3.344	175.658	4.51	1.624	101.539	189.9	1.977	46.337
Jan 28	9.29	3.344	179.002	4.51	1.624	103.163	102.8	1.07	47.407
Jan 29	9.29	3.344	182.346	4.51	1.624	104.787	102.8	1.07	48.477
Jan 30	9.29	3.344	185.69	4.51	1.624	106.411	102.8	1.07	49.547
Jan 31	9.29	3.344	189.034	4.51	1.624	108.035	102.8	1.07	50.618
Feb 1	9.29	3.344	192.378	4.51	1.624	109.659	102.8	1.07	51.688
Feb 2	9.29	3.344	195.722	4.51	1.624	111.283	102.8	1.07	52.758
Feb 3	9.29	3.344	199.066	4.51	1.624	112.907	102.8	1.07	53.828
Feb 4	12.22	4.399	203.465	3.86	1.39	114.297	13.7	0.143	53.971
Feb 5 ^d	12.97	4.669	208.134	6.01	2.164	116.461	13.7	0.143	54.113
Feb 6	11.89	4.28	212.414	7.04	2.534	118.995	62.4	0.65	54.763
Feb 7	11.89	4.28	216.694	7.04	2.534	121.529	62.4	0.65	55.413
Feb 8	11.89	4.28	220.974	7.04	2.534	124.063	62.4	0.65	56.062
Feb 9	13.67	4.921	225.895	3.54	1.274	125.337	562.8	5.859	61.921
Feb 10	13.67	4.921	230.816	3.54	1.274	126.611	562.8	5.859	67.78
Feb 11	12	4.32	235.136	4.42	1.591	128.202	264.2	2.75	70.531
Feb 12	12	4.32	239.456	4.42	1.591	129.793	264.2	2.75	73.281
Feb 13	13.48	4.853	244.309	0.01	0.004	129.797	323.7	3.37	76.651
Feb 14	13.48	4.853	249.162	0.01	0.004	129.801	323.7	3.37	80.021
Feb 15	13.48	4.853	254.015	0.01	0.004	129.805	323.7	3.37	83.391
Feb 16	13.48	4.853	258.868	0.01	0.004	129.809	323.7	3.37	86.761
Feb 17	13.48	4.853	263.721	0.01	0.004	129.813	323.7	3.37	90.13
Feb 18 ^e	23.17	8.341	272.062	0.26	0.094	129.907	3159.8	32.895	123.025
Feb 19	37.22	13.399	285.461	0.14	0.05	129.957	466.3	4.854	127.88
Feb 20	37.22	13.399	298.86	0.14	0.05	130.007	466.3	4.854	132.734
Feb 21	37.22	13.399	312.259	0.14	0.05	130.057	466.3	4.854	137.588
Feb 22	37.22	13.399	325.658	0.14	0.05	130.107	466.3	4.854	142.443
Feb 23	26.91	9.688	335.346	0.04	0.014	130.121	466.3	4.854	147.297
Feb 24	26.91	9.688	345.034	0.04	0.014	130.135	466.3	4.854	152.151
Feb 25	39.12	14.083	359.117	11	3.96	134.095	466.3	4.854	157.006
Feb 26	39.12	14.083	373.2	11	3.96	138.055	466.3	4.854	161.86
Feb 27 ^f	11.99	4.316	377.516	4.19	1.508	139.563	466.3	4.854	166.715
Feb 28 ^g	11.99	4.316	381.832	4.19	1.508	141.071	466.3	4.854	171.569
Mar 1 ^{h,i}	15.83	5.699	387.531	5.82	2.095	143.166	466.3	4.854	176.423

Table A3 (continued): Sulphur mass balance for laboratory-scale Biofilter 1 - Dec. 1992 to March 1993 (Source: Coleman and Dombroski 1995)

IN				OUT					
Date	H ₂ S ppm	H ₂ S mmoles/d	Cum. H ₂ S mmoles	H ₂ S ppm	H ₂ S mmoles/d	Cum. H ₂ S mmoles	SO ₄ ²⁻ mg/d	SO ₄ ²⁻ mmoles/d	Cum. SO ₄ ²⁻ mmoles
Mar 2	NA	0	387.531	NA	0	143.166	466.3	4.854	181.278
Mar 3	NA	0	387.531	NA	0	143.166	466.3	4.854	186.132
Mar 4	NA	0	387.531	NA	0	143.166	378.9	3.945	190.077
Mar 5	NA	0	387.531	NA	0	143.166	378.9	3.945	194.021
Mar 6	NA	0	387.531	NA	0	143.166	181.3	1.887	195.908
Mar 7	NA	0	387.531	NA	0	143.166	181.3	1.887	197.796
Mar 8	NA	0	387.531	NA	0	143.166	181.3	1.887	199.683
Mar 9	NA	0	387.531	NA	0	143.166	181.3	1.887	201.571
Mar 10	NA	0	387.531	NA	0	143.166	181.3	1.887	203.458
Mar 11	NA	0	387.531	NA	0	143.166	181.3	1.887	205.346
Mar 12	NA	0	387.531	NA	0	143.166	181.3	1.887	207.233
mmoles H ₂ S in		387.531	mmoles H ₂ S out		143.166	mmoles SO ₄ ²⁻ out		207.233	
% out as H ₂ S		36.943							
% out as SO ₄ ²⁻		53.475							
% unaccounted		9.582							

^a Biofilter packed with 2.1 L (196 g) coarse peat. Air turned on.

^b H₂S turned on at 1100h December 9.

^c Water turned on at 1350h December 15.

^d Inoculate with seed bacteria 1400h February 5.

^e H₂S flow increased 1045h February 18.

^f H₂S flow turned off 2000h February 27 due to safety sensor system shutdown.

^g H₂S flow turned back on 1330h February 28.

^h H₂S flow increased slowly March 1.

ⁱ H₂S flow turned off 1345 March 1 due to safety sensor system shutdown.

^j NA – not analysed

Table A4: Hydrogen sulphide profiles for laboratory-scale biofilters operated during the first experiment – April 1999 (Source: Budwill and Coleman 1999)

Biofilter 1			Biofilter 2		
Time (days)	Inlet (ppm)	Outlet (ppm)	Time (days)	Inlet (ppm)	Outlet (ppm)
1	39.6	33.4	1	14.4	1.17
2	30	1	2	13.5	0.35
4	20	3	4	29	2.6
7	76	2.26	7	81	2.3
8	48	0	8	45	0
9	72	0	9	65	0
10	33.8	1.2	10	31.1	1.3
11	102.6	1.5	14	84.8	0
14	89.2	0	15	194.4	77
15	176.8	34	16	319.77	43.35
16	348.77	57.62	18	317	0
18	336	0	22	457.3	0.17
22	478.55	0.34	23	780	1.87
24	912	1.34	24	779.5	10.74
29	796.52	0.61	29	723.47	0.42
30	888.9	1.36	30	734.9	1.25
31	1173.9	2.49	31	974.8	8.78
32	1070.4	2.09	32	885.5	1.96
35	1008	3.03	35	840.5	2.87
36	949.59	2.897	36	818	2.72
37	1286.89	2.708	37	1193.85	2.493
38	746.2	0.15	38	701.2	0.0169
39	1055.7	0.198	39	940.74	0.133
42	1182.4	36.18	42	1053.67	22.36
43	1725.04	2.88	43	1530.75	2.59
44	1788	6.77	44	1554.5	5.74
45	1923	5.43	45	1386.17	3.35
50	618.7	1.65	50	619.9	75.4
51	780.4	0.31	51	780.4	63.99
52	795.98	0.86	52	795.98	48.7
53	758.97	0.709	53	800.46	32.2
56	2320.7	6.07	56	2397.2	6.05
57	689	1.44	57	677.2	1.54
58	1003.86	1.76	58	912.15	1.35
59	803.5	0.27	59	668.1	0.13
60	1026.6	0.697	60	940.41	0.208
63	1111.47	768.76	63	1010.85	12.6
64	31.3	4.34	64	1111.32	1.28
65	138.99	88.05	65	949	56.87
67	37.1	16.15	67	977.94	139.46
70	427.19	154.2	70	857.57	328.45

Table A5: Hydrogen sulphide profiles for laboratory-scale biofilters operated during the second experiment – July 1999 (Source: Budwill and Coleman 1999)

Biofilter 1			Biofilter 2		
Time (days)	Inlet (ppm)	Outlet (ppm)	Time (days)	Inlet (ppm)	Outlet (ppm)
1	20.74	9.63	1	15.3	6.19
2	20	2.57	2	13.72	0.57
5	22.14	0	5	14.46	0
6	89.01	0.6997	6	85.68	0.913
7	95.7	0.1199	7	87.11	1.79
8	179.87	0.078	8	169.18	0.587
9	292.2	0.0436	9	277.9	0.1543
13	433.2	398.96	13	380.41	3.8
14	62.2	61.2	14	294.2	2.29
15	48.7	47.4	15	402.1	12.4
16	46.04	44.3	16	378.3	35
19	59.47	24.41	19	496.6	172.5
20	61.2	30.1	20	524.9	265.95
21	56.5	1.27	21	231.3	15.5
22	120.5	0.92	22	155.7	12.4
23	290.5	5.16	23	317.2	36.8
26	329.5	0.1297	26	318.26	0.15057
27	451.91	0.471	27	471.3	0.47
28	409.1	0.146	28	398.5	0.221
29	621.9	69.9	29	604.28	55.98
30	832.7	92.88	30	774.3	6.14
33	892.997	31.35	33	911.97	8.91
34	866.88	46.13	34	864.18	28.8
35	1213	41.14	35	1171.1	16.7
36	1423.7	27.8	36	1567.04	31.4
37	984.4	5.95	37	1223.9	5.6
40	1356.6	48.11	40	1129.92	20.07
41	1292.75	2.57	41	1099.4	42.5
42	1415.7	2.56	42	993.4	57.8
43	1610.78	217	43	1130	195.4
44	919.4	38.98	44	939.8	45.51
47	1007.46	40.15	47	791.6	192.8
48	962.25	37.04	48	803.9	53.8
49	816.7	39.4	49	812.2	217.9

Table A6: Hydrogen sulphide profiles for laboratory-scale biofilters operated during the third experiment – August 1999 (Source: Budwill and Coleman 1999)

Biofilter 1			Biofilter 2		
Time (days)	Inlet (ppm)	Outlet (ppm)	Time (days)	Inlet (ppm)	Outlet (ppm)
1	88.6	11.5	1	79.3	1.07
1.6	81.99	15.5	1.6	78.5	2.99
4	170.1	0.371	4	96.6	0.332
4.6	271.8	0.344	4.6	214.4	0.322
5	216.5	1.21	5	222.7	0.186
5.6	204.9	0.31	5.6	212.2	0.304
6	317.4	0.258	6	276.5	0.22
7	1034.87	32.2	7	934.7	1.14
8	838.4	0.995	8	899.9	0.65
8.6	1048.3	2.53	8.6	1070.9	1.92
11	1428.4	8.95	11	1357.2	2.113
11.6	1020.3	14.38	11.6	1021.1	2.245
12	1107.2	42.7	12	1089.6	11.15
12.6	1188.7	63.3	12.6	1229.3	41.97
13	1195.95	58.1	13	1167	3.31
13.6	1501	105.3	13.6	1437	5.37
14	1176.6	136.6	14	1177.5	12
15	367.05	82.64	15	1135.87	9.65
15.6	305.13	0.954	15.6	1051.41	1.27
18	381.6	1.212	18	1091.1	7.01
18.6	661.2	1.51	18.6	1135.2	40.33
19	754.1	2.21	19	1046.2	42.74
20	1095.9	27.3	20	1185.4	47.7
20.6	1117.4	2.4	20.6	1090.7	2.53
21	1026.96	2.62	21	1014.7	2.45
21.6	1493.6	40.8	21.6	1359.1	14.3
22	1136.8	76.4	22	1178.8	64.9
26	310.3	2.3	26	298.6	1.98
27	1225.6	121.3	27	1239.1	97.6
28	1210.8	43.2	28	1200.3	5.4
29	1776.4	1550.5	29	1881.97	4.46
32	1661.9	414.3	32	2119.2	3.6
33	1247.7	919.5	33	1391.25	4.68
35	51.2	0.58	34	2447.1	6.66
			35	1622.1	5.5

Appendix B – Model code

B.1 Main model

```
model := proc()
local Ch, Sh, i, Ch0, Ch16, G, B, j, Hh, Dh, Da, Pe, Di, EC, Vm, Ks, N, delta, Z, W, A,
    E, U, V, Cin, rho, k, ns, ans, XSh1, z, Chp, Sv, Enew, Etime, Vs, Vstime, M,
    Mtime, count, t, sumVs, sumM;
restart;
with(linalg);
with(plots);
read "equations.m";
read "sulphur.m";
Ch := linalg[vector](17, [Ch0, Ch1, Ch2, Ch3, Ch4, Ch5, Ch6, Ch7, Ch8, Ch9, Ch10,
    Ch11, Ch12, Ch13, Ch14, Ch15, Ch16]); # gas phase concentration vector
Sh := linalg[matrix](15, 10, [Sh01, Sh11, Sh12, Sh13, Sh14, Sh15, Sh16, Sh17, Sh18,
    Sh19, Sh02, Sh21, Sh22, Sh23, Sh24, Sh25, Sh26, Sh27, Sh28, Sh29, Sh03,
    Sh31, Sh32, Sh33, Sh34, Sh35, Sh36, Sh37, Sh38, Sh39, Sh04, Sh41, Sh42,
    Sh43, Sh44, Sh45, Sh46, Sh47, Sh48, Sh49, Sh05, Sh51, Sh52, Sh53, Sh54,
    Sh55, Sh56, Sh57, Sh58, Sh59, Sh06, Sh61, Sh62, Sh63, Sh64, Sh65, Sh66,
    Sh67, Sh68, Sh69, Sh07, Sh71, Sh72, Sh73, Sh74, Sh75, Sh76, Sh77, Sh78,
    Sh79, Sh08, Sh81, Sh82, Sh83, Sh84, Sh85, Sh86, Sh87, Sh88, Sh89, Sh09,
    Sh91, Sh92, Sh93, Sh94, Sh95, Sh96, Sh97, Sh98, Sh99, Sh010, Sh101, Sh102,
    Sh103, Sh104, Sh105, Sh106, Sh107, Sh108, Sh109, Sh011, Sh111, Sh112,
    Sh113, Sh114, Sh115, Sh116, Sh117, Sh118, Sh119, Sh012, Sh121, Sh122,
    Sh123, Sh124, Sh125, Sh126, Sh127, Sh128, Sh129, Sh013, Sh131, Sh132,
    Sh133, Sh134, Sh135, Sh136, Sh137, Sh138, Sh139, Sh014, Sh141, Sh142,
    Sh143, Sh144, Sh145, Sh146, Sh147, Sh148, Sh149, Sh015, Sh151, Sh152,
    Sh153, Sh154, Sh155, Sh156, Sh157, Sh158, Sh159]);
#liquid phase concentration vector
for i to 15 do Sh[i, 1] := Ch[i + 1]/Hh end do; # gas-liquid boundary condition
for i to 15 do Sh[i, 10] := Sh[i, 9] end do; # liquid-solid boundary condition
Ch0 := Ch[2] - Ch[2]*U*Z/(W*Di) + Cin*U*Z/(W*Di); # inlet gas boundary
condition
Ch16 := Ch15; # outlet gas boundary condition
```



```

G := linalg[vector](15); # vector of gas phase equations
B := linalg[matrix](15, 8); # vector of liquid phase equations
for i to 15 do G[i] := Da*(Ch[i + 2] - 2*Ch[i + 1] + Ch[i])*W^2/Z^2 - U*(Ch[i + 1] -
Ch[i])*W/Z + Dh*A*(Sh[i, 2] - Sh[i, 1])*N/(E*delta) end do;
for i to 15 do for j to 8 do B[i, j] := Dh*N^2*(Sh[i, j + 2] - 2*Sh[i, j + 1] +
Sh[i, j])/delta^2 - EC end do end do;

Hh := .3885563; # Henry's law coefficient
Dh := .161*10^(-8); # diffusivity of H2S in water, m2/s
Da := Di; # diffusivity of H2S in air, m2/s
Pe := 17; # Peclet number
Di := U*Z/Pe; # dispersion coefficient, m2/s
EC := 413/1800000*1/Hh; # elimination capacity, kg/m3s
Vm := .680873*10^(-5); # maximum elimination capacity, kg/m3s
Ks := .000134167; # half saturation constant, kg/m3
N := 8; # number of x-divisions in biofilm
delta := .000175; # biofilm thickness, m
Z := 1; # length of biofilter, m
W := 15; # number of z-divisions in biofilter
A := 950; # specific surface area of peat, m2/m3
E := .45; # porosity
U := .2195837726*1/π; # gas velocity, m/s
V := evalf(.00064516*π*Z); # biofilter volume, m3
Cin := .004126574104; # inlet H2S concentration, kg/m3
rho := 2000; # density of sulphur, kg/m3
ks := .00581051; # chemical sulphur formation rate constant, (kg/m3)0.38 s-1
ns := .61609103; # chemical sulphur formation reaction order
equations();
for i to 135 do eq[i] := eq[i] end do;
_EnvAllSolutions := true;
ans := solve({eq1 = 0, eq2 = 0, eq3 = 0, eq4 = 0, eq5 = 0, eq6 = 0, eq7 = 0, eq8 = 0,
eq9 = 0, eq10 = 0, eq11 = 0, eq12 = 0, eq13 = 0, eq14 = 0, eq15 = 0, eq16 = 0,
eq17 = 0, eq18 = 0, eq19 = 0, eq20 = 0, eq21 = 0, eq22 = 0, eq23 = 0, eq24 = 0,
eq25 = 0, eq26 = 0, eq27 = 0, eq28 = 0, eq29 = 0, eq30 = 0, eq31 = 0, eq32 = 0,
eq33 = 0, eq34 = 0, eq35 = 0, eq36 = 0, eq37 = 0, eq38 = 0, eq39 = 0, eq40 = 0,
eq41 = 0, eq42 = 0, eq43 = 0, eq44 = 0, eq45 = 0, eq46 = 0, eq47 = 0, eq48 = 0,
eq49 = 0, eq50 = 0, eq51 = 0, eq52 = 0, eq53 = 0, eq54 = 0, eq55 = 0, eq56 = 0,

```


$eq57 = 0, eq58 = 0, eq59 = 0, eq60 = 0, eq61 = 0, eq62 = 0, eq63 = 0, eq64 = 0,$
 $eq65 = 0, eq66 = 0, eq67 = 0, eq68 = 0, eq69 = 0, eq70 = 0, eq71 = 0, eq72 = 0.$
 $eq73 = 0, eq74 = 0, eq75 = 0, eq76 = 0, eq77 = 0, eq78 = 0, eq79 = 0, eq80 = 0,$
 $eq81 = 0, eq82 = 0, eq83 = 0, eq84 = 0, eq85 = 0, eq86 = 0, eq87 = 0, eq88 = 0,$
 $eq89 = 0, eq90 = 0, eq91 = 0, eq92 = 0, eq93 = 0, eq94 = 0, eq95 = 0, eq96 = 0,$
 $eq97 = 0, eq98 = 0, eq99 = 0, eq100 = 0, eq101 = 0, eq102 = 0, eq103 = 0,$
 $eq104 = 0, eq105 = 0, eq106 = 0, eq107 = 0, eq108 = 0, eq109 = 0, eq110 = 0,$
 $eq111 = 0, eq112 = 0, eq113 = 0, eq114 = 0, eq115 = 0, eq116 = 0, eq117 = 0,$
 $eq118 = 0, eq119 = 0, eq120 = 0, eq121 = 0, eq122 = 0, eq123 = 0, eq124 = 0,$
 $eq125 = 0, eq126 = 0, eq127 = 0, eq128 = 0, eq129 = 0, eq130 = 0, eq131 = 0,$
 $eq132 = 0, eq133 = 0, eq134 = 0, eq135 = 0\}, \{Ch1, Ch2, Ch3, Ch4, Ch5, Ch6,$
 $Ch7, Ch8, Ch9, Ch10, Ch11, Ch12, Ch13, Ch14, Ch15, Sh11, Sh12, Sh13,$
 $Sh14, Sh15, Sh16, Sh17, Sh18, Sh21, Sh22, Sh23, Sh24, Sh25, Sh26, Sh27,$
 $Sh28, Sh31, Sh32, Sh33, Sh34, Sh35, Sh36, Sh37, Sh38, Sh41, Sh42, Sh43,$
 $Sh44, Sh45, Sh46, Sh47, Sh48, Sh51, Sh52, Sh53, Sh54, Sh55, Sh56, Sh57,$
 $Sh58, Sh61, Sh62, Sh63, Sh64, Sh65, Sh66, Sh67, Sh68, Sh71, Sh72, Sh73,$
 $Sh74, Sh75, Sh76, Sh77, Sh78, Sh81, Sh82, Sh83, Sh84, Sh85, Sh86, Sh87,$
 $Sh88, Sh91, Sh92, Sh93, Sh94, Sh95, Sh96, Sh97, Sh98, Sh101, Sh102,$
 $Sh103, Sh104, Sh105, Sh106, Sh107, Sh108, Sh111, Sh112, Sh113, Sh114,$
 $Sh115, Sh116, Sh117, Sh118, Sh121, Sh122, Sh123, Sh124, Sh125, Sh126,$
 $Sh127, Sh128, Sh131, Sh132, Sh133, Sh134, Sh135, Sh136, Sh137, Sh138,$
 $Sh141, Sh142, Sh143, Sh144, Sh145, Sh146, Sh147, Sh148, Sh151, Sh152,$
 $Sh153, Sh154, Sh155, Sh156, Sh157, Sh158\});$

assign(ans);

$Ch := \text{linalg}[\text{vector}](17, [Ch0, Ch1, Ch2, Ch3, Ch4, Ch5, Ch6, Ch7, Ch8, Ch9, Ch10,$
 $Ch11, Ch12, Ch13, Ch14, Ch15, Ch16]);$

$Sh := \text{linalg}[\text{matrix}](15, 10, [Sh01, Sh11, Sh12, Sh13, Sh14, Sh15, Sh16, Sh17, Sh18,$
 $Sh19, Sh02, Sh21, Sh22, Sh23, Sh24, Sh25, Sh26, Sh27, Sh28, Sh29, Sh03,$
 $Sh31, Sh32, Sh33, Sh34, Sh35, Sh36, Sh37, Sh38, Sh39, Sh04, Sh41, Sh42,$
 $Sh43, Sh44, Sh45, Sh46, Sh47, Sh48, Sh49, Sh05, Sh51, Sh52, Sh53, Sh54,$
 $Sh55, Sh56, Sh57, Sh58, Sh59, Sh06, Sh61, Sh62, Sh63, Sh64, Sh65, Sh66,$
 $Sh67, Sh68, Sh69, Sh07, Sh71, Sh72, Sh73, Sh74, Sh75, Sh76, Sh77, Sh78,$
 $Sh79, Sh08, Sh81, Sh82, Sh83, Sh84, Sh85, Sh86, Sh87, Sh88, Sh89, Sh09,$
 $Sh91, Sh92, Sh93, Sh94, Sh95, Sh96, Sh97, Sh98, Sh99, Sh010, Sh101, Sh102,$
 $Sh103, Sh104, Sh105, Sh106, Sh107, Sh108, Sh109, Sh011, Sh111, Sh112,$
 $Sh113, Sh114, Sh115, Sh116, Sh117, Sh118, Sh119, Sh012, Sh121, Sh122,$


```

    Sh123, Sh124, Sh125, Sh126, Sh127, Sh128, Sh129, Sh013, Sh131, Sh132,
    Sh133, Sh134, Sh135, Sh136, Sh137, Sh138, Sh139, Sh014, Sh141, Sh142,
    Sh143, Sh144, Sh145, Sh146, Sh147, Sh148, Sh149, Sh015, Sh151, Sh152,
    Sh153, Sh154, Sh155, Sh156, Sh157, Sh158, Sh159));
for i to 15 do Sh[i, 1] := Ch[i + 1]/Hh end do;
for i to 15 do Sh[i, 10] := Sh[i, 9] end do;
print(Sh);
print(Ch);
for i to 15 do Sh|| i := linalg[vector](10) end do;
for j to 15 do for i to 10 do Sh|| j[i] := Sh[j, i] end do end do;
XShI := linalg[vector](10);
XShI[1] := 0;
XShI[2] := 1/16*delta;
XShI[3] := 3/16*delta;
XShI[4] := 5/16*delta;
XShI[5] := 7/16*delta;
XShI[6] := 9/16*delta;
XShI[7] := 11/16*delta;
XShI[8] := 13/16*delta;
XShI[9] := 15/16*delta;
XShI[10] := delta;
convert(XShI, 'list');
for i to 15 do convert(Sh|| i, 'list') end do;
plots[pointplot](zip((x, y) -> [x, y], XShI, ShI), style = line, color = red, labels =
    ["Distance into biofilm, m", "Concentration, kg/m3"], labeldirections = [horizontal,
    vertical], title = "Liquid phase concentration profile (H2S) at inlet");
plots[pointplot](zip((x, y) -> [x, y], XShI, ShI0), style = line, color = red, labels =
    ["Distance into biofilm, m", "Concentration, kg/m3"], labeldirections = [horizontal,
    vertical], title = "Liquid phase concentration profile (H2S) at outlet");
z := linalg[vector](15);
Ch := linalg[vector](15, [Ch1, Ch2, Ch3, Ch4, Ch5, Ch6, Ch7, Ch8, Ch9, Ch10, Ch11,
    Ch12, Ch13, Ch14, Ch15]);
Chp := linalg[vector](15);
for i to 15 do Chp[i] := 726995.3050*Ch[i] end do;
for i to 15 do z[i] := 1/15*i - 1/30 end do;
print(z);

```



```

plots[pointplot](zip((x, y) -> [x, y], z, Chp), style = line, color = red, labels =
  ["Distance along biofilter, m", "Concentration, ppm"], labeldirections = [horizontal,
    vertical], title = "Gas phase concentration profile - H2S");
for i to 15 do if Ch[i] < 0 then Ch[i] := 0 end if end do;
for i to 15 do evalf(E*V/W) end do;
Sv := linalg[vector](15, %); # vector of available void space in biofilter, m3
Enew := linalg[vector](15, E); # vector of new porosity values
Etime := linalg[vector]; # vector of porosity values at each time step
Vs := linalg[vector](15, 0); # vector of volume of sulphur formed, m3
Vstime := linalg[vector]; # vector of volume of sulphur at each time step
M := linalg[vector](15, 0); # vector of concentration of sulphur formed, kg/m3
Mtime := linalg[vector]; # vector of concentration of sulphur formed at each time step
count := 0; # counter variable
t := 0; # time, d
sumVs := 0; # sum of volume of sulphur formed, m3
sumM := 0; # sum of concentration of sulphur formed, kg/m3
while 0 < Sv[14] do sulphur(Ch, ks, ns, Vm, Ks, V, W, kbiolsulphate, nbiolsulphate,
  rho) end do;
evalf(t);
E;
print(Sv);
print(Vs);
evalf(sumVs);
evalf(sumM);
print(Enew);
print(M);
print(Etime);
print(Vstime);
print(Mtime)
end proc
save model, "model.m"

```


B.2 Defining equations

```
equations := proc()  
global G, B, Ch, Sh, eq;  
  eq[1] := G[1];  
  eq[2] := G[2];  
  eq[3] := G[3];  
  eq[4] := G[4];  
  eq[5] := G[5];  
  eq[6] := G[6];  
  eq[7] := G[7];  
  eq[8] := G[8];  
  eq[9] := G[9];  
  eq[10] := G[10];  
  eq[11] := G[11];  
  eq[12] := G[12];  
  eq[13] := G[13];  
  eq[14] := G[14];  
  eq[15] := G[15];  
  eq[16] := B[1, 1];  
  eq[17] := B[2, 1];  
  eq[18] := B[3, 1];  
  eq[19] := B[4, 1];  
  eq[20] := B[5, 1];  
  eq[21] := B[6, 1];  
  eq[22] := B[7, 1];  
  eq[23] := B[8, 1];  
  eq[24] := B[9, 1];  
  eq[25] := B[10, 1];  
  eq[26] := B[11, 1];  
  eq[27] := B[12, 1];  
  eq[28] := B[13, 1];  
  eq[29] := B[14, 1];  
  eq[30] := B[15, 1];
```


$eq[31] := B[1, 2];$
 $eq[32] := B[2, 2];$
 $eq[33] := B[3, 2];$
 $eq[34] := B[4, 2];$
 $eq[35] := B[5, 2];$
 $eq[36] := B[6, 2];$
 $eq[37] := B[7, 2];$
 $eq[38] := B[8, 2];$
 $eq[39] := B[9, 2];$
 $eq[40] := B[10, 2];$
 $eq[41] := B[11, 2];$
 $eq[42] := B[12, 2];$
 $eq[43] := B[13, 2];$
 $eq[44] := B[14, 2];$
 $eq[45] := B[15, 2];$
 $eq[46] := B[1, 3];$
 $eq[47] := B[2, 3];$
 $eq[48] := B[3, 3];$
 $eq[49] := B[4, 3];$
 $eq[50] := B[5, 3];$
 $eq[51] := B[6, 3];$
 $eq[52] := B[7, 3];$
 $eq[53] := B[8, 3];$
 $eq[54] := B[9, 3];$
 $eq[55] := B[10, 3];$
 $eq[56] := B[11, 3];$
 $eq[57] := B[12, 3];$
 $eq[58] := B[13, 3];$
 $eq[59] := B[14, 3];$
 $eq[60] := B[15, 3];$
 $eq[61] := B[1, 4];$
 $eq[62] := B[2, 4];$
 $eq[63] := B[3, 4];$
 $eq[64] := B[4, 4];$
 $eq[65] := B[5, 4];$
 $eq[66] := B[6, 4];$


```

eq[67] := B[7, 4];
eq[68] := B[8, 4];
eq[69] := B[9, 4];
eq[70] := B[10, 4];
eq[71] := B[11, 4];
eq[72] := B[12, 4];
eq[73] := B[13, 4];
eq[74] := B[14, 4];
eq[75] := B[15, 4];
eq[76] := B[1, 5];
eq[77] := B[2, 5];
eq[78] := B[3, 5];
eq[79] := B[4, 5];
eq[80] := B[5, 5];
eq[81] := B[6, 5];
eq[82] := B[7, 5];
eq[83] := B[8, 5];
eq[84] := B[9, 5];
eq[85] := B[10, 5];
eq[86] := B[11, 5];
eq[87] := B[12, 5];
eq[88] := B[13, 5];
eq[89] := B[14, 5];
eq[90] := B[15, 5];
eq[91] := B[1, 6];
eq[92] := B[2, 6];
eq[93] := B[3, 6];
eq[94] := B[4, 6];
eq[95] := B[5, 6];
eq[96] := B[6, 6];
eq[97] := B[7, 6];
eq[98] := B[8, 6];
eq[99] := B[9, 6];
eq[100] := B[10, 6];
eq[101] := B[11, 6];
eq[102] := B[12, 6];

```



```

eq[103] := B[13, 6];
eq[104] := B[14, 6];
eq[105] := B[15, 6];
eq[106] := B[1, 7];
eq[107] := B[2, 7];
eq[108] := B[3, 7];
eq[109] := B[4, 7];
eq[110] := B[5, 7];
eq[111] := B[6, 7];
eq[112] := B[7, 7];
eq[113] := B[8, 7];
eq[114] := B[9, 7];
eq[115] := B[10, 7];
eq[116] := B[11, 7];
eq[117] := B[12, 7];
eq[118] := B[13, 7];
eq[119] := B[14, 7];
eq[120] := B[15, 7];
eq[121] := B[1, 8];
eq[122] := B[2, 8];
eq[123] := B[3, 8];
eq[124] := B[4, 8];
eq[125] := B[5, 8];
eq[126] := B[6, 8];
eq[127] := B[7, 8];
eq[128] := B[8, 8];
eq[129] := B[9, 8];
eq[130] := B[10, 8];
eq[131] := B[11, 8];
eq[132] := B[12, 8];
eq[133] := B[13, 8];
eq[134] := B[14, 8];
eq[135] := B[15, 8]

```

end proc

save equations, "equations.m"

B.3 Calculating sulphur plugging

```

sulphur := proc(Ch, ks, ns, Vm, Ks, V, W, kbiolsulphate, nbiolsulphate, rho)
local rchem, rbiol, rbiolsulfate, Vslice, i, sumE;
global Sv, t, Vs, E, M, Enew, Etime, Vstime, sumVs, count, Cin, sumM, Mtime;
  rchem := linalg[vector](15); # vector of chemical sulphur formation rate, kg/m3s
  rbiol := linalg[vector](15); # vector of net biological sulphur formation, kg/m3s
  Vslice := evalf(V/W); # volume available for plugging in each layer, m3
  for i to 15 do rchem[i] := .004789272031*ks*Ch[i]^ns/(Cin*W)^1.05 end do;
  for i to 15 do rbiol[i] := Vm*Ch[i]/(Ks + Ch[i]) end do;
  for i to 15 do M[i] := M[i] + rchem[i] + rbiol[i] end do;
  for i to 15 do Vs[i] := evalf(M[i]*Vslice/rho) end do;
  for i to 15 do if Vs[i] < 0 then Vs[i] := 0 end if end do;
  for i to 15 do M[i] := Vs[i]*rho/Vslice end do;
  for i to 15 do Enew[i] := evalf(.45*Vslice - Vs[i])*W/V end do;
  for i to 15 do if evalf(Enew[i]) < .05 then Enew[i] := .05 end if end do;
  for i to 14 do if evalf(Vs[i] - Sv[i]) > 0 then Vs[i + 1] := Vs[i + 1] + Vs[i] - Sv[i];
    Sv[i] := 0 else Sv[i] := evalf(.45*Vslice - Vs[i])
    end if
  end do;
  for i to 15 do if Vs[i] < 0 then Vs[i] := 0 end if end do;
  sumE := 0;
  for i to 15 do sumE := sumE + Enew[i] end do;
  t := t + 1/86400;
  E := evalf(sumE/W);
  count := count + 1;
  sumVs := 0;
  for i to 15 do sumVs := evalf(sumVs + Vs[i]) end do;
  sumM := 0;
  for i to 15 do sumM := sumM + M[i] end do;
  for i to 100 do if count = 86400*i then Etime[i] := E; Vstime[i] := sumVs;
    Mtime[i] := sumM end if end do
end proc
save sulphur, "sulphur.m"
```


Appendix C – Chemical oxidation experiments data

C.1 Physical data

MW H ₂ S	34.08 g/mol
ρ H ₂ S	1.19
STP	22.4 L/mol 0.0224 m ³ /mol
ρ H ₂ S (corrected)	0.0267 m ³ /mol 26.7 L/mol

C.2 Flowrates

H ₂ S-High	25 mL/min 1.5 L/h 2940 ppm 4.05 g/m ³
H ₂ S-Low	8.63 mL/min 0.518 L/h 1020 ppm 1.40 g/m ³
Air	8.5 L/min 510 L/h

C.3 Experimental data

Table C1: Sulphur recovery during the chemical oxidation experiments – January to March 2000

Experiment	Length	H ₂ S on	H ₂ S off	Time (h)	S-peat (g)	S-SO ₄ ²⁻ (g)	S-extracted (g)	S-total (g)
1	7 days	9:23	9:00	171	36	0.24	na	-
2	7 days	14:53	14:30	172	39	0.17	13	53
3	7 days	13:28	11:02	168	42	0.81	10	53
5	2 days	10:44	9:01	47	3	0	7	11
7	3 days	10:46	11:52	75	35	0	8	43
6	5 days	10:45	8:37	119	70	3.88	32	107
4	7 days	15:54	8:48	162	68	0.20	10	79
Abiotic	7 days	9:51	9:28	168	na	0.54	9	-
Peat control	6 days	12:30	10:00	142	na	0.20	na	-

Table C2: Sulphur recovery from the peat core, during the chemical oxidation experiments. The core was labelled from inlet (BF-1) to outlet (BF-4).

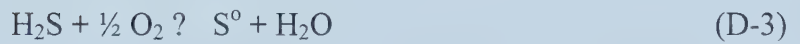
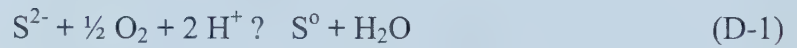
Experiment	Length	H ₂ S (ppm)	BF-1 (g)	BF-2 (g)	BF-3 (g)	BF-4 (g)	Total (g)
1	7 days	1000	16.54	9.30	4.53	5.23	35.61
2	7 days	1000	30.58	0	8.72	0	39.29
3	7 days	1000	17.16	9.00	7.09	9.00	42.24
4	7 days	3000	42.61	19.64	0	5.66	67.91
5	2 days	3000	0	2.84	0	0	2.84
6	5 days	3000	40.84	13.34	9.60	6.21	69.99
7	3 days	3000	18.49	6.89	4.92	4.41	34.72

The data from Experiment 6 were disregarded for all analyses, because of consistently high results. It is likely that there were problems with the experimental flow rates during this experiment, so that much higher concentrations than 3000 ppm were actually flowing through the column.

Appendix D - Determining rate laws

D.1 Chemical sulphur formation

The raw data from the chemical oxidation experiments are shown in Appendix C. To determine the appropriate kinetic expression for sulphur formation, the following equations were used. “Sulphide” is converted to solid sulphur in the presence of oxygen:



The species “S⁰” is a general designation for the sulphur that is formed in the presence of water and air in the biofilter. It is likely some form of colloidal sulphur. The following rate expression can be derived:

$$r_{\text{s,chem}} = \frac{dC_{\text{S}}}{dt} \quad (\text{D-4})$$

The rate of sulphur deposition, based on the total amount of sulphur recovered (both on the peat and washed out with the effluent as S and SO₄²⁻) can be expressed as:

$$r_{\text{s,chem}} = k_{\text{S}} C_{\text{h}}^{n_{\text{S}}} \quad (\text{D-5})$$

In equation D-5, C_h refers to the concentration of H₂S in the inlet stream. Excess oxygen is assumed, so that the rate constants shown are actually pseudo-rate constants, where:

$$k = k' [\text{O}]^{n_{\text{O}}} \quad (\text{D-6})$$

The amount of sulphur recovered versus time was plotted at two different influent concentrations of H₂S. The resulting curves are shown in Figure D1. Regression analysis was performed to measure the rate of sulphur formation.

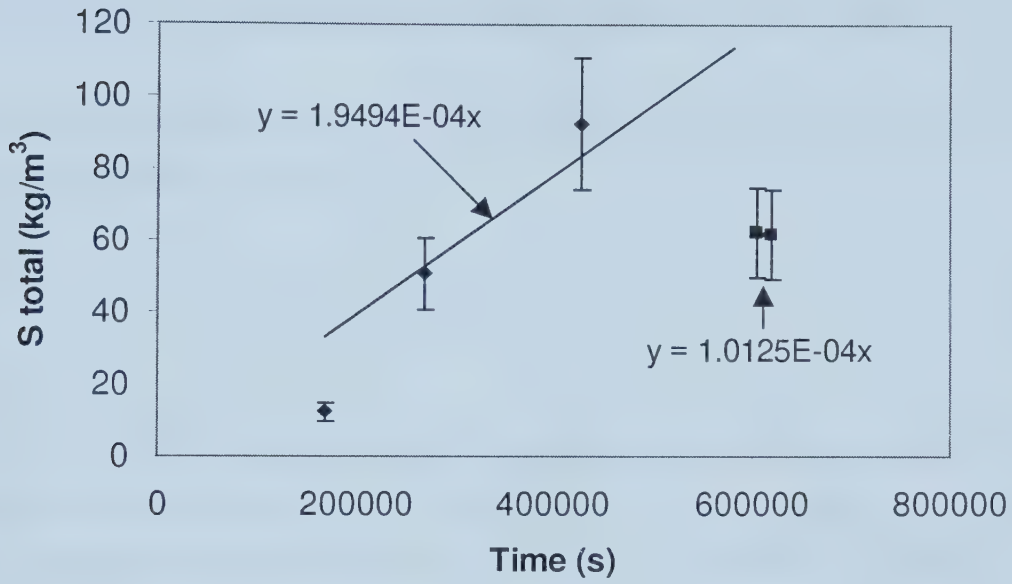


Figure D1: Chemical sulphur formation in the H₂S biofilter, at influent H₂S concentrations of 1000 (○) and 3000 (◆) ppm

Figure D1 shows the two different rates of sulphur formation that were obtained in these experiments. Using equation D-5, this creates a system of two equations and two unknowns, as follows:

$$r_1 = k_s C_1^{n_s} \quad (D-7)$$

$$r_2 = k_s C_2^{n_s} \quad (D-8)$$

where C_1 and C_2 are the influent H₂S concentrations (1000 and 3000 ppm). Solving this system gives:

$$k_s = 0.0058 (\text{kg/m}^3)^{0.38} \text{ s}^{-1}$$

$$n_s = 0.616$$

D.2 H₂S depletion during the chemical oxidation experiments

The rate of H₂S depletion from the gas phase during the chemical oxidation experiments, r_{chem} , can be defined as follows:

$$r_{\text{chem}} = \frac{dC_h}{dt} = k_h C_n^{n_h} \quad (\text{D-9})$$

A similar analysis to that described above was performed on the data from the chemical oxidation experiments. A plot of sulphur (as H₂S) in the exit stream of the biofilter versus time gives a system of equations similar to those described by equations D-7 and D-8. The plot is shown in Figure D2.

The rate constants for H₂S depletion from the gas phase during the chemical oxidation experiments are:

$$k_h = 0.748 (\text{m}^3/\text{kg})^{0.35} \text{ s}^{-1}$$

$$n_h = 1.35$$

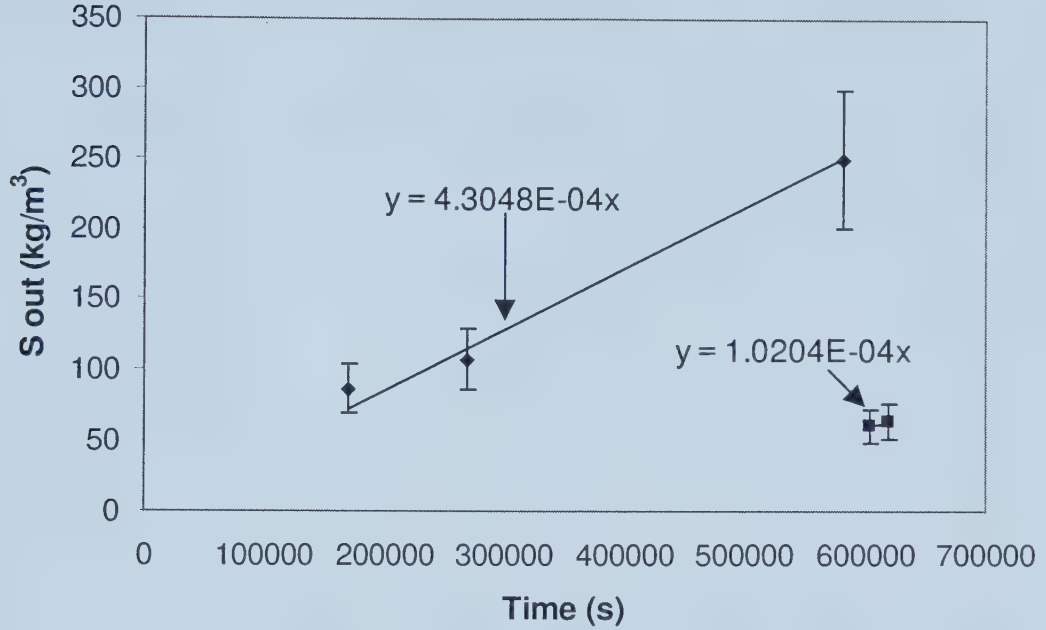


Figure D2: Effluent sulphur (as H₂S) in the H₂S biofilter, at influent H₂S concentrations of 1000 (□) and 3000 (◆) ppm

D.3 Determining lumped kinetic parameters

The biofilter data from ARC were analysed using Michaelis-Menten kinetics, to obtain values of V_m and K_s that describe the net biological activity in the biofilter. The linearised form of the Michaelis-Menten rate expression is (Fogler 1992):

$$\frac{1}{R} = \frac{1}{V_m} + \frac{K_s}{V_m} \frac{1}{C} \quad (\text{D-10})$$

In this case R is calculated as $r - r_{\text{chem}}$, where r is calculated from the ARC data using to equation D-11, and r_{chem} is calculated using to equation D-9.

$$r = \frac{Q}{V} (C_{h,\text{in}} - C_{h,\text{out}}) \quad (\text{D-11})$$

A sample plot is shown in Figure D3.

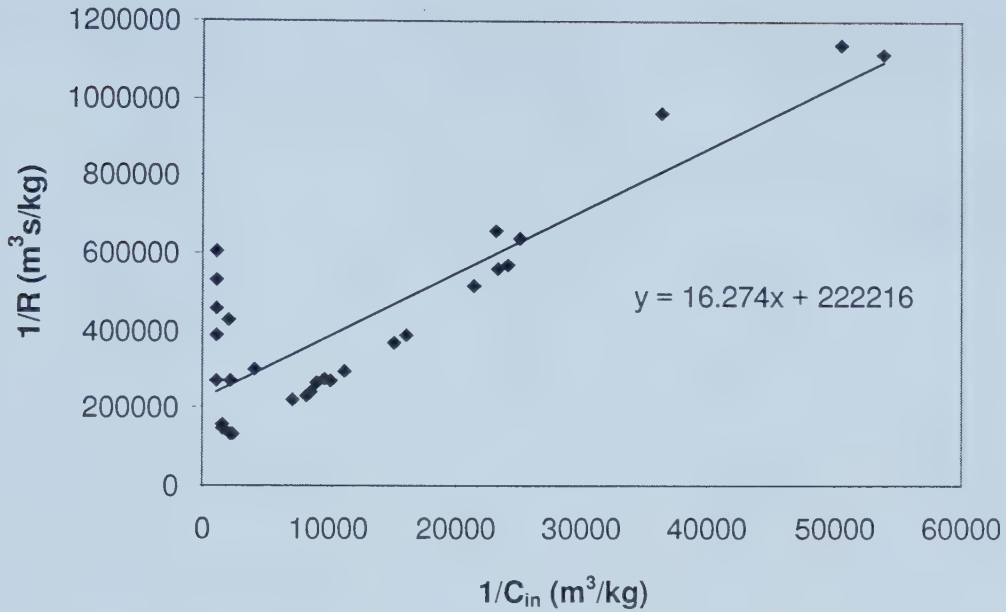


Figure D3: Modified Michaelis-Menten kinetics for the first ARC experiment – April 1999 (Budwill and Coleman 1999)

From Figure D3, V_m and K_s can be calculated from the slope and intercept as:

$$V_m = 4.50\text{E-}06 \text{ kg/m}^3\text{s}$$

$$K_s = 7.32\text{E-}05 \text{ kg/m}^3$$

Averages of the kinetic calculations on all ARC data were used to calculate the model parameters. The values of V_m and K_s used in the model are:

$$V_m = 6.81\text{E-}06 \text{ kg/m}^3\text{s}$$

$$K_s = 1.34\text{E-}04 \text{ kg/m}^3$$

Appendix E – Edmonton water quality parameters

Table E1: Summary of major chemical, physical, and microbiological parameters of Edmonton drinking water for March 2001 (Source: Water quality reports, EPCOR website, www.epcor.ca). The biofilter experiments were conducted in February and March 2001.

Parameter	Monthly Average	2001 Range	Approval Requirements
Alkalinity, total (mg/L as CaCO ₃)	117	106 – 141	n/a
Aluminium, total (mg/L)	0.03	0.03 – 0.04	<0.1
Arsenic (mg/L)	<0.002	<0.002	<0.025
Cadmium (mg/L)	<0.001	<0.001	<0.005
Chloride (mg/L)	3.8	2.2 – 8.3	<250
Chlorine, (total) residual (mg/L)	1.99	1.75 – 2.13	0.5 – 2.5
Chromium (mg/L)	<0.001	<0.001	<0.05
Coliforms, fecal (cfu/100 mL)	<1	<1	0
Coliforms, total (cfu/100 mL)	<1	<1	<10
Colour (TCU Pt-Co)	1	1	<15
Conductivity (µS/cm)	345	344 – 387	n/a
Copper (mg/L)	<0.003	<0.003	<1.0
<i>Cryptosporidium</i> (cysts/100 L)	<0.1	<0.1	n/a
Fluoride (mg/L)	0.79	0.74 – 0.83	0.7 – 0.9
<i>Giardia</i> (cysts/100 L)	<0.1	<0.1	n/a
Hardness, calcium (mg/L as CaCO ₃)	113	106 – 136	n/a
Hardness, total (mg/L as CaCO ₃)	166	156 – 199	n/a
Iron (mg/L)	<0.003	<0.003	<0.3
Lead (mg/L)	<0.0005	<0.0005	<0.01
Manganese (mg/L)	<0.0005	<0.0005 – 0.0007	<0.05
Mercury (mg/L)	<0.0001	<0.0001	<0.001
Nitrate (mg/L as N)	0.07	0.06 – 0.09	<10.0
Nitrite (mg/L as N)	<0.01	<0.01	<1.0
pH	7.9	7.4 – 8.0	6.5 – 9.0
Potassium (mg/L)	0.6	0.6 – 0.8	n/a
Sodium (mg/L)	7.4	6.6 – 7.8	<200
Sulphate (mg/L)	59.9	55.9 – 68.6	<500
Total dissolved solids (calc.) (mg/L)	200	195 – 223	<500
Total organic carbon (mg/L)	0.6	0.6 – 1.3	n/a
Trihalomethanes (mg/L)	0.006	0.002 – 0.014	<0.1
Turbidity (NTU)	0.06	0.03 – 0.09	<1.0
Uranium (mg/L)	<0.05	<0.05	<0.1
Zinc	<0.005	<0.005	<5

Appendix F – RTD analysis

The residence time distribution of an inert tracer, also called the exit age distribution for a pulse input, $E(t)$, is defined as:

$$E(t) = \frac{C(t)}{\int_0^{\infty} C(t)dt} \cong \frac{C_i}{\sum C_i \Delta t_i} \quad (F-1)$$

The two most important variables obtained from RTD studies are the first moment of the RTD function, $E(t)$, which gives the mean residence time, t_m (equation F-2), and the second moment about the mean, which gives the variance, σ^2 (equation F-3):

$$t_m = \int_0^{\infty} t E dt \cong \sum t_i E_i \Delta t_i \quad (F-2)$$

$$\sigma^2 = \int_0^{\infty} (t - t_m)^2 E dt \cong \sum (t_i - t_m)^2 E_i \Delta t_i \quad (F-3)$$

Table F1 presents the calculations of the first moment (mean residence time) and second moment (variance) about the origin for the RTD function obtained from a representative set of pulse tracer test data. The real data (obtained in the tracer studies) were not used in the sample calculations, because of the prohibitively high number of data points. Similar calculations and analyses were conducted with the raw data from the tracer tests.

Table F1: Sample calculation of the RTD function analysis

t_i (min)	C_i^* ^a	Δt_i (min)	$E_i(t)$ (min ⁻¹)	$t_i E_i \Delta t_i$ (min)	$(t_i - t_m)^2$ (min ²)	$(t_i - t_m)^2 E_i \Delta t_i$ (min ²)
0	0	0	0	0.000	19.349	0
0.5	0.002	0.5	0.0005	0.000	15.201	0.004
1.0	0.035	0.5	0.011	0.005	11.552	0.063
1.5	0.083	0.5	0.026	0.020	8.403	0.109
2.0	0.212	0.5	0.067	0.067	5.754	0.192
2.5	0.388	0.5	0.122	0.153	3.605	0.220
3.0	0.656	0.5	0.206	0.310	1.957	0.202
3.5	0.774	0.5	0.243	0.426	0.808	0.098
4.0	1.000	0.5	0.315	0.629	0.159	0.025
4.5	0.770	0.5	0.242	0.545	0.010	0.001
5.0	0.743	0.5	0.234	0.584	0.361	0.042
5.5	0.608	0.5	0.191	0.526	1.213	0.116
6.0	0.481	0.5	0.151	0.454	2.564	0.194
6.5	0.266	0.5	0.084	0.271	4.415	0.184
7.0	0.135	0.5	0.043	0.149	6.766	0.144
7.5	0.089	0.5	0.028	0.104	9.617	0.134
8.0	0.060	0.5	0.019	0.075	12.969	0.122
8.5	0.039	0.5	0.012	0.052	16.820	0.104
9.0	0.012	0.5	0.004	0.017	21.171	0.041
9.5	0.004	0.5	0.001	0.006	26.022	0.017
10.0	0.003	0.5	0.001	0.005	31.373	0.015
Sum C_i^*	6.36		t_m	4.40	σ_t^2	2.02786
					σ_t	4.05572

^a Normalised response, used in all calculations

Appendix G – Biofilter calculations

Sour gas in Alberta contains an average of 1.5 percent H₂S (Johnson et al. 2001). It is difficult to obtain reliable estimates of solution gas flow rates, but a “typical” flow rate encountered might be 43 m³/h (Johnson et al. 2001). Using the physical properties of H₂S listed in Appendix C, the mass loading of H₂S from a well containing 1.5 percent H₂S content can be calculated as follows:

$$43 \frac{\text{m}^3}{\text{h}} \times 0.015 = 0.43 \frac{\text{m}^3}{\text{h}} \text{H}_2\text{S}$$

$$0.43 \frac{\text{m}^3}{\text{h}} \text{H}_2\text{S} \div 0.0224 \frac{\text{m}^3}{\text{mol}} (\text{STP}) \times 34.09 \frac{\text{g}}{\text{mol}} \text{H}_2\text{S} = 652 \frac{\text{g}}{\text{h}} \text{H}_2\text{S}$$

On average, the ARC biofilter was capable of removing 400 g H₂S/m³h (Budwill and Coleman 1999). The volume of biofilter needed to treat the solution gas from a well containing 1.5 percent H₂S is:

$$652 \frac{\text{g}}{\text{h}} \text{H}_2\text{S} \div 400 \frac{\text{g}}{\text{m}^3 \text{h}} \text{H}_2\text{S} = 1.63 \text{ m}^3$$

Assuming a diameter of 1 m, the biofilter would need to be 2 m high.

Similar calculations can be performed for various different mass loading rates of H₂S, depending on the solution gas composition of the particular well in question.

University of Alberta Library



0 1620 1493 7831

B45617